THE UNIVERSITY OF CALGARY

A Low-Cost Integrated INS/GPS System

by

Gengsheng Zhang

A THESIS

SUBMITTED TO THE FACULTY OF GRADUATE STUDIES

IN PARTIAL FULFILLMENT OF THE REQUIREMENTS FOR THE

DEGREE OF MASTER OF SCIENCE

DEPARTMENT OF GEOMATICS ENGINEERING

CALGARY, ALBERTA

MARCH, 1995

THE UNIVERSITY OF CALGARY

FACULTY OF GRADUATE STUDIES

The undersigned certify that they have read, and recommend to the Faculty of Graduate Studies for acceptance, a thesis entitled "A Low-Cost Integrated INS/GPS System" submitted by Gengsheng Zhang in partial fulfillment of the requirements for the degree of Master of Science.

Dr. K.P. Schwarz K.P. Schwarz

Supervisor, Department of Geomatics Engineering

Dr. M.E. Cannon

Department of Geomatics Engineering

Dr. M.J. Collins Michael Lee Collins

Department of Geomatics Engineering

Dr. E.P. Nowicki

Department of Electrical and Computer Engineering

13.4.95

Date

ABSTRACT

This thesis describes the development of a low-cost integrated INS/GPS system for airborne resource mapping applications. The prototype system integrates the MotionPak, a low-cost inertial sensor assembly, with differential GPS as well as a GPS multi-antenna system. The analogue outputs of the MotionPak are converted into digital data and compensated. A centralized Kalman filter approach is developed to combine the MotionPak measurements with double differenced GPS pseudorange and Doppler observations as well as heading measurements of a GPS multi-antenna system. The system design is verified by tests. Test results show that the integration of the MotionPak with differential GPS can meet the accuracy requirements of airborne resource mapping applications except in heading, and all accuracy requirements can be satisfied by integrating the MotionPak with differential GPS and a GPS dual-antenna system.

ACKNOWLEDGEMENTS

I would like to express my deepest gratitude to my supervisor, Dr. Klaus-Peter Schwarz, for his continuous support, encouragement and guidance throughout my graduate studies. Dr. M.E. Cannon, Dr. M.J. Collins and Dr. E.P. Nowicki are also thanked for their valuable advice on the thesis.

Special thanks are extended to many of my teachers and colleagues at Northwestern Polytechnical University, China, but particularly, to Professor Jixiang Yu, supervisor of my first M.Sc degree, for his continuous guidance and great encouragement during the eight years I worked with him.

Thanks go to Mr. Z. Liu for his help in data acquisition software development and data collection, and Dr. A. El-Mowafy for his help in data collection and providing attitude results of the GPS multi-antenna system. I also wish to thank Dr. M. Wei, Mr. Y. Li, Q. Zhang, Z. Li, N. El-Sheimy and V. Argeseanu for many fruitful discussions and valuable assistance during system development.

Financial support for this research was obtained through a Strategic Grant and an Operating Grant of the Natural Sciences and Engineering Research Council of Canada (NSERC). This is gratefully acknowledged.

Finally, my deepest thanks goes to my wife, Yingfang Zhang, and our son, Hongliang Zhang, for sharing the troubles and triumphs of a foreign graduate student.

TABLE OF CONTENTS

LIST OF TABLES

Table

LIST OF FIGURES

Figure

NOTATION

A CONVENTIONS

A.1 Matrices are uppercase and bold

A.2 Vectors are lowercase and bold

A.3 Transformation Matrices between two coordinate systems are specified by a subscript and a superscript, e.g. $\mathbf{C}_b^l$ indicates the transformation matrix from the body frame to the local-level frame.

A.4 Vector means coordinates of a vector. A superscript will be used if necessary to indicate the particular coordinate frame in which the vector is represented.

A.5 The operators are defined as:

(-)	pre-measurement update value
(+)	post-measurement update value
$\dot{a}$	derivation with respect to time
$\mathbf{A}^T$	matrix transpose
$\mathbf{A}^{-1}$	matrix inverse
$\hat{\mathbf{x}}$	estimated value
δ	error
Δ	single difference between receivers
∇	single difference between satellites

B COORDINATE FRAMES

B.1 Body Frame (b-frame)

origin: at the mass center of the vehicle

x-axis: pointing to the right-handed side when looking forward

y-axis: pointing forward along the longitudinal axis of the vehicle

z-axis: completes a right-handed system

B.2 Earth-Fixed Frame (e-frame)

origin: at the mass center of the earth

x-axis: towards the mean Greenwich meridian, in the equatorial plane

y-axis: completes a right-handed system

z-axis: mean rotation axis of the earth

B.3 Operational Inertial Frame (i-frame)

origin: at the mass center of the earth

x-axis: towards the mean vernal equinox

y-axis: completes a right-handed system

z-axis: coincident with the mean rotation axis of the earth

B.4 Local-Level Frame (l-frame)

origin: at topocenter

x-axis: ellipsoidal east

y-axis: ellipsoidal north

z-axis: pointing up along the ellipsoidal normal

C SYMBOLS

A	accelerometer output
b	accelerometer bias
c	speed of light
d	gyro bias
f	specific force
F	dynamics matrix
g	gravity
I	identity matrix
K	Kalman filter gain matrix
P	covariance matrix
p	pseudorange
x	system state vector
V	velocity
dT	receiver clock error
dt	satellite clock error
Φ	carrier phase
Φ	transition matrix
γ	normal gravity
φ	roll
θ	pitch
ψ	yaw
ω_e	mean rotation rate of the Earth
ϕ	geographic latitude
λ	geographic longitude
ε	misalignment

D ACRONYMS

C/A Code	Clear/Acquisition Code
DC	Direct Current
GPS	Global Positioning System
IMU	Inertial Measurement Unit
INS	Inertial Navigation System
ISA	Inertial Sensor Assembly
MTBF	Mean Time Between Failures
P Code	Precise Code
PDOP	Position Dilution of Precision
PPS	Pulse Per Second
RMS	Root Mean Square
VDC	Direct-Current Volts

CHAPTER 1

INTRODUCTION

1.1 BACKGROUND AND OBJECTIVE

In applications which require attitude as well as position and velocity, such as airborne photogrammetry and remote sensing, the integration of an Inertial Navigation System (INS) with Global Positioning System (GPS) receivers offers significant advantages. INS can provide high data rate attitude, position and velocity with excellent short-term stability, but its position and velocity deteriorate quickly with time due to gyro drifts and accelerometer biases. GPS, on the other hand, can provide position and velocity with excellent long-term accuracy. Attitude determination is also possible with a GPS multi-antenna system. GPS measurements, however, are currently restricted to data rates between 0.1 to 10 Hz, which means GPS can not sense dynamic changes rapidly enough for many of the intended applications. Other problems with GPS are that the results are too noisy and that the trajectory solution may be interrupted if less than four satellites are observed. By optimally integrating the data streams from INS and GPS, use can be made of the strength of each system. That means that high data rate attitude, position and velocity with the superior short-term error behaviour of the INS as well as the superior long-term error behaviour of GPS can be obtained.

Many integrated INS/GPS systems have been developed for a wide range of applications, e.g. Brown et al. (1992), Cannon (1991), Cox (1978), Kwan et al. (1993), Lapucha (1990), Meyer-Hilberg (1994), Nelthropp et al. (1992), Tazartes and Mark (1988), Upadhyay et al. (1994), and Woolven et al. (1994). Traditionally, navigation-grade inertial navigation systems are used in the integration. Because these inertial navigation systems are designed for stand-alone navigation, they are expensive, usually over US$100,000. The use of integrated INS/GPS systems has thus been seriously limited by the high costs. For applications which need only moderate accuracy, low cost is an important constraint and a low-cost integrated INS/GPS system is highly desirable. For example, applications such as airborne resource mapping with a multi-spectral scanner require attitude accuracies of 0.3 to 0.5 degrees root mean square (RMS) error and position accuracies of 2 to 5 metres (RMS), This information is needed at 20-30 Hz (Schwarz et al., 1993 and 1994a).

The high accuracy of GPS has redefined the traditional role of inertial navigation systems and has redirected attention to their uses as components of integrated navigation systems. Thus, low-cost integrated INS/GPS systems have become an attractive option. In the integrated INS/GPS system, GPS information can ensure the long-term navigation performance and improve the performance capability achievable with INS significantly since the velocity errors, position errors, attitude errors and inertial sensor errors are continuously estimated from GPS updates. The long-term position accuracy of the integrated system is almost independent of INS and only the short-term performance of the INS is needed for the integration. As long as adequate error modelling and calibration is performed, even a low-cost, low-quality inertial sensor assembly can be used to develop an integrated INS/GPS system to provide a navigation solution for applications that only require moderate accuracy.

Companies, such as Litton, Rockwell and Systron Donner, have recognized the need for low-cost, small-size and lightweight inertial sensors and are in the process of developing solid-state inertial sensors with post-compensation accuracy of about 10 deg/h for gyro drifts and 1 mg ($9.81\times10^{-3}ms^{-2} \approx$ 1Gal) for accelerometer biases. Advances in the technology of GPS receivers and solid-state inertial sensors have continued to improve the performance while reducing size and cost to the point where a low-cost integrated INS/GPS system becomes viable and attractive for many applications. Recently, companies and universities have begun to design and develop low-cost integrated systems for different applications, e.g. Bader (1993), Baumker and Mattissek (1992), McMillan and Arden (1994b), Schwarz and Zhang (1994b), Shale and Bader (1994), Silva and Murray (1994), and Vieweg (1994). The objective of this research is to develop a low-cost integrated INS/GPS system which can provide an affordable, operationally effective reference for airborne resource mapping applications.

1.2 THESIS OUTLINE

The research documented in this thesis is presented in eight chapters.

In chapter 2, the MotionPak, a low-cost inertial sensor assembly, and its analogue-to-digital conversion design are described. The static outputs of the MotionPak are presented and analyzed.

In chapter 3, methods of compensating the MotionPak inertial sensor errors are developed. The algorithm of strapdown inertial navigation in the earth-fixed frame is discussed and the navigation capability of the MotionPak is analyzed.

In chapter 4, GPS measurements used in the low-cost integrated INS/GPS system are reviewed and their observation equations are given.

In chapter 5, hardware and software design of the low-cost integrated INS/GPS system are presented in detail.

In chapter 6, tests conducted to verify the system design, tune the Kalman filter and evaluate the system accuracy achievable are described. Test results using double differenced pseudorange and Doppler observations are given and analyzed.

In Chapter 7, heading measurements from a GPS dual-antenna system are added to the integration. Test results are analyzed and compared to those of the integration in Chapter 6.

In chapter 8, conclusions of this research are drawn. Some recommendations for further research and system development are given.

CHAPTER 2

LOW-COST INERTIAL MEASUREMENT UNIT

A key element in developing a low-cost integrated INS/GPS system is the design and testing of a low-cost inertial measurement unit (IMU) which has sufficient accuracy to meet the needs of the intended applications. Advances in the technology of low-cost solid-state inertial sensors have brought the price of a full inertial sensor assembly (ISA) down to about US$10,000. One of these inertial sensor assemblies, Systron Donner's MotionPak, has been used to develop the low-cost inertial measurement unit for this research. This chapter describes this inertial sensor assembly in detail. The design of the data sampling system is then discussed and static data from the MotionPak is analyzed.

2.1 LOW-COST INERTIAL SENSOR ASSEMBLY

The inertial measurement unit used in the prototype low-cost integrated INS/GPS system is based on the MotionPak, an inertial sensor assembly manufactured by the Systron Donner Inertial Division of BEI Electronics Company. The MotionPak has three gyros, three accelerometers and one temperature sensor, sealed in a compact, rugged package with internal regulation and signal conditioning electronics. It is directly powered by a DC battery and provides three analogue DC angular rate signal outputs, three analogue DC

acceleration signal outputs and one analogue DC temperature output. The MotionPak is suitable for a wide variety of applications that require high reliability, small size, light weight and low cost. Table 2.1 summarizes its characteristics (BEI Electronics Company, 1993).

Table 2.1 Summary of MotionPak Characteristics

Physical	
Weight	0.82kg
Size	$7.6x7.6x9.0\,cm^3$
Input Voltage	±12.8 to ±18.0 VDC
Input Power	< 3.3 watts
Mounting	4 mounting bolts
Operating Range	
Angular Rate	± 50 deg/s
Linear Acceleration	± 2g
Reliability	
Operating Life	10 years
MTBF	> 100000 hours
Environmental	
Operating Temperature	-40°C to +80°C
Storage Temperature	-55°C to +100°C
Vibration Survival	10g rms, 20 to 2000 Hz random
Vibration Operating	4g rms, 20 to 2000 Hz random
Shock Survival	100g, 2 milliseconds
Start-up Time	< 1 second

The MotionPak utilizes small, batch-fabricated quartz inertial sensors to achieve low cost and small size. The angular rates are sensed using vibrating quartz tuning forks, while linear accelerations are sensed using servoed quartz flexture accelerometers.

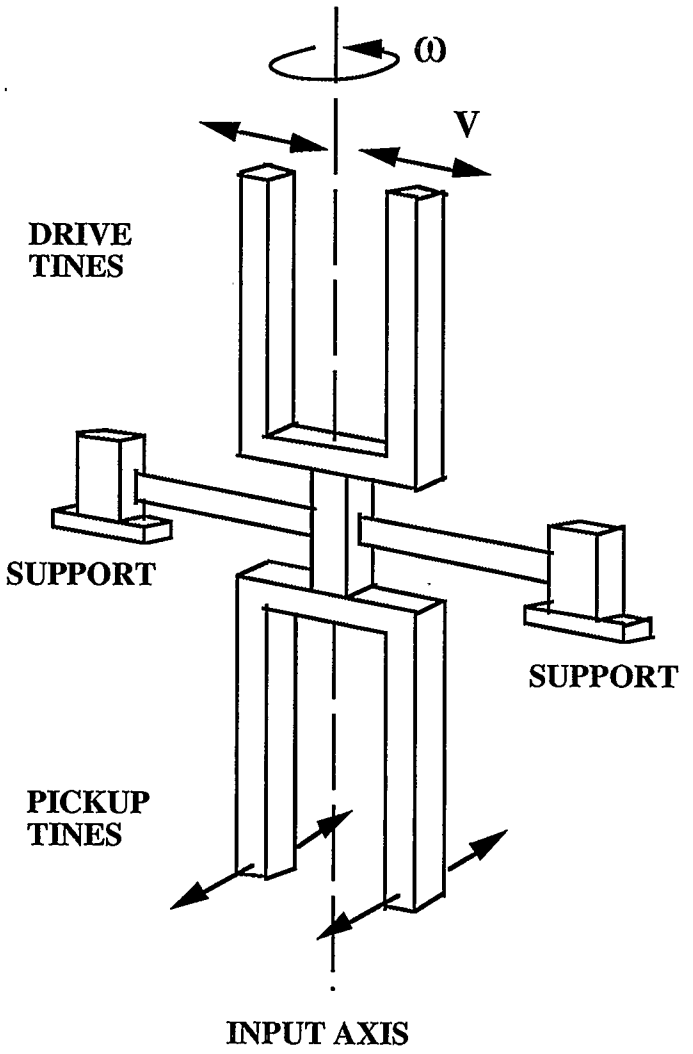

Figure 2.1 Block Diagram of the Vibrating Quartz Tuning Fork

The vibrating quartz tuning fork shown in Figure 2.1 senses angular rates by acting as a Coriolis sensor. This sensor consists of a pair of tuning forks, support flexures and frame all fabricated from a wafer of single-crystal piezo-electric quartz. The piezo-electric drive

tines are activated by an oscillator at a precise amplitude, causing the tines to move toward and away from each other at a high frequency. Each tine will have a Coriolis force of $F = 2m\omega \times V$ acting on it , where the tine mass is m, instantaneous linear radial velocity is V and the input angular rate is ω. This force is perpendicular to both the input rate and the instantaneous radial velocity. Since each tine is moving in the opposite direction to the other, the forces are perpendicular to the plane of the fork assembly at each of the tines and in opposite directions, yielding a torque proportional to the input angular velocity. Since the radial linear velocity is sinusoidal, the torque produced is also sinusoidal at the frequency of the drive tines, and in-phase with the radial velocity of the tine. The pickup tines respond to the oscillating torque by moving in and out of the plane, causing output signals to be produced by the pickup amplifier. After amplification, those signals are demodulated by the synchronous demodulator. Thus, the output is a DC signal proportional to the angular rate. The input rate sensitivity is only about the axis of symmetry of the fork assembly, since that is the only motion which will, by Coriolis sensing, produce an oscillating torque at the frequency of the drive tines. The output signals are demodulated with respect to the drive tine oscillator signal since the rate signal is directly in-phase with the oscillator signal. The output signal of the MotionPak is a DC signal directly proportional to the input rate, reversing sign with the reversal of the input rate since the oscillating torque produced by Coriolis reverse phase when the input rate reverses.

In the servoed quartz flexture accelerometer, the deflection of a quartz beam under acceleration is measured and amplified, then fed back to restore the beam to its original position. The feedback current is proportional to acceleration and is used to produce a high level acceleration output signal.

Table 2.2 gives the design specifications of the MotionPak. Due to the low cost requirement, the quality of the MotionPak inertial sensors is very poor.

Table 2.2 Specifications of the MotionPak

Gyro	
Bandwidth	> 60 Hz
Linearity	< 0.05% of full range
Resolution	< 0.002 deg/s
g sensitivity	< 0.02 deg/s/g
Scale Factor Calibration	< 1.0% of value
Scale Factor T.C.	< 0.03%/°C
bias	< 1.8 deg/s
Bias Short Term	< 0.005 deg/s - 100 second at constant temperature
Bias Long Term	< 0.2 deg/s - one year at constant temperature
Misalignment	< 1.0 deg
Noise	< 0.03 deg/s/$\sqrt{\text{Hz}}$
Accelerometer	
Bandwidth	> 300 Hz
Zero g Bias	< ±12.5mg
Bias T.C.	< 0.1mg/°C
Scale Factor T.C	< 0.01%/°C
Misalignment	< ±1.0 deg

2.2 DATA ACQUISITION OF THE MOTIONPAK

In the low-cost integrated INS/GPS system, the seven analogue outputs of the MotionPak are digitized to produce a high quality digital representation by using AT-MIO-16X, a data acquisition board manufactured by National Instruments.

The AT-MIO-16X is a software-configurable, high performance analogue, digital, and timing I/O board, and can be directly plugged into all standard PCs. With the self-calibration function, high-speed settling to 16 bits and low noise, the board can perform high accuracy analogue-to-digital conversions. Table 2.3 summarizes the main characteristics of its analogue input (National Instruments, 1993).

Table 2.3 Characteristics of AT-MIO-16X Analogue Input

Input channel number	16 single-ended or 8 differential
Analogue resolution	16-bit
Analogue input range	± 10 V or 0 to +10 V, software-selectable
Gains	1, 2, 5, 10, 20, 50, and 100, software-selectable
Maximum sampling rate	100 ksample/s
Relative accuracy	±1LSB maximum

The AT-MIO-16X offers three different input modes, nonreferenced single-ended input, referenced single-ended input, and differential input. Since the seven analogue output signals of the MotionPak are low level and have their own return signals, the MotionPak outputs are connected to the AT-MIO-16X board using the differential analogue input configuration. That means the difference between each signal and its reference is measured. The difference input configuration reduces pick-up noise and performs high accuracy analogue-to-digital conversion, see Dally et al. (1993) and Morrison (1984).

In order to achieve the highest possible conversion accuracy, the analogue angular rate outputs from the MotionPak are amplified. Since the AT-MIO-16X can only accept voltage

analogue inputs, the current analogue output from the temperature sensor is converted into voltage before connecting to the board.

The MotionPak outputs are connected to the AT-MIO-16X board through a cable, so only the MotionPak needs to be mounted onto the instrument or platform whose position and attitude needs to be measured. Since the MotionPak is small and light, it can be directly mounted onto any instrument or platform which contains the primary sensor to be oriented. Larger and heavier inertial systems can usually not be installed in this way and attitude errors are introduced by transferring the attitude from an inertial system to the instrument or platform.

In order to obtain the maximum measurement accuracy, the seven analogue outputs of the MotionPak are sampled at 640 Hz.

A major problem for the integrated INS/GPS system is the synchronization of measurements from the MotionPak and the GPS. In the low-cost integrated INS/GPS system, the synchronization is realized by using the GPS pulse per second (PPS) signal to trigger the MotionPak output sampling. This will be discussed in Chapter 3.

2.3 MOTIONPAK INERTIAL SENSOR PERFORMANCE

Static tests of the MotionPak have been conducted in the laboratory to evaluate its inertial sensor performance. Figures 2.2 and 2.3 are the static outputs of the MotionPak gyros and accelerometers sampled at 640 Hz. They show standard deviations of 1 to 2 mg for the accelerometer outputs and 0.19 to 0.34 deg/s for the gyro outputs.

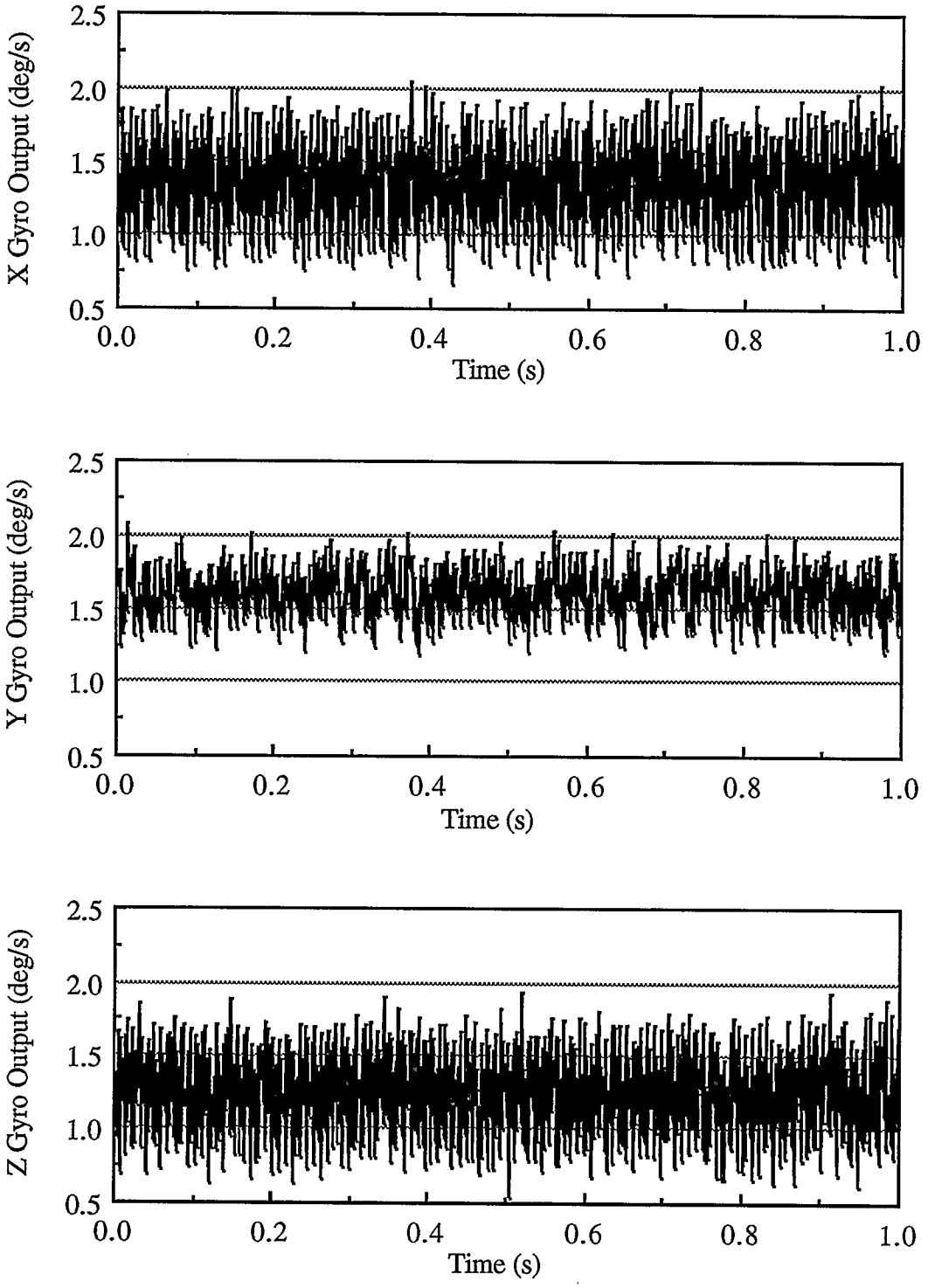

Figure 2.2 Static MotionPak Gyro Outputs

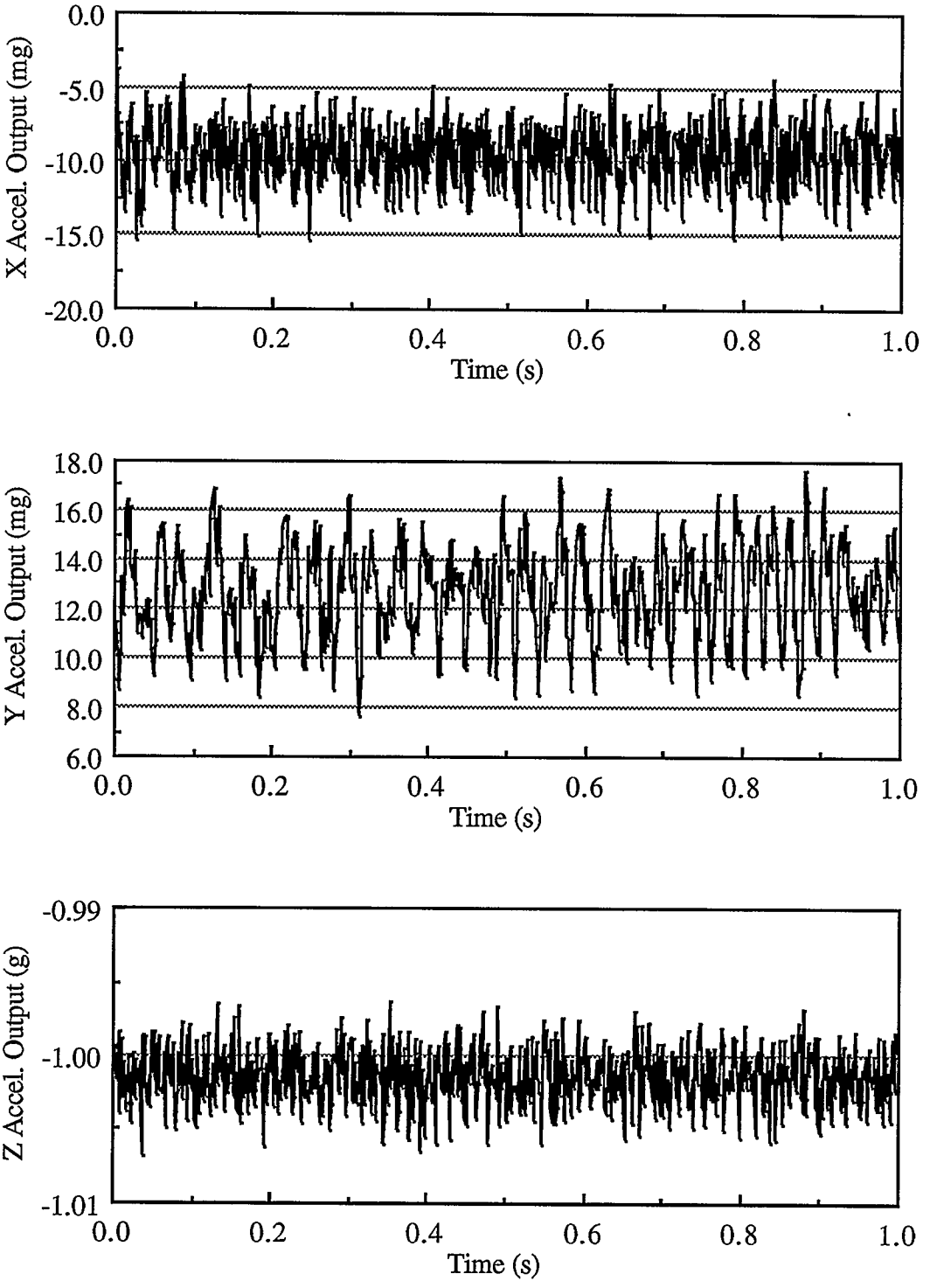

Figure 2.3 Static MotionPak Accelerometer Outputs

In order to analyze the characteristics of the MotionPak inertial sensors, an analysis of the amplitude spectrum for these data is shown in Figures 2.4 and 2.5. The static outputs of the MotionPak gyros and accelerometers have been sampled at 640 Hz. The results show that the accelerometer outputs are quite noisy and the gyro outputs have large peaks at about 260 Hz. They are 0.4 deg/s, 0.2 deg/s, and 0.3 deg/s for X, Y and Z gyro, respectively. The large peaks are caused by the tine motion inside the vibrating quartz tuning forks. The high frequency components in gyro and accelerometer outputs are cut off by a low-pass filter, see Chapter 3.

Because the MotionPak does not have an internal temperature control device, its internal temperature changes during operation, see Figure 2.6. In this figure, the temperature is represented by the voltage value of the temperature sensor output since its scale factor is not provided by the manufacturer. The change of the MotionPak internal temperature induces significant gyro drifts and accelerometer biases, see Figures 2.7 and 2.8. These temperature effects have to be compensated before the navigation solution is computed.

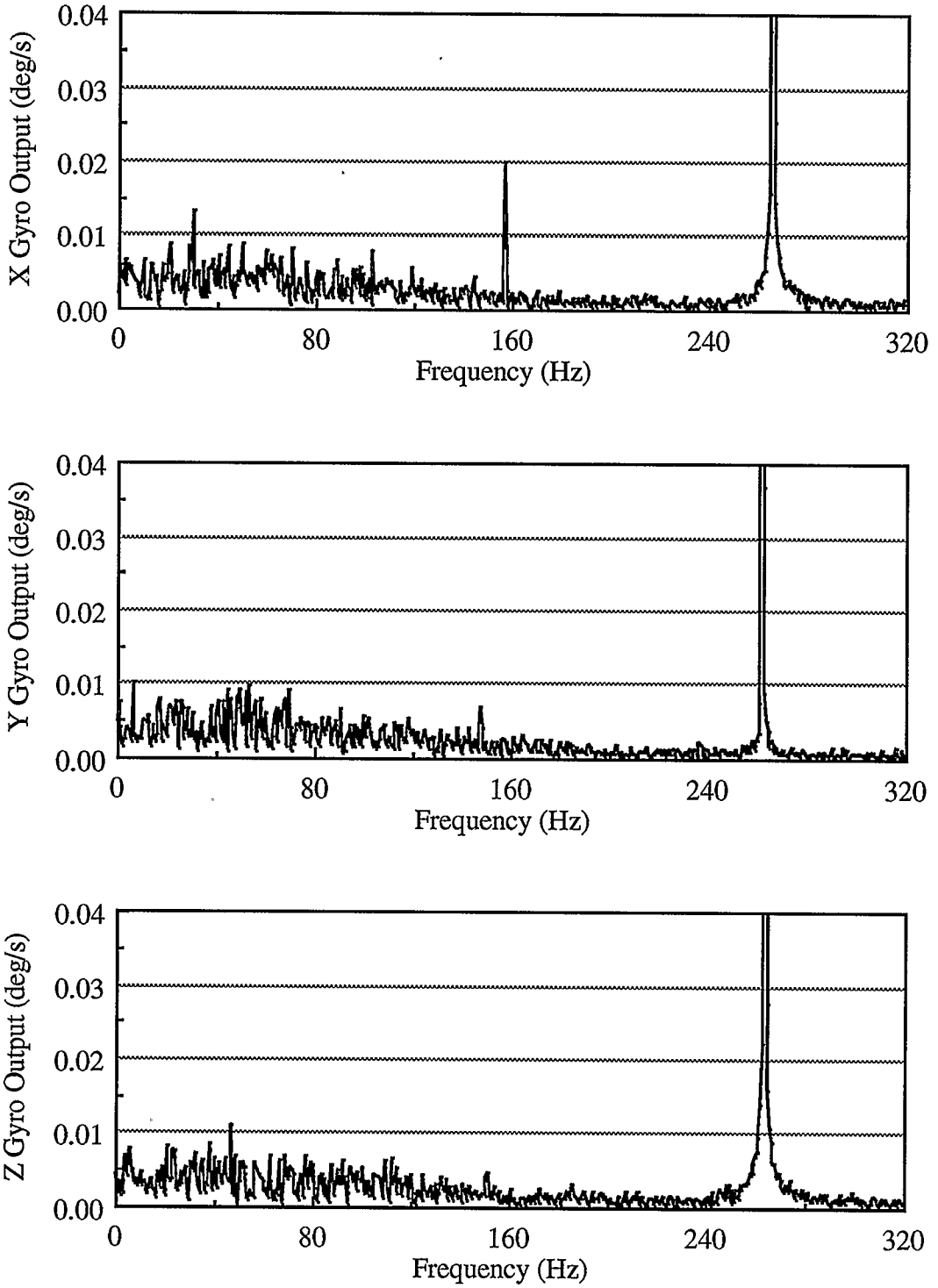

Figure 2.4 Amplitude Spectrum of Static MotionPak Gyro Outputs

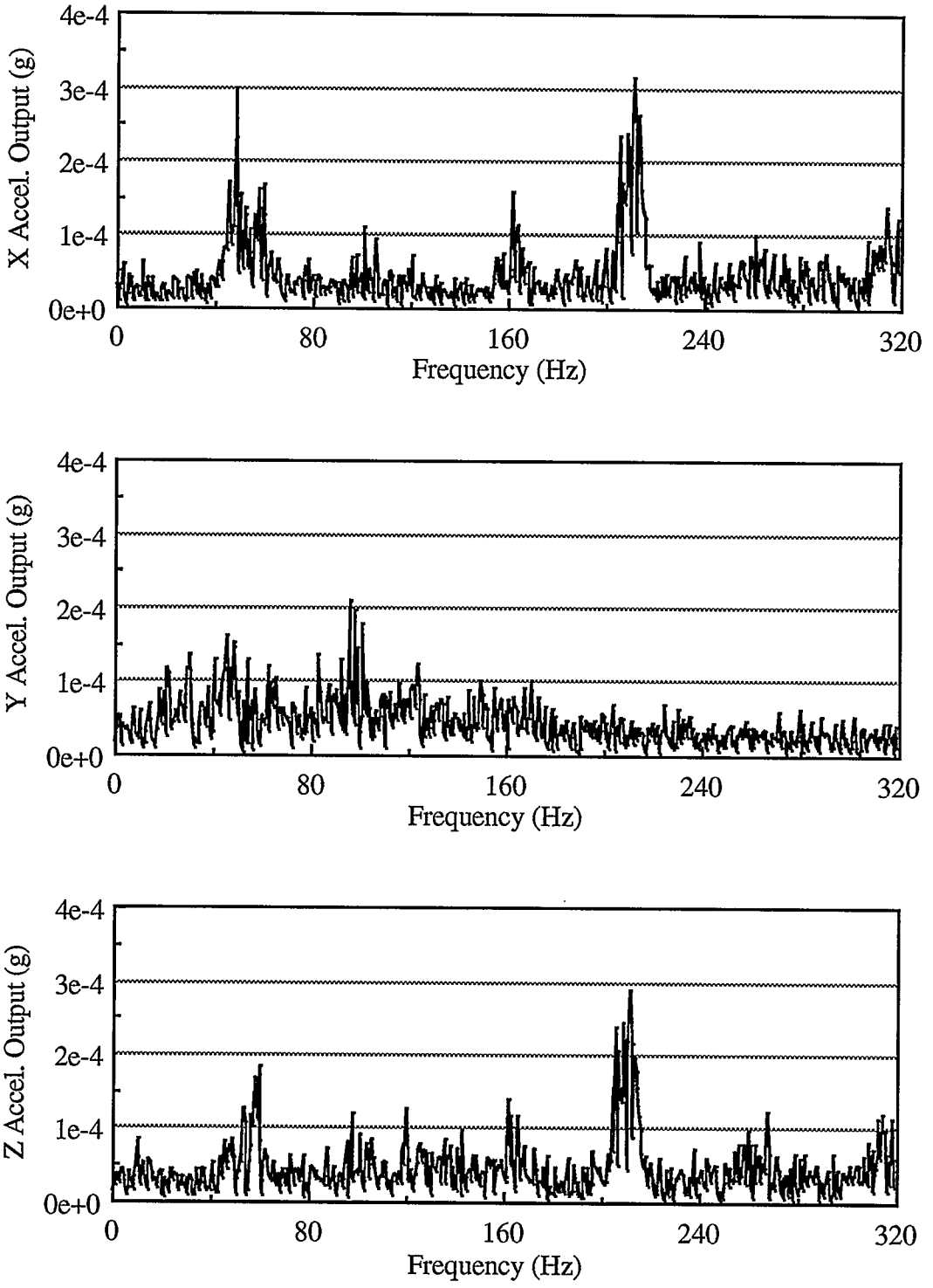

Figure 2.5 Amplitude Spectrum of Static Accelerometer Outputs

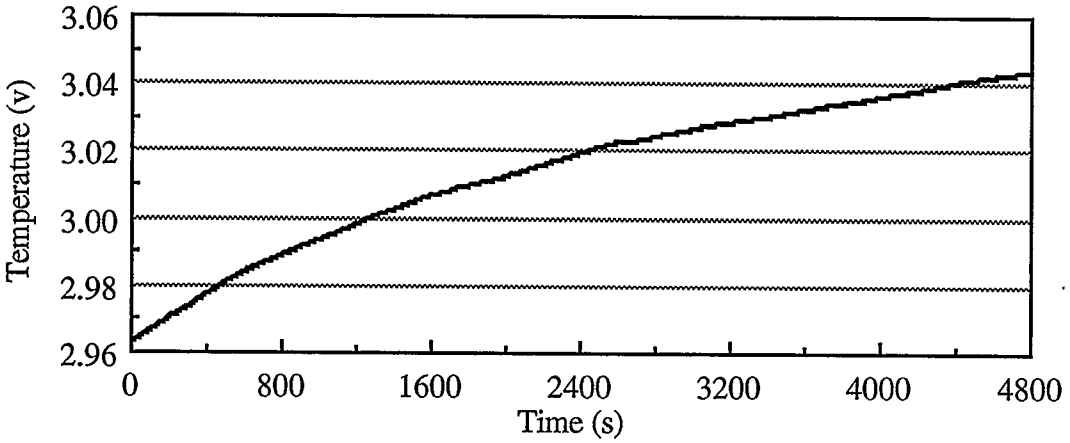

Figure 2.6 MotionPak Internal Temperature Change During Operation

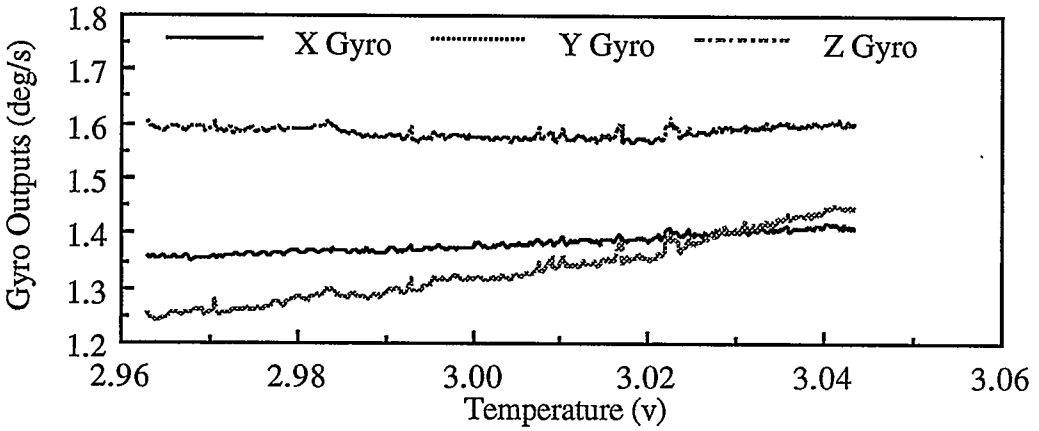

Figure 2.7 Temperature Effects on MotionPak Gyro Outputs

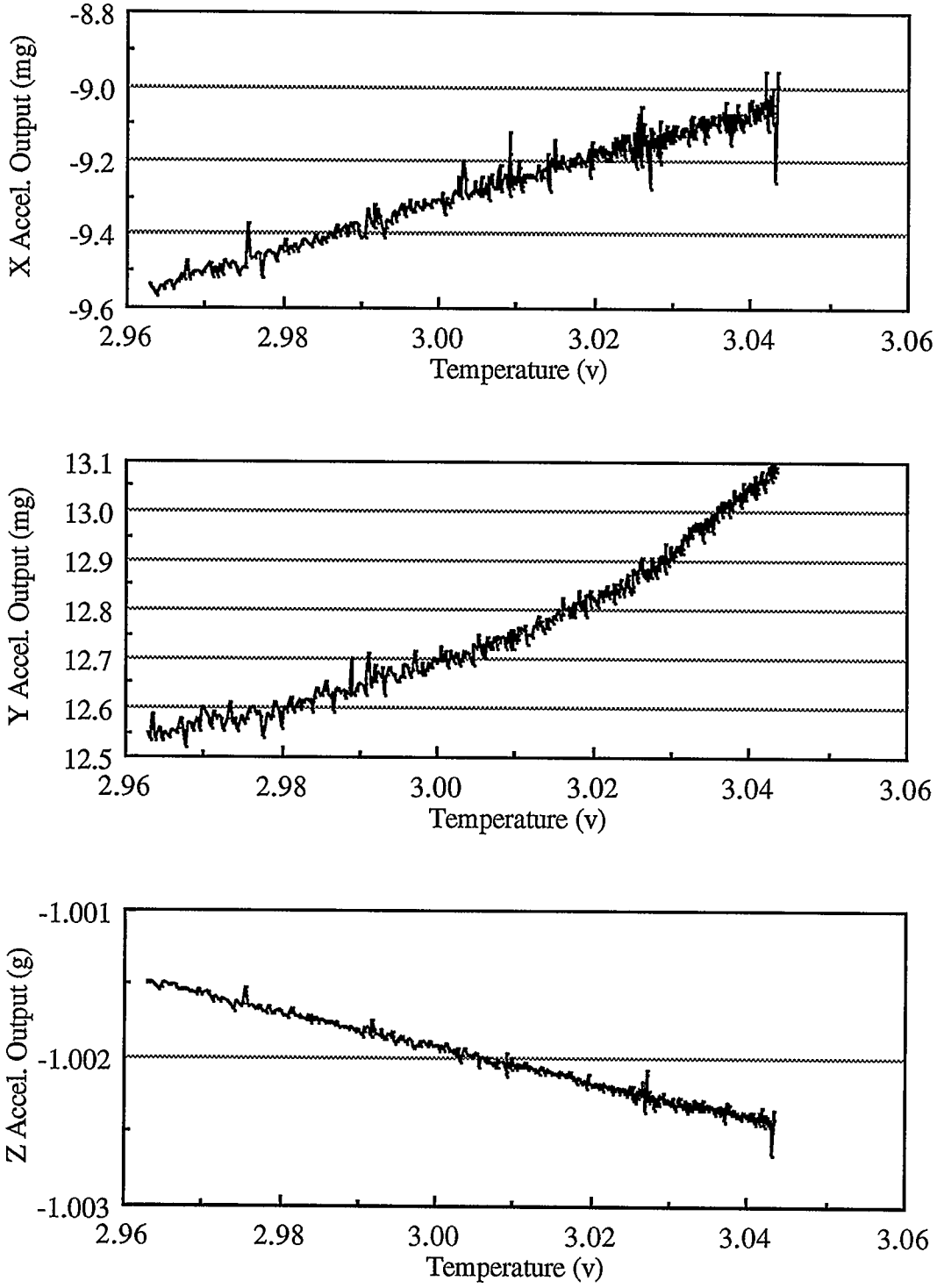

Figure 2.8 Temperature Effects on MotionPak Accelerometer Outputs

CHAPTER 3

STRAPDOWN INERTIAL NAVIGATION

The measurements of the MotionPak inertial sensors are used to compute the inertial navigation solution. This chapter discusses the strapdown inertial navigation algorithm for the MotionPak. First, all coordinate frames involved in the strapdown inertial navigation algorithm are defined. Then the inertial sensor error compensation is discussed. After presenting the algorithm, static navigation results of the MotionPak are given.

3.1 COORDINATE FRAMES

In order to develop the strapdown navigation algorithm, the coordinate frames involved in the algorithm are defined first.

3.1.1 Inertial Frame (i-frame)

The mean right-ascension system with geocentric origin is chosen as the operational inertial frame. The definition of this inertial frame is as follows:

origin: at the mass center of the earth;

x-axis: towards the mean vernal equinox;

y-axis: completes a right-handed system.

z-axis: coincident with the mean rotation axis of the earth.

3.1.2 Earth-Fixed Frame (e-frame)

The earth-fixed frame is defined as follows:

origin: at the mass center of the earth;

x-axis: towards the mean Greenwich meridian, in the equatorial plane;

y-axis: completes a right-handed system.

z-axis: mean axis of rotation of the Earth;

Due to the above definition, the rotation of the earth-fixed frame with respect to the inertial frame is constant and given by

$$\omega_{ie}^{e} = \begin{bmatrix} 0 \\ 0 \\ \omega_e \end{bmatrix} = \begin{bmatrix} 0 \\ 0 \\ 7.2921158 \times 10^{-5} \text{rad/s} \end{bmatrix} \tag{3.1}$$

3.1.3 Local-Level Frame (l-frame)

The local-level frame refers to the chosen reference ellipsoid and is a coordinate frame similar to the local geodetic frame. The definition of the local-level frame is as follows:

origin: at topocenter;

x-axis: ellipsoidal east (also denoted as E axis);

y-axis: ellipsoidal north (also denoted as N axis);

z-axis: pointing up along the ellipsoidal normal (also denoted as U axis).

The transformation matrix from the local-level frame to the earth-fixed frame is

$$C_I^e = \begin{bmatrix} -\sin\lambda & -\sin\phi\cos\lambda & \cos\phi\cos\lambda \\ \cos\lambda & -\sin\phi\sin\lambda & \cos\phi\sin\lambda \\ 0 & \cos\phi & \sin\phi \end{bmatrix} \tag{3.2}$$

where ϕ and λ are the geographic latitude and longitude of the origin of the local-level frame respectively.

3.1.4 Body Frame (b-frame)

The body frame is defined as follows:

origin: at the mass center of the vehicle;

x-axis: pointing to the right-handed side when looking forward;

y-axis: pointing forward along the longitudinal axis of the vehicle;

z-axis: completes a right-handed system.

The transformation matrix from the body frame to the local-level frame is

$$C_b^l = \begin{bmatrix} \cos\psi\cos\varphi - \sin\psi\sin\theta\sin\varphi & -\sin\psi\cos\theta & \cos\psi\sin\varphi + \sin\psi\sin\theta\cos\varphi \\ \sin\psi\cos\varphi + \cos\psi\sin\theta\sin\varphi & \cos\psi\cos\theta & \sin\psi\sin\varphi - \cos\psi\sin\theta\cos\varphi \\ -\cos\theta\sin\varphi & \sin\theta & \cos\theta\cos\varphi \end{bmatrix} \tag{3.3}$$

where φ, θ, ψ are the attitude angles, roll, pitch and yaw of the vehicle, respectively, if the inertial sensor assembly is rigidly installed on the vehicle in such a way that the input axes of the inertial sensors coincide with the axes of the body frame.

3.2 INERTIAL SENSOR ERROR COMPENSATION

In order to achieve maximum performance, the inertial sensor errors must be compensated in strapdown inertial systems. Because the quality of MotionPak inertial sensors is poor,

the compensation of the inertial sensor errors is key to the system design. The accuracy of the compensation will be the main criterion for the system achievable accuracy. Figure 3.1 shows the concept of inertial sensor error compensation implemented in the software of the low-cost integrated INS/GPS system.

3.2.1 Low-Pass Filtering

As shown in Figures 2.4 and 2.5, the amplitude spectrum of the static MotionPak gyro and accelerometer outputs indicate that gyro drifts and accelerometer biases have large high frequency components. These high frequency components will cause large navigation errors and must therefore be removed. Since the useful information on the vehicle angular rate and acceleration is usually low frequency, the high frequency components can be cut off by a low-pass filter. In the integrated INS/GPS system, a third-order Butterworth digital low-pass filter is used for this purpose. For the inertial navigation computation, 64 Hz data are needed. They are obtained by averaging 10 subsequent samples of the filtered 640Hz data, thus obtaining integrated data at 64 Hz.

3.2.2 Temperature Effect Compensation

As shown in Figures 2.7 and 2.8, changes in internal temperature affects gyro drifts and accelerometer biases significantly. The temperature effects on gyro drifts and accelerometer biases have been modelled for each inertial sensor using a curve fitting approach.

3.2.3 Scale Factor Error and Misalignment Compensation

In principle, the input axes of the gyros and accelerometers should be orthogonal and coincide with the axes of the body frame. In fact, however, there are small misalignment angles between the body frame axes and the inertial sensor input axes. The misalignment for each gyro or accelerometer can be described by two small angles, shown in Figure 3.2.

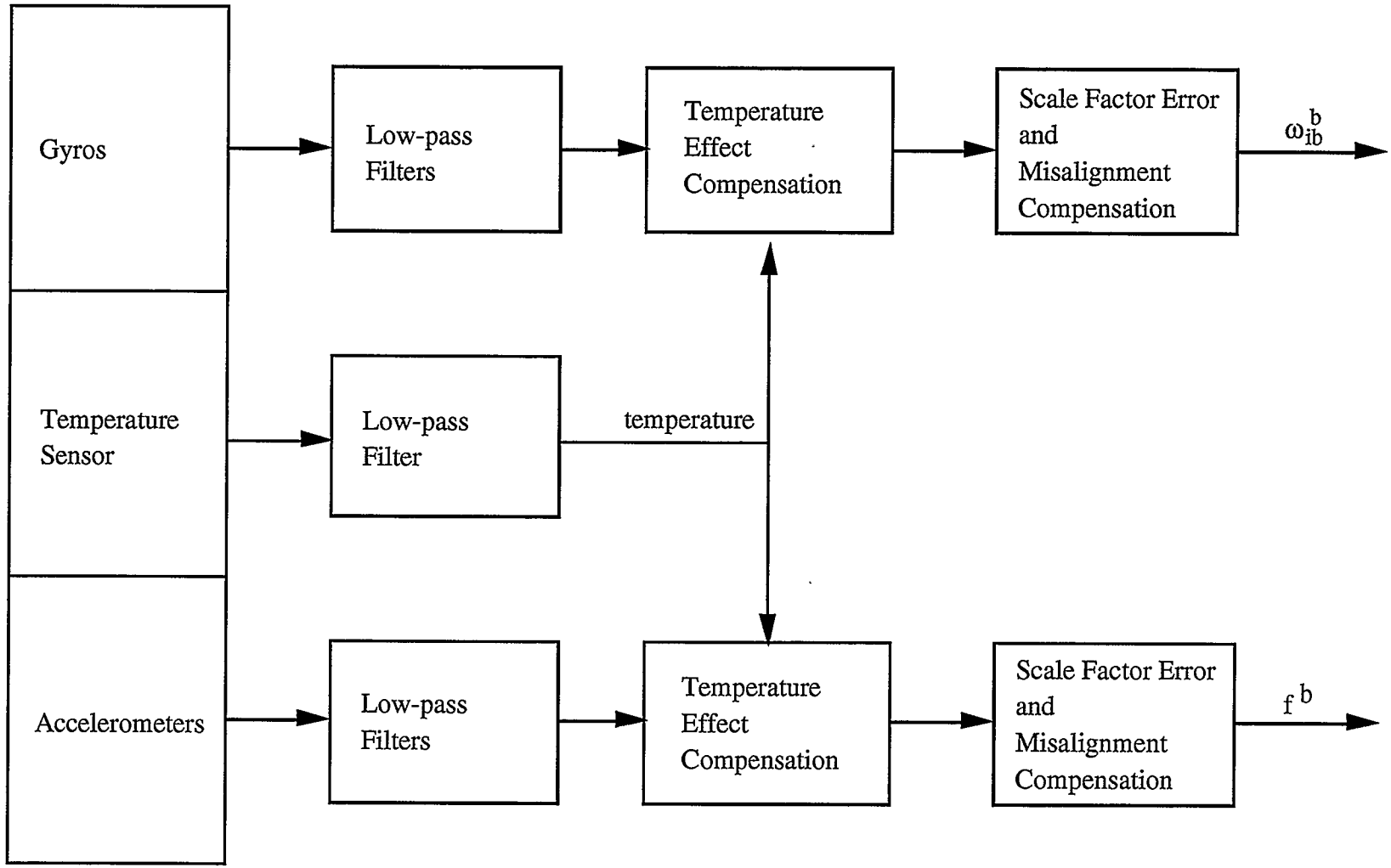

Figure 3.1 Inertial Sensor Error Compensation

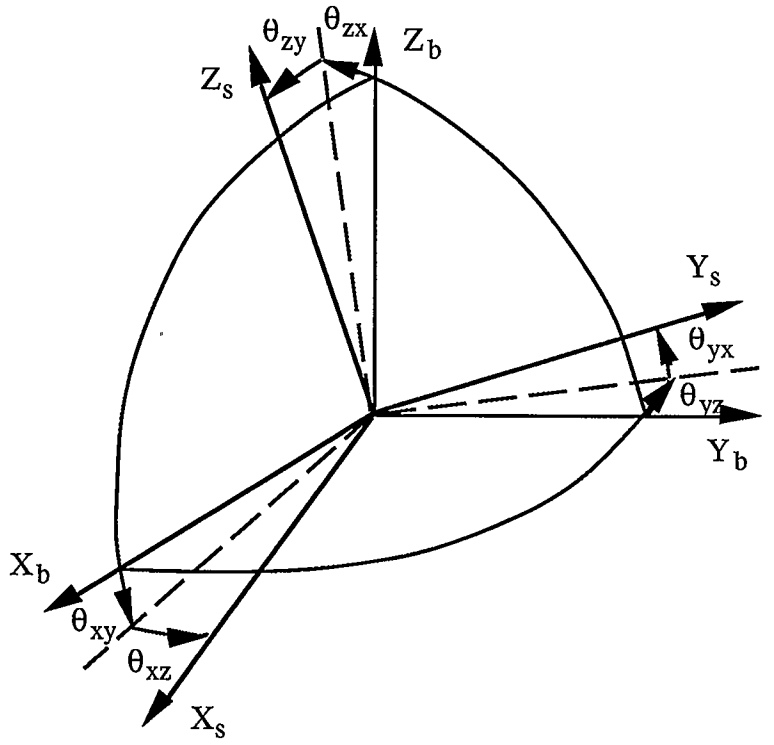

Figure 3.2 Misalignments of the Inertial Sensors

The gyro and accelerometer errors due to the scale factor errors and misalignments are compensated by the following models, see Britting (1971) and Schmidt (1978).

$$\begin{bmatrix} \delta f_x^b \\ \delta f_y^b \\ \delta f_z^b \end{bmatrix} = \begin{bmatrix} \delta K_x^a & \theta_{xz}^a & -\theta_{xy}^a \\ -\theta_{yz}^a & \delta K_y^a & \theta_{yx}^a \\ \theta_{zy}^a & -\theta_{zx}^a & \delta K_z^a \end{bmatrix} \begin{bmatrix} f_x^b \\ f_y^b \\ f_z^b \end{bmatrix} \tag{3.4}$$

$$\begin{bmatrix} \delta \omega_x^b \\ \delta \omega_y^b \\ \delta \omega_z^b \end{bmatrix} = \begin{bmatrix} \delta K_x^g & \theta_{xz}^g & -\theta_{xy}^g \\ -\theta_{yz}^g & \delta K_y^g & \theta_{yx}^g \\ \theta_{zy}^g & -\theta_{zx}^g & \delta K_z^g \end{bmatrix} \begin{bmatrix} \omega_x^b \\ \omega_y^b \\ \omega_z^b \end{bmatrix} \tag{3.5}$$

where X_s, Y_s and Z_s are the sensor input axes, δK_i (i=x, y, z) indicates the scale factor error of sensor i, θ_{ij} (i=x, y, z, j=x, y, z, $i \neq j$) indicates the small misalignment angle, the

superscript a indicates the accelerometer and the superscript g indicates the gyro. Scale factor errors and misalignments are assumed to be constant. After compensation, the accuracies of gyros and accelerometers are at the level of 10 deg/h and 1 mg, respectively.

3.3 MECHANIZATION EQUATIONS IN THE EARTH-FIXED FRAME

The INS mechanization equations are used to compute the navigation solution from the gyro and accelerometer measurements. A strapdown inertial navigation system can be mechanized in different coordinate systems, such as the local-level frame or the earth-fixed frame. In the low-cost integrated INS/GPS system, a strapdown inertial algorithm using the earth-fixed frame has been implemented since it is more efficient in computation and convenient for the integration with GPS. Figure 3.3 illustrates the mechanization equations.

After inertial sensor error compensation, the outputs of the MotionPak are angular rates and linear accelerations in the body frame. In the strapdown inertial algorithm using the earth-fixed frame, the measured angular rates are integrated to update the transformation matrix from the body frame to the earth-fixed frame using the quaternion approach. Then the linear accelerations in the body frame are transformed to the earth-fixed frame to compute velocity and position. For a detailed mathematical formulation of the algorithm, see Wei and Schwarz (1990a) or Schwarz and Wei (1995).

3.4 INITIAL ALIGNMENT

The initial alignment of a strapdown inertial navigation system determines the initial transformation matrix from the body frame to the local-level frame. For a high-accuracy

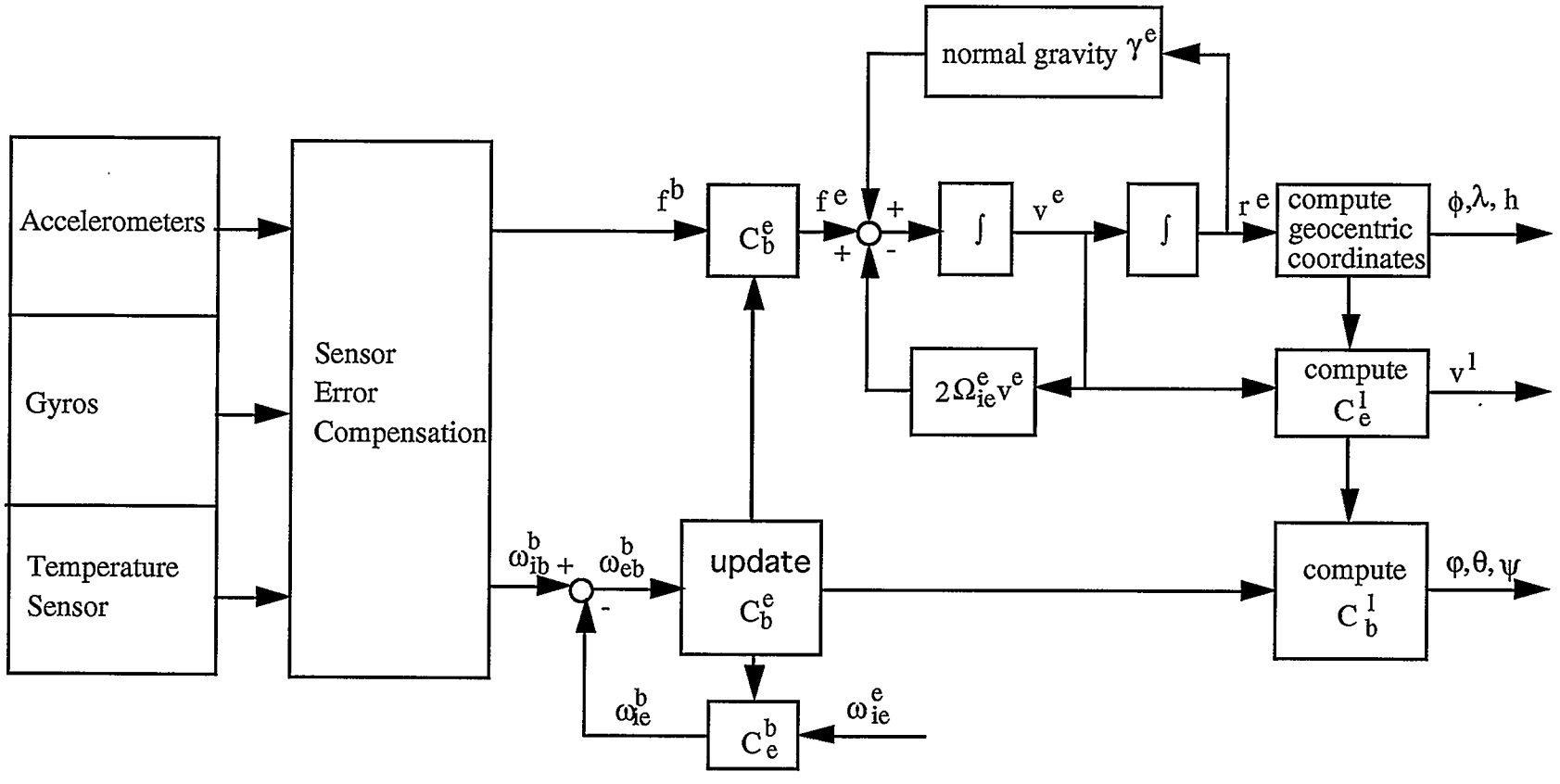

Figure 3.3 Mechanization Equations in the Earth-Fixed Frame

strapdown inertial navigation system, the initial alignment can be done autonomously by measuring the direction of earth rotation and the gravity vector with its sensors (Liu, 1992). For the MotionPak, however, the initial azimuth alignment can only be realized by using external measurements since its gyro drifts are too large. In the low-cost integrated INS/GPS system, the heading is either computed from the GPS velocity or taken from heading measurements of a GPS multi-antenna system, while roll and pitch are determined from the MotionPak accelerometer outputs:

$$\begin{aligned} \varphi &= \tan^{-1}(-A_x / A_z) \\ \theta &= \sin^{-1}(A_y / g) \\ \psi &= -\tan^{-1}(V_E / V_N) \end{aligned} \tag{3.6}$$

where A_x, A_y, A_z are the X, Y, Z accelerometer outputs, g is gravity, V_E and V_N are the GPS velocity components in east and north direction. Equation (3.3) is then used to compute the initial $\mathbf{C}_b^l$. The alignment equation (3.6) for the MotionPak is approximate. The initial alignment errors will be reduced after GPS updates, which will be discussed in Chapter 6. The initial position and velocity are taken from GPS results.

3.5 NAVIGATION RESULTS OF THE MOTIONPAK

Figures 3.4, 3.5 and 3.6 show the increase of MotionPak errors in position, velocity and attitude during two minutes, respectively. These figures indicate that the MotionPak navigation errors increase very fast with time due to the low quality inertial sensors. Thus the MotionPak has only short-term navigation capability. In the low-cost integrated INS/GPS system, GPS measurements will be used to provide the long-term navigation capability.

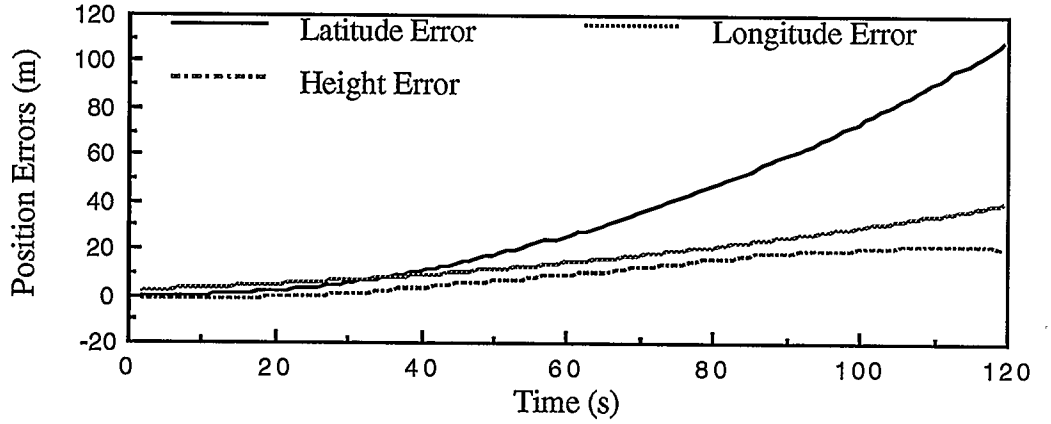

Figure 3.4 Position Errors of the MotionPak

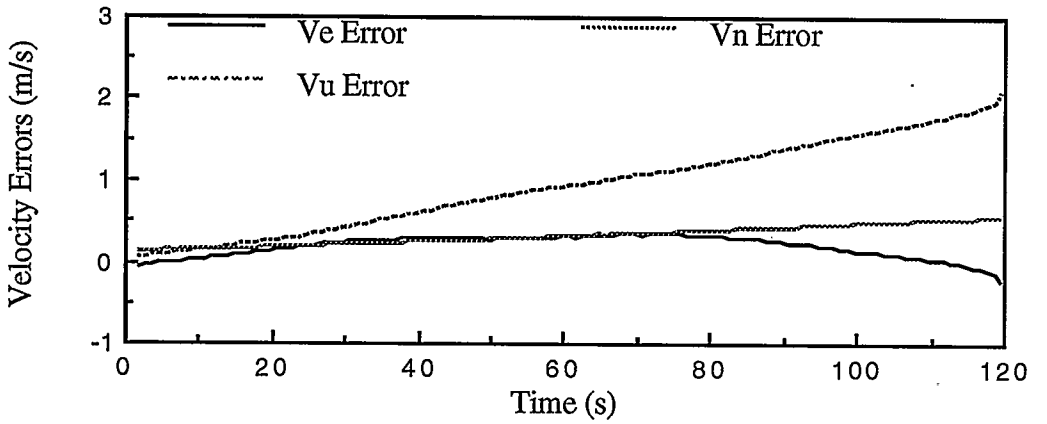

Figure 3.5 Velocity Errors of the MotionPak

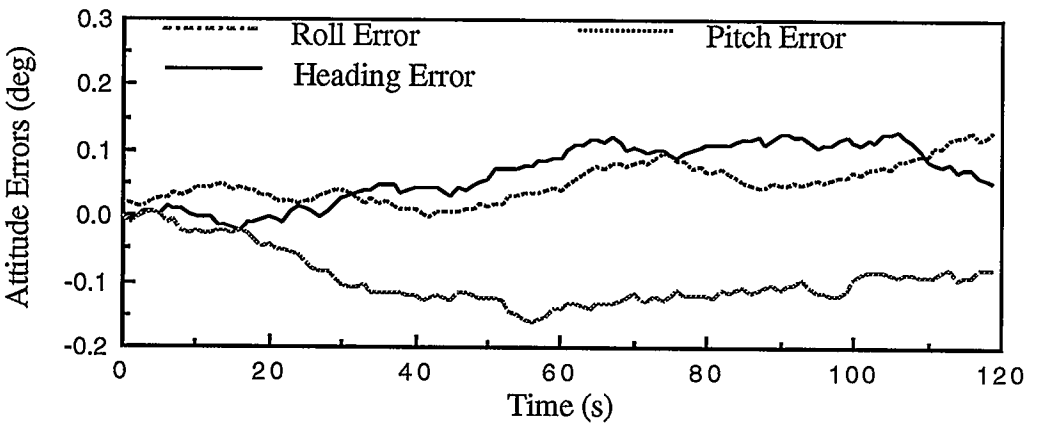

Figure 3.6 Attitude Errors of the MotionPak

CHAPTER 4

GLOBAL POSITIONING SYSTEM

GPS measurements are used to ensure the long-term navigation performance of the low-cost integrated INS/GPS system. This chapter introduces the concept of GPS and its fundamental observations. The method of observation differencing is discussed and the observation equations are given. Finally, three types of GPS measurements, which are double differenced pseudorange observations, double differenced Doppler observations and attitude measurements from a GPS multi-antenna system, are chosen to update the MotionPak based on INS error characteristics and system accuracy requirements.

4.1 GENERAL DESCRIPTION

The Global Positioning System is a satellite-based radionavigation system deployed by the United States Department of Defense. It provides accurate position, velocity and time anywhere on or near the Earth on a continuous basis (Wells et al., 1987). The system is composed of the space segment, the control segment, and the user segment.

The Space Segment consists of 24 GPS satellites at an altitude of about 20,200 km above the Earth's surface. These satellites are distributed in 6 orbital planes in a manner which ensures the visibility of four or more satellites at all locations on the Earth's surface at any

time. Each satellite continuously broadcasts signals on two L-band carrier frequencies, one is the L1 frequency of 1575.42 MHz and the other is the L2 frequency of 1227.60 MHz. Both carrier frequencies are modulated by Pseudo-Random Noise (PRN) codes. The L1 carrier frequency is modulated by both the coarse acquisition (C/A) code and the Precise (P) code while the L2 is only modulated by the P code. The navigation message, which contains information such as ephemerides, satellite clock corrections, satellite status and satellite health, is also modulated on both frequencies.

The Control Segment is composed of five ground-based tracking and control stations. These stations track the satellites, determine satellite orbits, upload the navigation message and control satellites.

The User Segment consists of GPS receivers. GPS receivers use the GPS signals from satellites to determine the user's position, velocity and time.

4.2 GPS OBSERVATIONS

There are three fundamental GPS observations: pseudorange observations, carrier phase observations, and Doppler observations.

4.2.1 Pseudorange Observation

The pseudorange observation is the difference between the signal transmission time at the satellite and reception time at the receiver. It is scaled to units of length using the speed of light. If the receiver clock is fully synchronized to GPS time, the measurement is the range between the user and the satellite. Since the satellite and receiver clocks are usually not

synchronized, the time difference includes the receiver clock error, and the range measured is referred to as the pseudorange. The pseudorange observation equation is given as:

$$p = \rho + c(dt - dT) + d_{ion} + d_{trop} + d\rho + \varepsilon_p \tag{4.1}$$

where p is the pseudorange observation, ρ is the range between the satellite and the receiver, c is the speed of light, dt is the satellite clock error, dT is the receiver clock error, d_{ion} is the error due to the ionosphere, d_{trop} is the error due to the troposphere, $d\rho$ is the satellite orbital error and ε_p is the pseudorange measurement noise. The range between the satellite and the receiver, ρ, has the following form

$$\rho = \sqrt{(x_s - x_r)^2 + (y_s - y_r)^2 + (z_s - z_r)^2} \tag{4.2}$$

where x_s, y_s, z_s are the satellite coordinates computed from the ephemeris, x_r, y_r, z_r are the unknown receiver coordinates. There are four unknowns in Equation (4.1), namely x_r, y_r, z_r and dT, and three parameters to be modeled or eliminated, namely d_{ion}, d_{trop}, $d\rho$. Thus, at least four satellites must be simultaneously observed to obtain a solution.

GPS pseudorange observations can be made on either C/A code or P code. Since civilian users are not given access to the P code, only C/A code pseudorange observations are used in this research.

4.2.2 Carrier Phase Observation

Carrier phase observations are made on a beat phase which is formed by differencing the incoming carrier phase with a reference signal generated in the receiver. Only the fractional part of one cycle can be measured accurately. The phase change is measured by the Doppler count which is the number of accumulated whole cycles. Therefore, the initial number of integer cycles in the carrier phase is unknown. This is called the carrier phase ambiguity.

The carrier phase observation equation is given as:

$$\Phi = \rho + d\rho + c(dt - dT) + \lambda N - d_{ion} + d_{trop} + \varepsilon_{\Phi} \tag{4.3}$$

where Φ is the carrier phase observation, ρ is the range between the satellite and the receiver, λ is the carrier wavelength, N is the unknown integer cycle ambiguity, c is the speed of light, dt is the satellite clock error, dT is the receiver clock error, d_{ion} is the error due to the ionosphere, d_{trop} is the error due to the troposphere, $d\rho$ is the satellite orbital error and ε_{Φ} is the carrier phase measurement noise.

In order to achieve high accuracy positioning by using GPS carrier phase observations, the correct integer carrier phase ambiguity must be resolved.

4.2.3 Doppler Observation

The Doppler observation is the instantaneous phase rate, and it is measured by determining the Doppler frequency shift of the incoming carrier frequency. This frequency shift is caused by the relative motion between the satellite and the receiver, and can be used to determine the user velocity. The Doppler observation equation is:

$$\dot{\Phi} = \dot{\rho} + d\dot{\rho} + c(d\dot{t} - d\dot{T}) - \dot{d}_{ion} + \dot{d}_{trop} + \varepsilon_{\dot{\Phi}} \tag{4.4}$$

where $\dot{\Phi}$ is the Doppler observation, $\dot{\rho}$ is the range rate, $d\dot{t}$ is the satellite clock drift, $d\dot{T}$ is the receiver clock drift, $\dot{d}_{ion}$ is the error due to the ionosphere, $\dot{d}_{trop}$ is the error due to the troposphere, $d\dot{\rho}$ is the satellite orbit drift, $\varepsilon_{\dot{\Phi}}$ is the Doppler measurement noise. The range rate between the satellite and the receiver is computed by the following equation:

$$\dot{\rho} = \frac{(x_s - x_r)(\dot{x}_s - \dot{x}_r) + (y_s - y_r)(\dot{y}_s - \dot{y}_r) + (z_s - z_r)(\dot{z}_s - \dot{z}_r)}{\sqrt{(x_s - x_r)^2 + (y_s - y_r)^2 + (z_s - z_r)^2}} \tag{4.5}$$

where x_s, y_s and z_s are satellite coordinates computed from the ephemeris, $\dot{x}_s$, $\dot{y}_s$ and $\dot{z}_s$ are the components of satellite velocity computed from the ephemeris, x_r, y_r and z_r are the unknown receiver coordinates, $\dot{x}_r$, $\dot{y}_r$ and $\dot{z}_r$ are the unknown components of receiver velocity. Since the Doppler observation does not have the ambiguity, Doppler measurements from at least four satellites can determine the four unknowns in Equation (4.4), $\dot{x}_r$, $\dot{y}_r$, $\dot{z}_r$ and $d\dot{T}$.

4.3 DIFFERENCING OF GPS OBSERVATIONS

Equations (4.1) to (4.4) show that there are several error sources in the GPS fundamental observations. These errors will affect the accuracy of GPS position and velocity results significantly. In order to achieve higher system accuracy, differencing of GPS observations is usually used to remove or reduce a number of these errors.

In order to obtain differenced GPS observations, two GPS receivers have to be used. One located at a known point is the master station, and the other mounted on the vehicle is the remote station. Single differencing between receivers is done by subtracting the observations at the master station from that of the same satellite at the remote station. Double differenced observations can be obtained by further differencing two single differenced observations across two satellites.

Differencing reduces or eliminates many GPS observation errors. Satellite clock errors are canceled by single differencing between receivers while the receiver clock errors are eliminated by single differencing between satellites. Ionospheric, tropospheric and orbital errors are greatly reduced, depending on the distance between receivers.

The double differenced GPS observation equations for pseudorange, carrier phase and Doppler are:

$$\Delta\nabla p = \Delta\nabla\rho + \Delta\nabla d_{ion} + \Delta\nabla d_{trop} + \Delta\nabla d\rho + \varepsilon_{\Delta\nabla p} \tag{4.6}$$

$$\Delta\nabla\Phi = \Delta\nabla\rho + \lambda\Delta\nabla N - \Delta\nabla d_{ion} + \Delta\nabla d_{trop} + \Delta\nabla d\rho + \varepsilon_{\Delta\nabla\Phi} \tag{4.7}$$

$$\Delta\nabla\dot{\Phi} = \Delta\nabla\dot{\rho} - \Delta\nabla\dot{d}_{ion} + \Delta\nabla\dot{d}_{trop} + \Delta\nabla d\dot{\rho} + \varepsilon_{\Delta\nabla\dot{\Phi}} \tag{4.8}$$

where $\Delta\nabla$ is the double difference operator.

The $\Delta\nabla\rho$ and $\Delta\nabla\dot{\rho}$ in Equations (4.6) to (4.8) can be written as:

$$\begin{aligned}\Delta\nabla\rho = &\left(\sqrt{(x_{s1}-x_r)^2+(y_{s1}-y_r)^2+(z_{s1}-z_r)^2}\right.\\ &\left.-\sqrt{(x_{s2}-x_r)^2+(y_{s2}-y_r)^2+(z_{s2}-z_r)^2}\right)\\ -&\left(\sqrt{(x_{s1}-x_m)^2+(y_{s1}-y_m)^2+(z_{s1}-z_m)^2}\right.\\ &\left.-\sqrt{(x_{s2}-x_m)^2+(y_{s2}-y_m)^2+(z_{s2}-z_m)^2}\right)\end{aligned} \tag{4.9}$$

$$\begin{aligned}\Delta\nabla\dot{\rho} = &\left(\frac{(x_{s1}-x_r)(\dot{x}_{s1}-\dot{x}_r)+(y_{s1}-y_r)(\dot{y}_{s1}-\dot{y}_r)+(z_{s1}-z_r)(\dot{z}_{s1}-\dot{z}_r)}{\sqrt{(x_{s1}-x_r)^2+(y_{s1}-y_r)^2+(z_{s1}-z_r)^2}}\right.\\ &\left.-\frac{(x_{s2}-x_r)(\dot{x}_{s2}-\dot{x}_r)+(y_{s2}-y_r)(\dot{y}_{s2}-\dot{y}_r)+(z_{s2}-z_r)(\dot{z}_{s2}-\dot{z}_r)}{\sqrt{(x_{s2}-x_r)^2+(y_{s2}-y_r)^2+(z_{s2}-z_r)^2}}\right)\\ -&\left(\frac{(x_{s1}-x_m)\dot{x}_{s1}+(y_{s1}-y_m)\dot{y}_{s1}+(z_{s1}-z_m)\dot{z}_{s1}}{\sqrt{(x_{s1}-x_m)^2+(y_{s1}-y_m)^2+(z_{s1}-z_m)^2}}\right.\\ &\left.-\frac{(x_{s2}-x_m)\dot{x}_{s2}+(y_{s2}-y_m)\dot{y}_{s2}+(z_{s2}-z_m)\dot{z}_{s2}}{\sqrt{(x_{s2}-x_m)^2+(y_{s2}-y_m)^2+(z_{s2}-z_m)^2}}\right)\end{aligned} \tag{4.10}$$

The subscripts s1 and s2 indicate satellite 1 and 2, and the subscripts r and m indicate remote receiver and master receiver.

Double differenced carrier phase measurements can provide much higher positioning accuracy than double differenced pseudorange measurements. The major problem of using carrier phase measurements is that the initial ambiguity must be resolved and cycle slips must be fixed correctly.

4.4 ATTITUDE FROM A GPS MULTI-ANTENNA SYSTEM

With the recent development in GPS attitude determination, a new type of GPS measurement, attitude, is now available for integration with an inertial system. The concept of attitude determination using GPS is to mount two or more antennas on the vehicle. The GPS carrier phase observations collected by these antennas are processed to determine the baseline vector between antennas mounted on the vehicle. From the baseline vector, the vehicle attitude can be extracted. A minimum of two antennas is required for heading determination while at least three are needed to obtain roll, pitch and heading. Either a dedicated GPS multi-antenna system which has a number of channels divided between several antennas or a nondedicated system which is made up of individual antenna/receivers can be used for attitude determination. The achievable accuracy is mainly a function of baseline length between antenna pairs, i.e. the longer the separation the higher the accuracy. For a detailed discussion of attitude determination using GPS, see El-Mowafy (1994) and Lu et al. (1994).

4.5 GPS MEASUREMENTS USED IN THE LOW-COST INTEGRATED INS/GPS SYSTEM

Table 4.1 summarizes the GPS positioning accuracy that is currently achievable (Schwarz et al., 1994a). Since the position performance of the low-cost integrated INS/GPS system mainly depends on the GPS positioning accuracy, differential GPS has to be used to meet the position accuracy requirement of resource mapping applications. Differential GPS can also provide more accurate velocity measurements, which are very important for misalignment estimation.

Table 4.1 GPS Positioning Accuracy

Model	Baseline Length	Accuracy
Pseudorange Point Positioning	N/A	100 m horizontal 150 m vertical
Smoothed Pseudorange Differential Positioning	10 km	1-3 m horizontal 1-4 m vertical
	500 km	3-7 m horizontal 4-8 m vertical
Carrier Phase Differential Positioning	10 km	3-20 cm horizontal 5-30 cm vertical
	50 km	15-30 cm horizontal 20-40 cm vertical

For the applications considered in this research, either single differencing between receivers or double differencing can be used. In the first case, the receiver clock error and its drift must be modelled, but the observation noise will be about 30 percent lower than in double differencing. In the second case, the effects of the receiver clock error and its drift are

eliminated, and they are not needed to be modelled in the Kalman filter. Since both method give adequate accuracy for the intended applications, double differencing was chosen in this research.

In an INS, misalignments directly affect the velocity and thus affect the position. Since the INS position is obtained by integrating the velocity, position errors do not contain more information about misalignments than the velocity errors do (Stambough, 1973). Misalignments can be estimated faster by velocity measurements than by position measurements. Therefore, combining INS information with GPS information for misalignment estimation should be done at the velocity level, i.e. using Doppler observations rather than at the position level, i.e. using pseudorange or carrier phase observations. In the low-cost integrated INS/GPS system, Doppler observations are used to estimate velocity errors and misalignments.

However, the sensitivity of Doppler observations to position errors is low. The estimation of INS position error proceeds much slower and position accuracy does not approach the accuracy inherent in GPS range measurement. Therefore, range measurements are still needed to be used to estimate position errors. Since position measurements have only a small contribution to misalignment estimation and the sensitivity of the Doppler observations to position errors is low, the choice of position measurements for the low-cost integrated INS/GPS system only depends on the position accuracy requirements. Because the differenced GPS pseudorange observations can meet the position accuracy requirements of resource mapping applications and are better suited for kinematic positioning, they are used in the low-cost integrated INS/GPS system rather than carrier phase observations.

The misalignment estimation using Doppler observations is affected by vehicle maneuvers and the achievable accuracy is limited by accelerometer biases, which will be discussed in

Chapter 6. In order to obtain better attitude accuracy and ensure attitude accuracy in the case where constant velocity is the desired operational environment, attitude measurements from a GPS multi-antenna system can be used in the low-cost integrated INS/GPS system. As will be shown later, it is usually sufficient to have independent heading information. Pitch and roll are well determined by GPS velocity aiding of INS measurements.

The integration of the MotionPak with GPS using double differenced pseudorange and Doppler observations are discussed in Chapter 5 and 6. Chapter 7 will investigate the integration using not only double differenced pseudorange and Doppler observations, but also heading measurements from a GPS multi-antenna system.

CHAPTER 5

INS/GPS INTEGRATION

In the prototype low-cost integrated INS/GPS system, all the measurements from the MotionPak and GPS receivers are collected during the operation and then post-processed. This chapter discusses the data collection and processing in detail.

5.1 SYSTEM HARDWARE AND DATA COLLECTION

The hardware components used in the prototype low-cost integrated INS/GPS include the MotionPak, the AT-MIO-16X data acquisition board, two GPS receivers, a data collection computer and a power supply.

A portable computer is used to control the data collection process and record the MotionPak and GPS data. The AT-MIO-16X is plugged in the data acquisition computer. The GPS data output cable through the COM1 port, and the GPS 1PPS signal through the LPT1 port are connected to the data collection computer, see Figure 5.1.

The integration Kalman filter pre-supposes that measurements from the INS and the GPS are made at the same time epoch. The measurements between the GPS and the MotionPak have therefore to be synchronized. Required synchronization accuracy is at the level of one

millisecond. This corresponds to a position error of 0.1m when flying at a velocity of 300 km/h. In the low-cost integrated INS/GPS, the synchronization is accomplished by interrupting the computer time chip upon receiving the GPS PPS signal. The computer time tick will be used to solve the variable time offset between the GPS time and the computer time. All time tags are put in the GPS time frame.

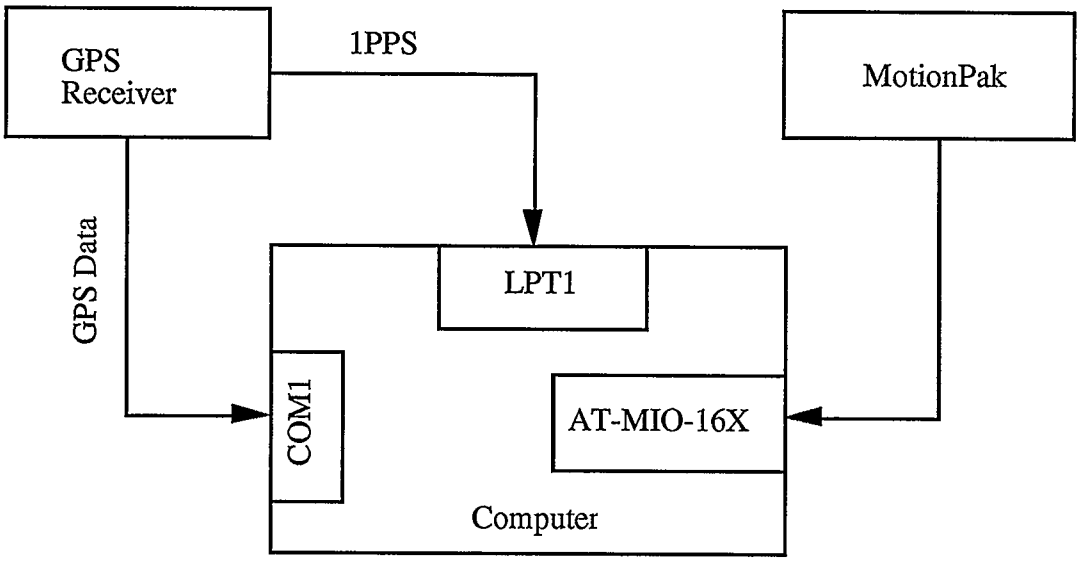

Figure 5.1 Hardware Components of the Low-Cost Integrated INS/GPS System

The data collection computer controls the whole data acquisition process through programmed interrupt processes. The well-defined hardware interrupts are used to perform the following functions:

(1) store the satellite ephemeris and measurements in the computer harddisk;

(2) interrupt the computer time chip upon receiving the GPS 1PPS signal from the GPS receiver;

(3) start the MotionPak data acquisition at a prescribed data rate of 640 Hz and record the data on the computer harddisk.

5.2 KALMAN FILTERING

The discrete Kalman filter is a standard tool to combine measurements in the integrated navigation system and much research has been done in this area, e.g. Hartman (1988), Howell and Tang (1994), Karatsinides (1994),Knight et al (1993), Lipman (1992), Schmidt (1989), Tang and Howell (1993). The essential formulas are briefly summarized in this section, for details, see Gelb (1974) and Maybeck (1979). For the discrete Kalman filter, the system is described by a linear dynamic model

$$x_k = \Phi_{k-1}x_{k-1} + w_{k-1} \tag{5.1}$$

and the measurements by a linear model

$$z_k = H_k x_k + v_k \tag{5.2}$$

where x is the system state vector, Φ_{k-1} is the state transition matrix over the interval k-1 to k, w is the process noise, z is the measurement vector, H is the design matrix, and v is the measurement noise. The other assumptions in the discrete Kalman filter are:

$$E[x_0] = \hat{x}_0 \qquad E\left[(x_0 - \hat{x}_0)(x_0 - \hat{x}_0)^T\right] = P_0$$

$$E[w_k] = 0 \qquad E\left[w_k w_j^T\right] = Q_k \delta_{kj}$$

$$E[v_k] = 0 \qquad E\left[v_k v_j^T\right] = R_k \delta_{kj}$$

$$E\left[w_k v_j^T\right] = 0$$

where Q is the process noise covariance and R is the measurement noise covariance. The Kalman filter first propagates the estimates from time k-1 to k

$$\hat{x}_k(-) = \Phi_{k-1}\hat{x}_{k-1}(+) \tag{5.3}$$

$$P_k(-) = \Phi_{k-1} P_{k-1}(+) \Phi_{k-1}^T + Q_{k-1} \tag{5.4}$$

where P is the system covariance, (-) refers to pre-measurement update values, (+) refers to post-measurement update values and ^ refers to estimates. The gain matrix can then be computed by

$$K_k = P_k(-) H_k^T \left[H_k P_k(-) H_k^T + R_k \right]^{-1} \tag{5.5}$$

and uses the measurements to obtain the best linear estimates of the system states

$$\hat{x}_k(+) = \hat{x}_k(-) + K_k \left[z_k - H_k \hat{x}_k(-) \right] \tag{5.6}$$

$$P_k(+) = \left[I - K_k H_k \right] P_k(-) \tag{5.7}$$

If the system dynamics is described by the first-order differential equation:

$$\dot{x}(t) = F(t) x(t) + w(t) \tag{5.8}$$

where F is the dynamics matrix and w is the random forcing function, this equation must be carefully discretized into Equation (5.1) by the expansion

$$\Phi_{k-1} = e^{-F\Delta t} = I + F\Delta t + \frac{(F\Delta t)^2}{2!} + \ldots \tag{5.9}$$

5.3 INS/GPS INTEGRATION

Either a centralized or decentralized Kalman filter can be used to integrate an INS with a double differenced GPS system, e.g. Gao et al. (1993), Schwarz and Wei (1994c), Wei and Schwarz (1990b). In the decentralized Kalman filter configuration, two Kalman filters are running in parallel. The GPS filter computes position and velocity from double

differenced GPS pseudorange and Doppler observations while the integration filter takes the position and velocity from the GPS filter to update the INS. The centralized Kalman filter, on the other hand, has only one Kalman filter and directly uses double differenced GPS pseudorange and Doppler observations to update the INS. Each of the configurations has its own advantages. In the low-cost integrated INS/GPS system, the centralized Kalman filter is used and its concept is shown in Figure 5.2.

The use of the centralized Kalman filter rather than the decentralized Kalman filter in the low-cost integrated INS/GPS system is based on the following consideration. The GPS filter in the decentralized Kalman filter configuration will only have an approximate model to describe vehicle motion. The GPS filter model error will cause some additional errors in GPS position and velocity, and decrease the whole system accuracy achievable. The centralized Kalman filter, however, uses the well-established inertial error model to describe the vehicle dynamics, which eliminates the accuracy degradation in the decentralized configuration.

5.3.1 System Dynamics Model

Since the Kalman filter can only give estimates of the system states, all navigation and sensor errors needed should be included in the state vector of the integration Kalman filter. Thus, theoretically the state vector should include the following components:

misalignment errors	3 states
position errors	3 states
velocity errors	3 states
gyro drifts	3 states
gyro scale factor errors	3 states

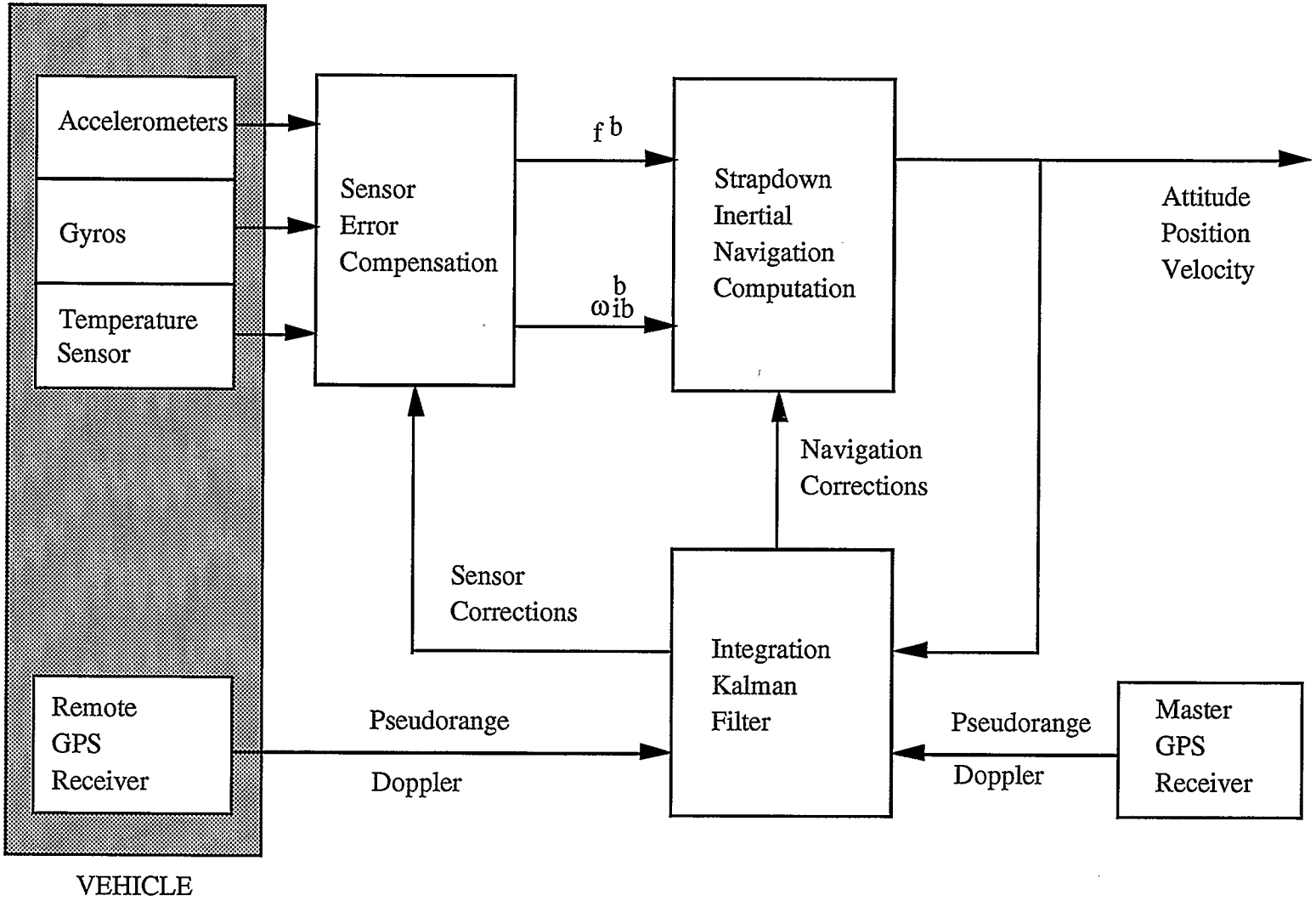

Figure 5.2 Block Diagram of the INS/GPS Integration

gyro misalignment errors	6 states
accelerometer biases	3 states
accelerometer scale factor errors	3 states
accelerometer misalignment errors	6 states

Since double differenced GPS pseudorange and Doppler observations are used, the state vector does not include components related to GPS errors. The state vector with 33 components was initially employed in the integration Kalman filter, and estimates of each state were obtained using laboratory and van test data. Many of these states, however, are weakly observable when using GPS updates only. Based on these results, the state vector was reduced to 15 error states which have been used in the Kalman filter of the low-cost integrated INS/GPS system. They are:

$$X = \left(\varepsilon_x^e \ \varepsilon_y^e \ \varepsilon_z^e \ \delta x^e \ \delta y^e \ \delta z^e \ \delta v_x^e \ \delta v_y^e \ \delta v_z^e \ d_x^b \ d_y^b \ d_z^b \ b_x^b \ b_y^b \ b_z^b\right)^T \tag{5.8}$$

where

ε_x^e, ε_y^e, ε_z^e are three misalignment errors in the earth-fixed frame;

δx^e, δy^e, δz^e are three position errors in the earth-fixed frame;

δv_x^e, δv_y^e, δv_z^e are three velocity errors in the earth-fixed frame;

d_x^b, d_y^b, d_z^b are three gyro drifts in the body frame, modelled as random walk;

b_x^b, b_y^b, b_z^b are three accelerometer biases in the body frame, modelled as random walk.

The linear dynamic model with this state vector is expressed as:

$$\begin{bmatrix}\dot{\varepsilon}_x^e\\ \dot{\varepsilon}_y^e\\ \dot{\varepsilon}_z^e\end{bmatrix}=\begin{bmatrix}0 & \omega_e & 0\\ -\omega_e & 0 & 0\\ 0 & 0 & 0\end{bmatrix}\begin{bmatrix}\varepsilon_x^e\\ \varepsilon_y^e\\ \varepsilon_z^e\end{bmatrix}+\begin{bmatrix}C_b^e(1,1) & C_b^e(1,2) & C_b^e(1,3)\\ C_b^e(2,1) & C_b^e(2,2) & C_b^e(2,3)\\ C_b^e(3,1) & C_b^e(3,2) & C_b^e(3,3)\end{bmatrix}\begin{bmatrix}d_x^b\\ d_y^b\\ d_z^b\end{bmatrix}+\begin{bmatrix}w_1\\ w_2\\ w_3\end{bmatrix} \tag{5.9}$$

$$\begin{bmatrix}\delta\dot{x}^e\\ \delta\dot{y}^e\\ \delta\dot{z}^e\end{bmatrix}=\begin{bmatrix}\delta v_x^e\\ \delta v_y^e\\ \delta v_z^e\end{bmatrix} \tag{5.10}$$

$$\begin{aligned}\begin{bmatrix}\delta\dot{v}_x^e\\ \delta\dot{v}_y^e\\ \delta\dot{v}_z^e\end{bmatrix}&=\begin{bmatrix}0 & f_z^e & -f_y^e\\ -f_z^e & 0 & f_x^e\\ f_y^e & -f_x^e & 0\end{bmatrix}\begin{bmatrix}\varepsilon_x^e\\ \varepsilon_y^e\\ \varepsilon_z^e\end{bmatrix}+\begin{bmatrix}N_{11} & N_{12} & N_{13}\\ N_{21} & N_{22} & N_{23}\\ N_{31} & N_{32} & N_{33}\end{bmatrix}\begin{bmatrix}\delta x^e\\ \delta y^e\\ \delta z^e\end{bmatrix}\\ &+\begin{bmatrix}0 & 2\omega_e & 0\\ -2\omega_e & 0 & 0\\ 0 & 0 & 0\end{bmatrix}\begin{bmatrix}\delta v_x^e\\ \delta v_y^e\\ \delta v_z^e\end{bmatrix}+\begin{bmatrix}C_b^e(1,1) & C_b^e(1,2) & C_b^e(1,3)\\ C_b^e(2,1) & C_b^e(2,2) & C_b^e(2,3)\\ C_b^e(3,1) & C_b^e(3,2) & C_b^e(3,3)\end{bmatrix}\begin{bmatrix}b_x^b\\ b_y^b\\ b_z^b\end{bmatrix}+\begin{bmatrix}w_7\\ w_8\\ w_9\end{bmatrix}\end{aligned} \tag{5.11}$$

$$\begin{bmatrix}\delta\dot{d}_x^e\\ \delta\dot{d}_y^e\\ \delta\dot{d}_z^e\end{bmatrix}=\begin{bmatrix}w_{10}\\ w_{11}\\ w_{12}\end{bmatrix} \tag{5.12}$$

$$\begin{bmatrix}\delta\dot{b}_x^e\\ \delta\dot{b}_y^e\\ \delta\dot{b}_z^e\end{bmatrix}=\begin{bmatrix}w_{13}\\ w_{14}\\ w_{15}\end{bmatrix} \tag{5.13}$$

where f_x^e, f_y^e and f_z^e are the specific force components in the earth-fixed frame, w_1 to w_{15} are the process noise components. Detailed expressions for N_{11} to N_{33} can be found in Schwarz and Wei (1995).

The initial covariances used in the integration Kalman filter reflect the likely magnitude of the specific parameters. The initial covariance values for the inertial sensor errors are determined from their statistics. Position and velocity covariances are determined by the likely accuracy of the initial data.

The unmodelled inertial sensor errors, such as the uncompensated scale factor errors and misalignments, are treated as accounted for in the process noise. The time synchronization error between the INS and GPS measurements is considered as measurement noise.

5.3.2 Measurement Model

In the low-cost integrated INS/GPS system, double differenced GPS pseudorange and Doppler observations are used to estimate inertial navigation errors and inertial sensor errors of the MotionPak. Since a linear measurement model is needed, the real measurements of the integration Kalman filter are the residuals of the double differenced pseudorange and Doppler between the actual GPS observations and their predictions,

$$z(\rho) = \Delta\nabla\rho(\text{obs}) - \Delta\nabla\rho(\text{pred}) \tag{5.14}$$

$$z(\dot{\rho}) = \Delta\nabla\dot{\rho}(\text{obs}) - \Delta\nabla\dot{\rho}(\text{pred}) \tag{5.15}$$

The predicted values are computed using Equations (5.9) and (5.10). In order to get the predicted values, the position and velocity of each satellite observed are calculated from the ephemeris, and current GPS antenna position and velocity are determined from the inertial position and velocity solution.

Because the MotionPak and the remote GPS antenna are not installed at the same point, there is a spatial offset between them, which is called the lever arm. The lever arm causes position and velocity differences between the MotionPak and the remote GPS antenna. In order to get correct predicted values of the double differenced GPS pseudorange and Doppler, the lever arm effects on position and velocity must be compensated for, see Figure 5.3.

In order to compute the lever arm effects on position and velocity, the offset between GPS antenna and MotionPak is precisely measured in the body frame before each test. Supposing the offset from the MotionPak to GPS in the body frame is measured as $r^b_{GPS-INS}$, the lever arm effects on position and velocity are computed as follows:

$$r^e_{GPS} - r^e_{INS} = C^e_b r^b_{GPS-INS} \tag{5.16}$$

$$v^e_{GPS} - v^e_{INS} = C^e_b(\omega^b_{Ib} \times r^b_{GPS-INS}) \tag{5.17}$$

where r^e_{GPS} and v^e_{GPS} are the predictions of GPS antenna position and velocity in the earth-fixed frame respectively.

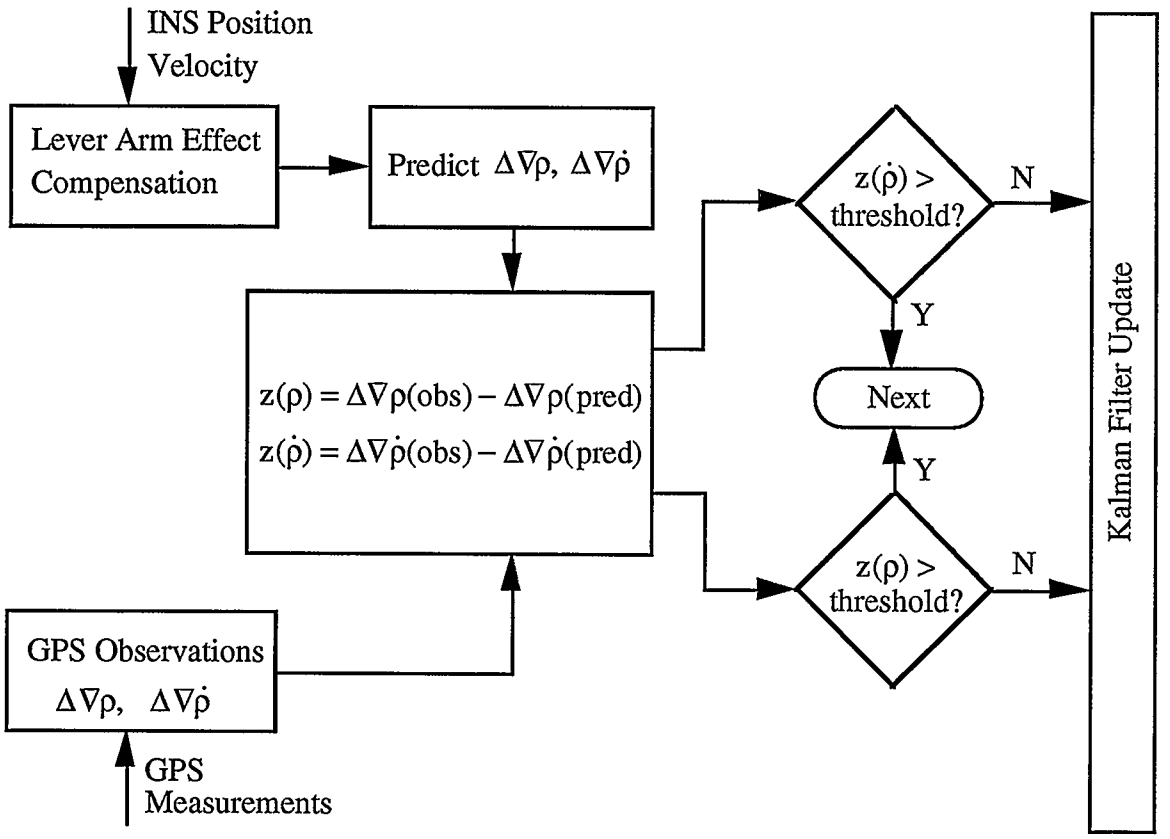

Figure 5.3 Lever Arm Effect Compensation and Measurement Validity Check

The measurement equations are derived from Equations (4.9) and (4.10) as follows:

$$z(\rho) = \frac{\partial \Delta\nabla\rho}{\partial x_r}\delta x^e + \frac{\partial \Delta\nabla\rho}{\partial y_r}\delta y^e + \frac{\partial \Delta\nabla\rho}{\partial z_r}\delta z^e \tag{5.18}$$

$$\begin{aligned} z(\dot{\rho}) = &\frac{\partial \Delta\nabla\dot{\rho}}{\partial x_r}\delta x^e + \frac{\partial \Delta\nabla\dot{\rho}}{\partial y_r}\delta y^e + \frac{\partial \Delta\nabla\dot{\rho}}{\partial z_r}\delta z^e \\ &+ \frac{\partial \Delta\nabla\dot{\rho}}{\partial \dot{x}_r}\delta v_x^e + \frac{\partial \Delta\nabla\dot{\rho}}{\partial \dot{y}_r}\delta v_y^e + \frac{\partial \Delta\nabla\dot{\rho}}{\partial \dot{z}_r}\delta v_z^e \end{aligned} \tag{5.19}$$

GPS measurements have to be validated to prevent incorrect measurements from being used by the integration Kalman filter. In the low-cost integrated INS/GPS, the data validity check is implemented by using a 3-σ test on the innovation process. That means the GPS measurements are used to update INS only if

$$\left|[z_k - H_k\hat{x}_k(-)](i)\right| \le 3\sqrt{\left[H_k P_k(-) H_k^T + R_k\right](i,i)} \tag{5.20}$$

where (i) indicates the i-th element, (i,i) indicates the i-th diagonal element.

In order to achieve maximum system accuracy, the integration Kalman filter has to be tuned. Tuning a filter is a time-consuming process which involves numerous trial-and-error iterations for the parameters that yield the best performance possible from the specified filter structure. For the low-cost integrated INS/GPS system, laboratory and van test data are used to tune the parameters in the integration Kalman filter.

The integration Kalman filter can be implemented in two distinct types, feedback and feedforward. In the low-cost integrated INS/GPS, the feedback configuration is used. The estimates of the navigation errors from the integration Kalman filter are fed back into the inertial navigation computation to correct the navigation errors, and the estimates of the

inertial sensor errors are fed back into the inertial sensor error compensation to calibrate the inertial sensor errors. The feedback corrections keep the errors of the MotionPak small and enhance the adequacy of the linear inertial error equations for the MotionPak, which is very important for a low-quality inertial system.

5.3.3 Software Development

The University of Calgary has developed an INS/GPS integration software package, KINGSPAD (KINematic Geodetic System for Position and Attitude Determination), which uses a decentralized Kalman filter to combine INS data and double differenced GPS carrier phase observations. Figure 5.4 is the block diagram of KINGSPAD.

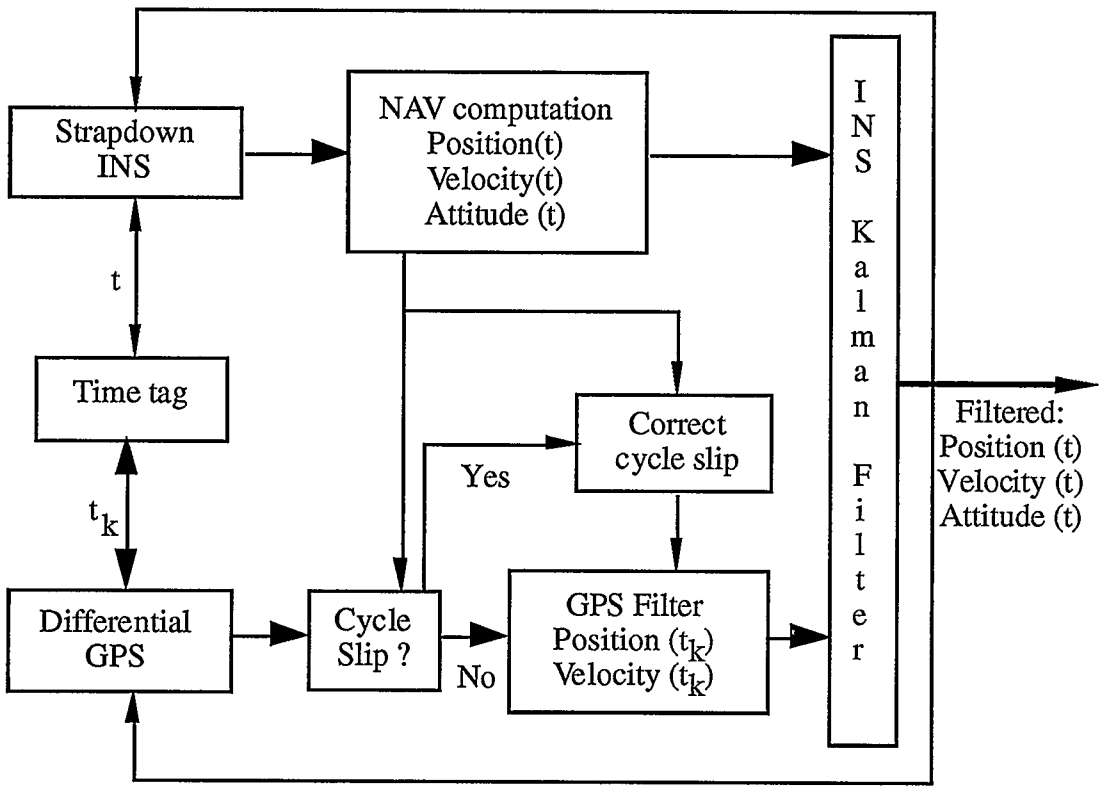

Figure 5.4 Block Diagram of KINGSPAD

The software used for the low-cost integrated INS/GPS system is a modified version of KINDSPAD. The modules for strapdown inertial navigation computation and GPS computation shown in Figure 5.2 are directly taken from the KINDSPAD software. The modules for sensor error compensation and the integration Kalman filter have been re-designd for the low-cost integrated INS/GPS system.

CHAPTER 6

TESTING AND RESULTS

A prototype low-cost integrated INS/GPS system was built by implementing the system hardware and software design described in the previous chapters. This system can provide a complete navigation solution at high data rates. The outputs include position (latitude, longitude, height), velocity (East, North, Up), attitude (roll, pitch, heading), 3-axis acceleration in the body frame and 3-axis angular rate in the body frame. All these outputs are available at any user selected data rate up to 64 Hz.

A number of tests were conducted with the low-cost integrated INS/GPS. This chapter describes these tests in detail. The test results are then analyzed and the achievable system performance is evaluated. The results given in this chapter will only use DGPS pseudorange and Doppler for updates. Updating by additional heading measurements from a GPS dual-antenna system will be discussed in the next chapter.

6.1 TEST OBJECTIVE

Three types of tests were planned for the low-cost integrated INS/GPS system. They are laboratory tests, van tests and flight tests. So far, the laboratory and van tests have been completed.

There are three main objectives for the tests of the low-cost integrated INS/GPS system, namely

(1) to verify the system hardware and software design;

(2) to tune the parameters of the integration Kalman filter;

(3) to assess the system performance achievable.

The laboratory tests are used to verify and modify the whole system hardware design and data collection. All software functions have also been checked by processing the laboratory test data.

Tuning a Kalman filter means that the parameters of the Kalman filter are iteratively adjusted to obtain the best performance possible. It is a very time-consuming task. The first two van test data sets were used to tune the parameters of the integration Kalman filter. After finishing the tuning, all filter parameters are fixed in the low-cost integrated INS/GPS system.

After the system design was verified and the integration Kalman filter was tuned, further van tests were conducted to evaluate the system accuracy achievable, which will be discussed in detail in the following.

6.2 TEST REFERENCE

A reference system which can provide much more accurate position, velocity and attitude outputs than the low-cost integrated INS/GPS system is needed for the tests. The University of Calgary has developed a high performance integrated INS/GPS system by

combining a LTN 90-100 strapdown inertial system and double differenced GPS carrier phase and Doppler observations. The software package for this integrated INS/GPS system is KINGSPAD. Since this integrated INS/GPS can provide position, velocity and attitude outputs with much higher accuracy than that of the low-cost integrated INS/GPS system, it was used as the test reference. During the tests, the MotionPak was mounted on top of the LTN 90-100, and the resulting differences between the low-cost integrated INS/GPS and the high performance integrated INS/GPS were considered as the errors of the low-cost integrated INS/GPS.

6.3 TEST DESCRIPTION

The hardware used in the van tests were the LTN 90-100 strapdown inertial system, the MotionPak, two Ashtech Z-XII GPS receivers, one Ashtech Three-Dimensional Direction Finding (3DF) system, and three computers. One Ashtech Z-XII GPS receiver was located on a known control point as the master station and its data was collected by using a computer. The LTN 90-100 was bolted to the van through a frame and the MotionPak was mounted on the top of the frame by use of a metal plate, see Figure 6.1. The GPS antennas for the remote GPS receiver and 3DF were mounted on the roof of the van. During the test, GPS measurements were collected at 1 Hz, LTN 90-100 data were recorded at 64 Hz, and the MotionPak outputs were sampled at 640 Hz. The measurements of both the LTN 90-100 and the MotionPak were synchronized with GPS measurements by using the GPS 1PPS signal. The offsets between the GPS antenna, the MotionPak and the center of the LTN 90-100 were measured for the compensation of the lever arm effect before the test.

At the beginning of each van test, about 30 minutes of static data were collected. These data were acquired for two reasons: firstly for the LTN 90-100 initial alignment and the

MotionPak levelling, and secondly for the initial GPS ambiguity determination in KINGSPAD. The van was then driven along the test course. Each test lasted about one hour.

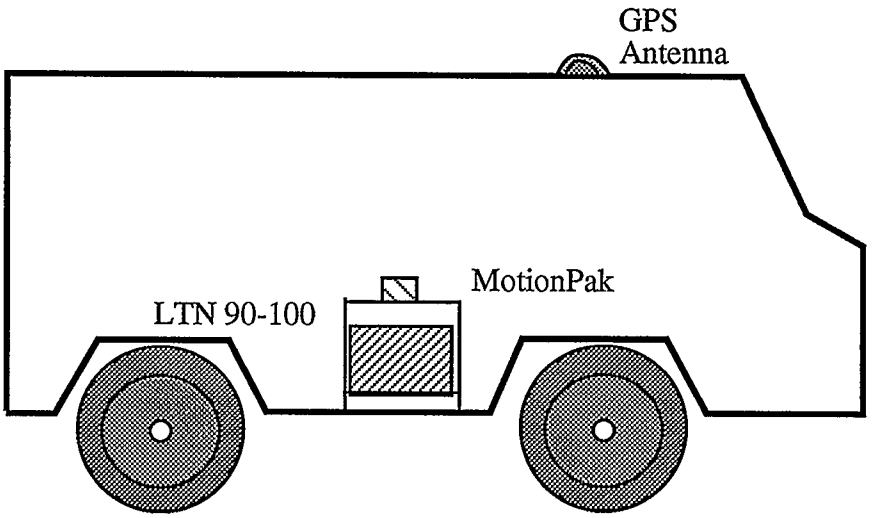

Figure 6.1 Test Equipment Configuration

6.4 RESULTS OF VAN TEST #1

Van test #1 was conducted on the Nortech baseline, a well-surveyed test traverse close to Calgary. The trajectory of van test #1 is shown in Figure 6.2. During this test, six to eight satellites were observed, and the PDOP was between 1.5 to 3.0, see Figures 6.3 and 6.4. The attitude and velocity of the van during the test is shown in Figures 6.5 and 6.6. The 360-degree jumps in heading are due to the vehicle movement with heading close to 180 degrees.

The velocity, position and attitude errors of the low-cost integrated INS/GPS system are shown in Figures 6.7, 6.8 and 6.9, respectively. Statistical values of these errors are

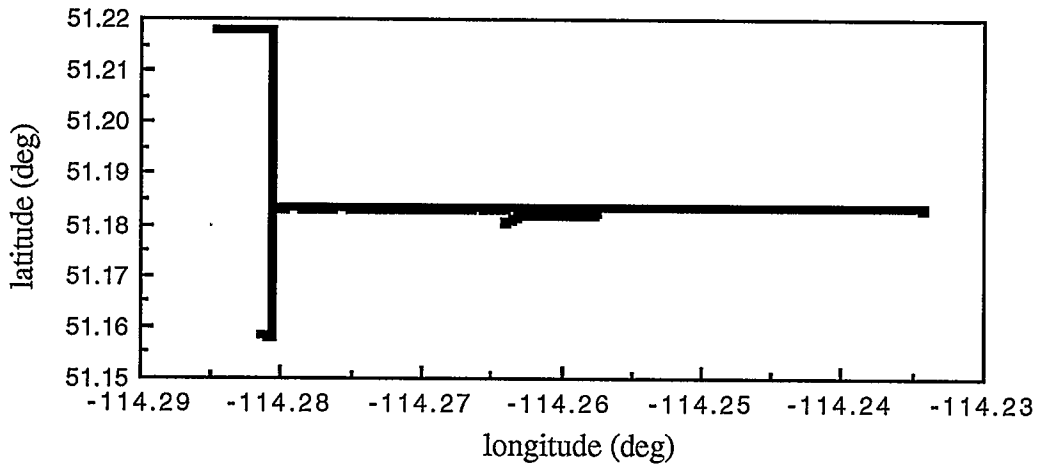

Figure 6.2 Trajectory of Van Test #1

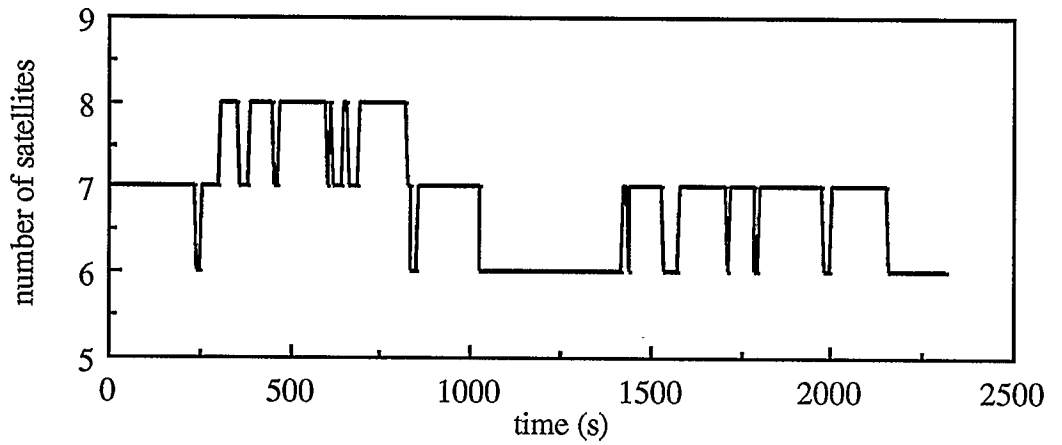

Figure 6.3 Number of Satellites Observed During Van Test #1

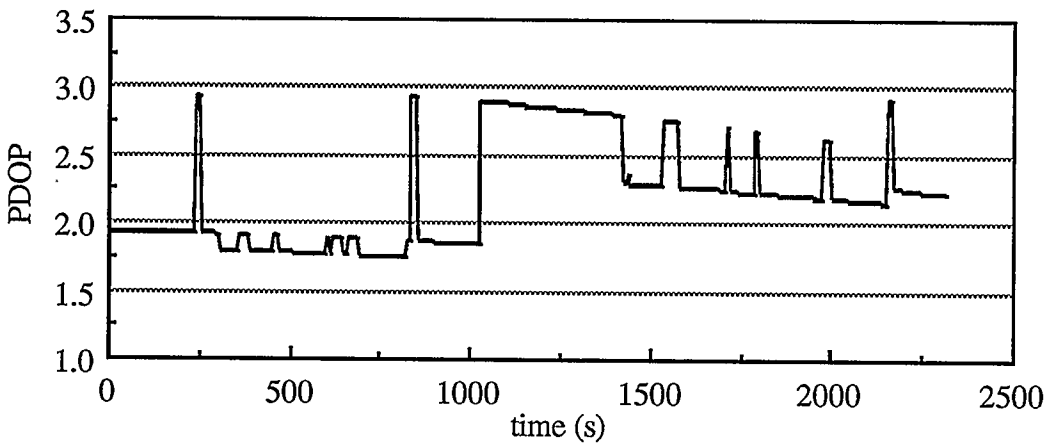

Figure 6.4 PDOP During Van Test #1

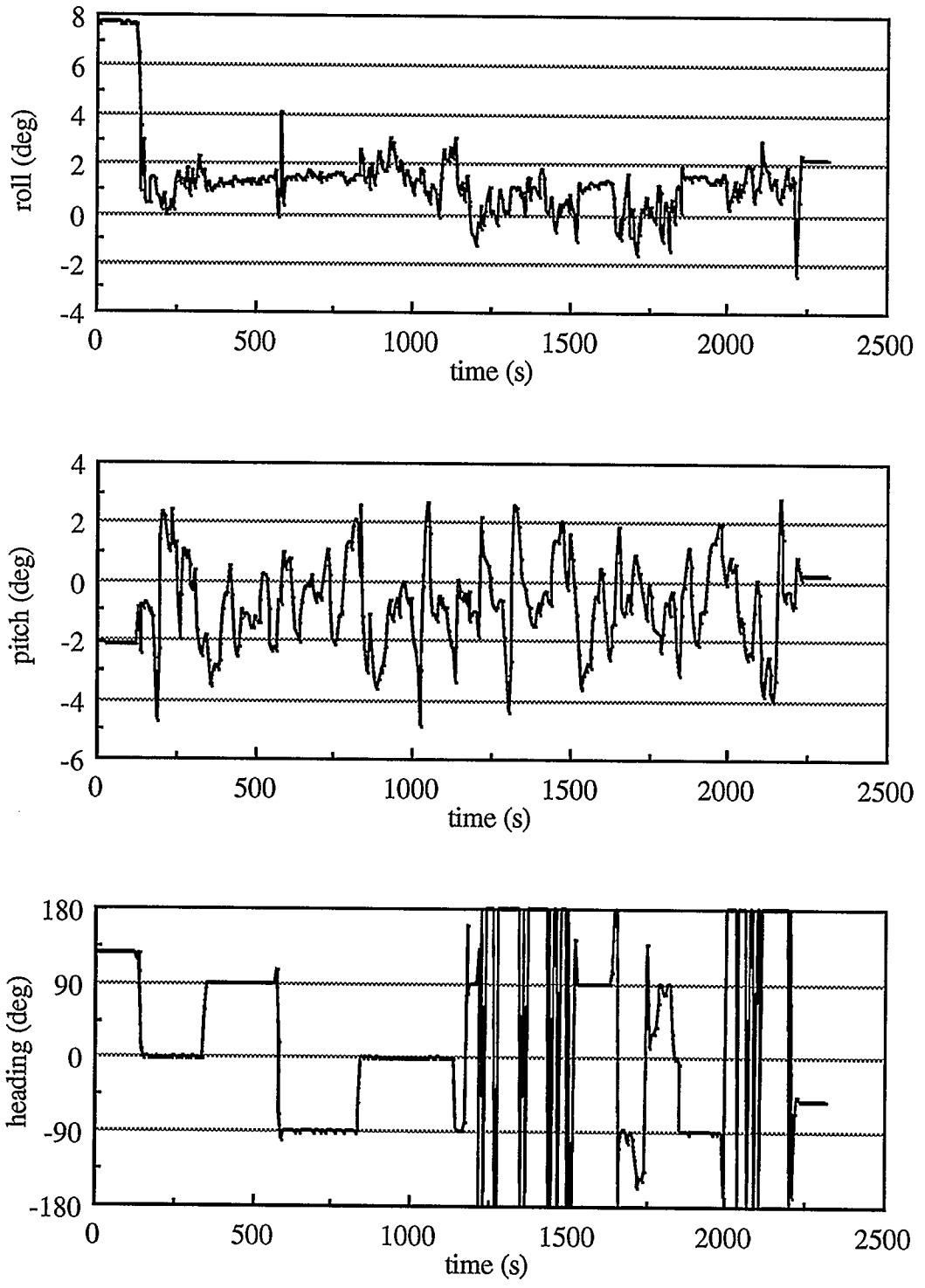

Figure 6.5 Attitude During Van Test #1

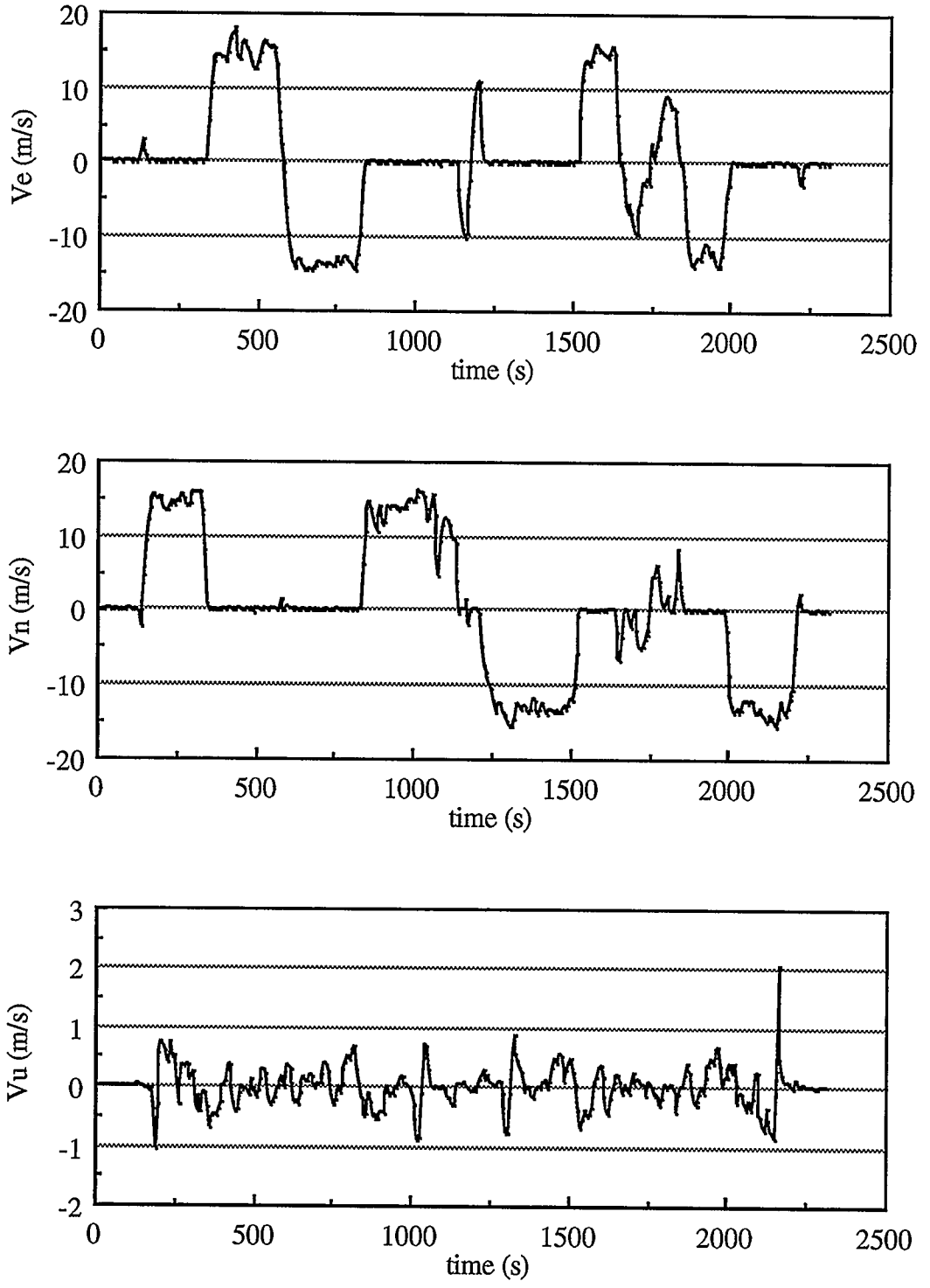

Figure 6.6 Velocity During Van Test #1

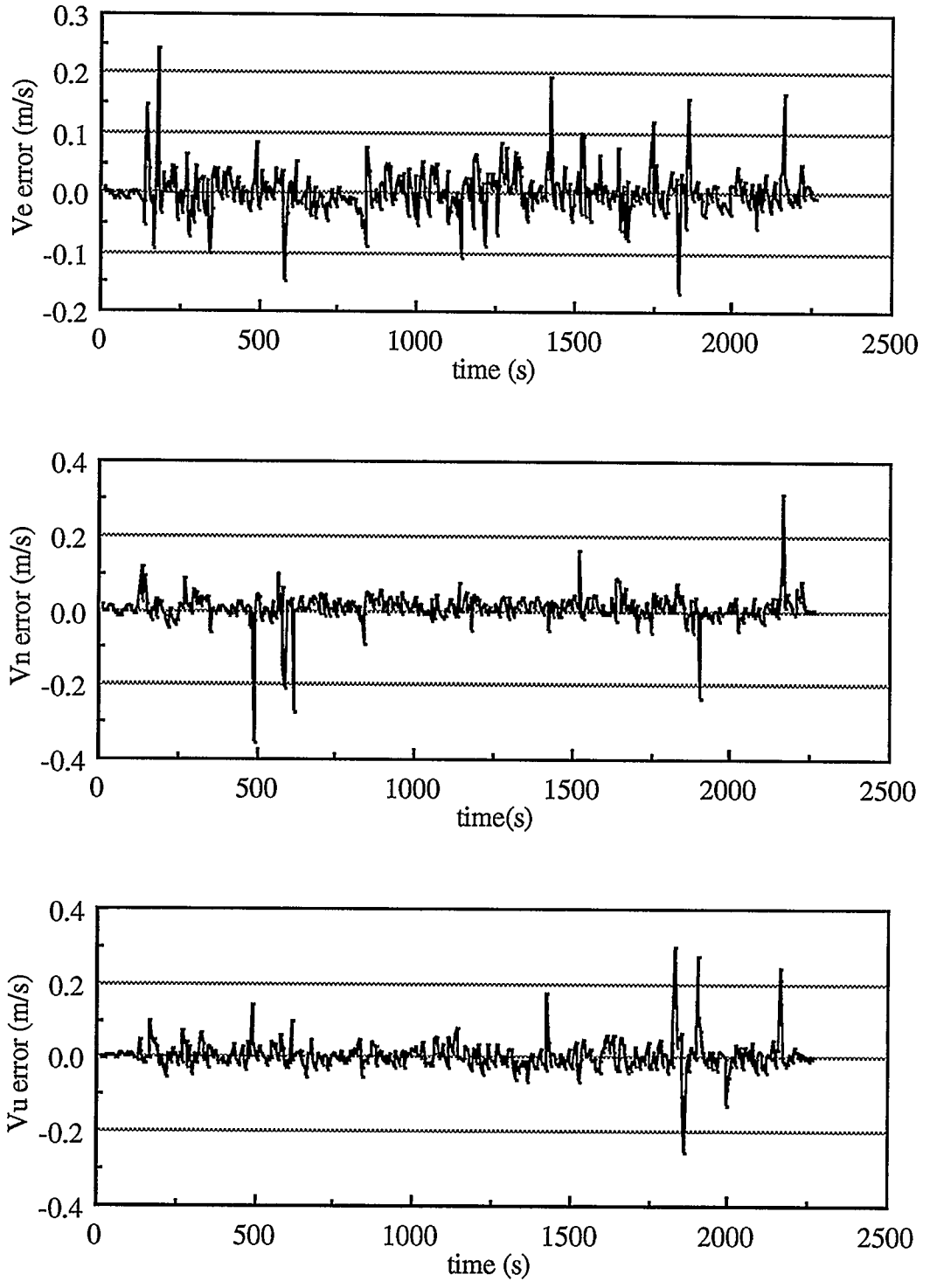

Figure 6.7 Velocity Errors of the Low-Cost Integrated INS/GPS

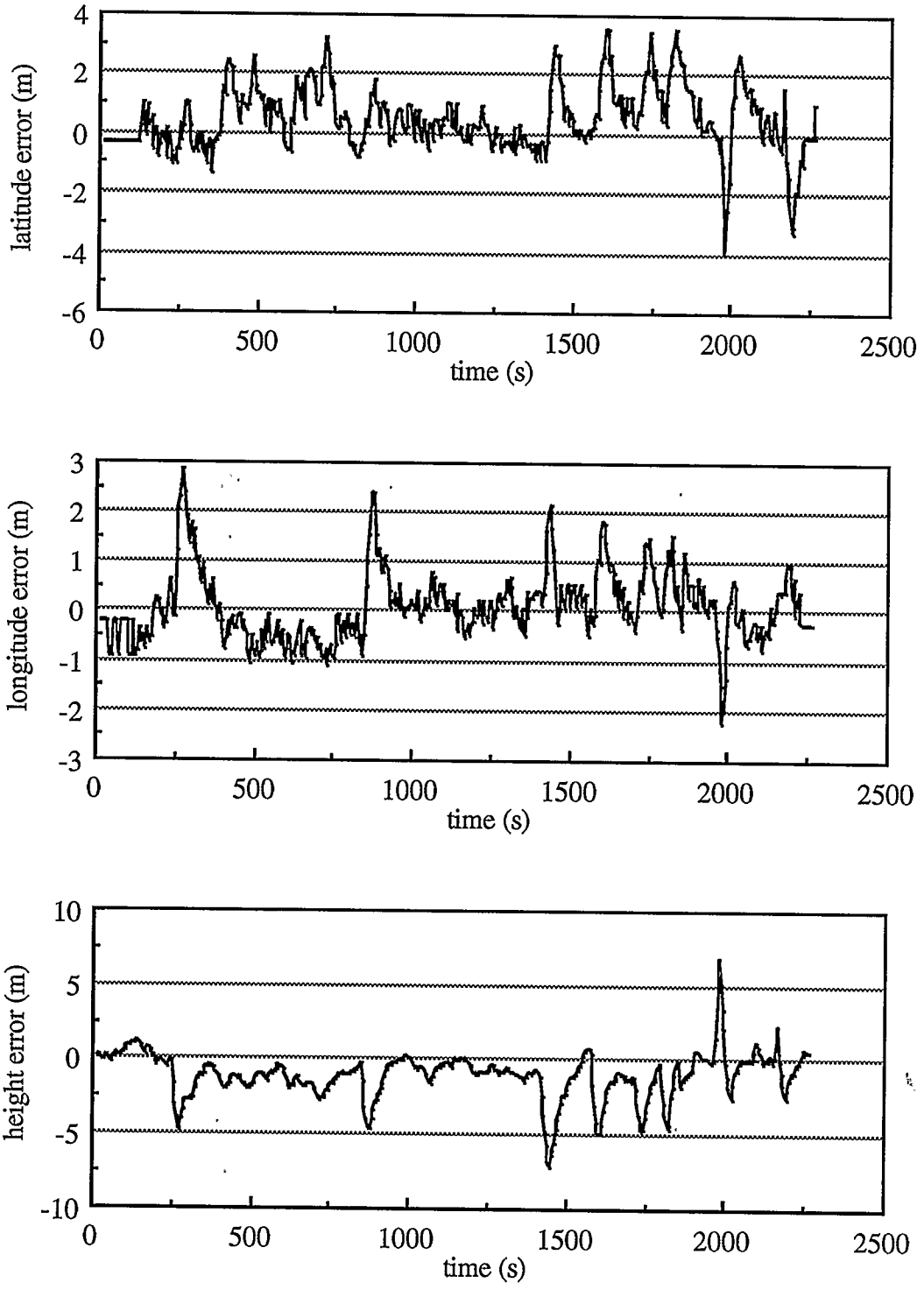

Figure 6.8 Position Errors of the Low-Cost Integrated INS/GPS

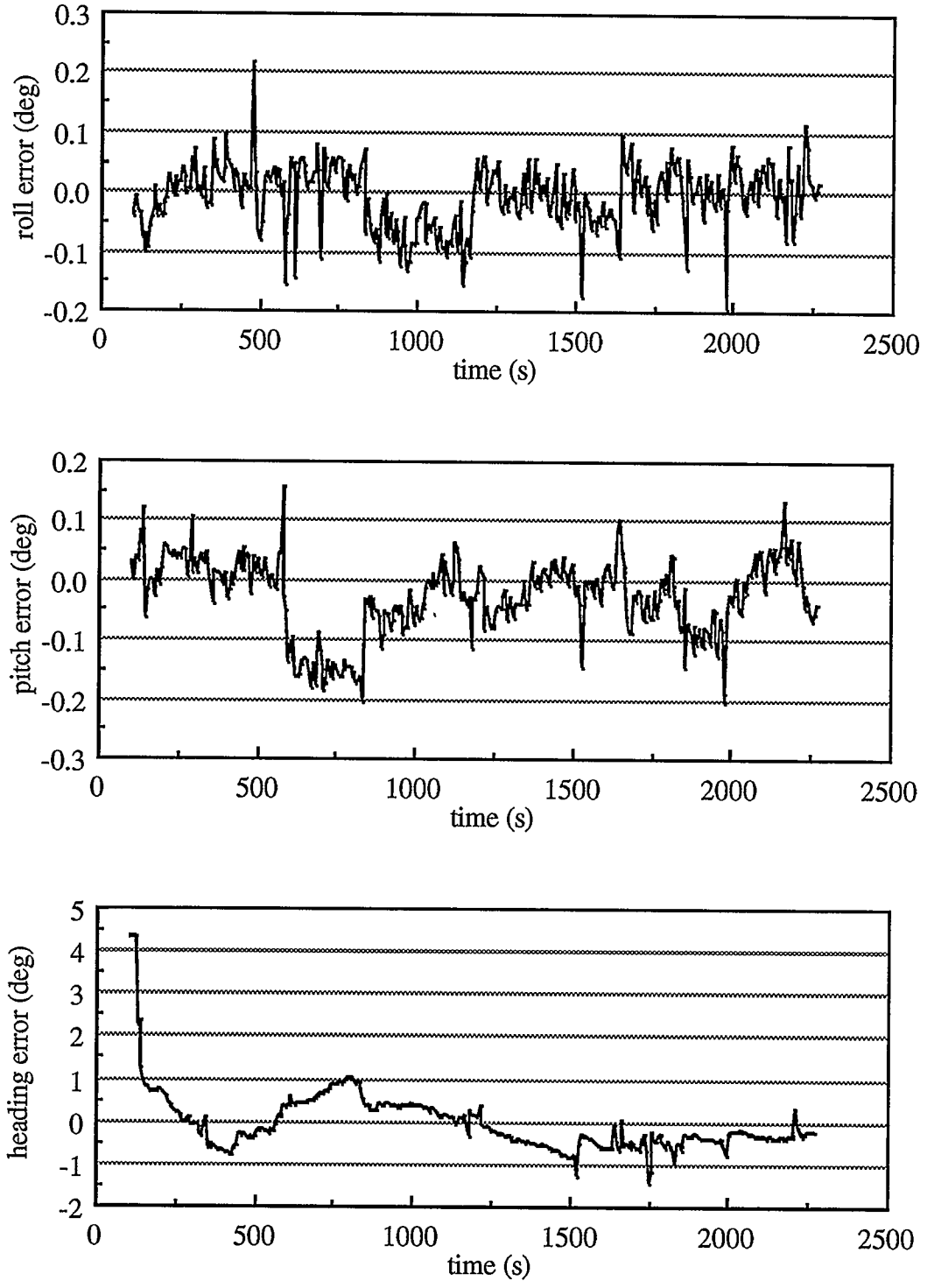

Figure 6.9 Attitude Errors of the Low-Cost Integrated INS/GPS

summarized in Tables 6.1, 6.2 and 6.3, respectively.

Figures 6.7 to 6.9 show clearly that due to the GPS updates the navigation errors of the low-cost integrated INS/GPS do not increase with time. The statistical values listed in Tables 6.1 to 6.3 indicate that the low-cost integrated system using double differenced pseudorange and Doppler observations can meet the accuracy requirements of resource mapping applications in position, roll and pitch, but the heading accuracy is marginal.

It should be noted, however, that RMS values may not be adequate to describe actual system requirements. Peaks in the data and quasi-systematic data drifts may actually limit the overall system accuracy.

Table 6.1 Velocity Errors of the Low-Cost Integrated INS/GPS

	Ve error	Vn error	Vu error
mean (m/s)	-0.000	0.004	0.003
RMS (m/s)	0.033	0.038	0.040

Table 6.2 Position Errors of the Low-Cost Integrated INS/GPS

	latitude error	longitude error	height error
mean (m)	0.461	0.091	-1.072
RMS (m)	1.173	0.705	1.860

Table 6.3 Attitude Errors of the Low-Cost Integrated INS/GPS

	roll error	pitch error	heading error
mean (deg)	-0.007	-0.029	-0.033
RMS (deg)	0.054	0.070	0.736

6.5 ANALYSIS OF RESULTS

The position and velocity accuracy of the low-cost integrated INS/GPS system mainly depends on the accuracy achievable from double differenced GPS pseudorange and Doppler observations. The geometry of the satellites observed as expressed by the PDOP value affects the position and velocity accuracy.

The test results show that the attitude accuracy has been significantly improved by using GPS updates and the performance in roll and pitch is much better than that of heading. In the following, the attitude performance is analyzed in detail.

In the local-level frame, the INS velocity errors due to misalignments and accelerometer biases can be written in component form as:

$$\begin{aligned} \delta\dot{v}_e &= f_u\varepsilon_n^l - f_n\varepsilon_u^l + b_e \\ \delta\dot{v}_n &= -f_u\varepsilon_e^l + f_e\varepsilon_u^l + b_n \\ \delta\dot{v}_u &= f_n\varepsilon_e^l - f_e\varepsilon_n^l + b_u \end{aligned} \tag{6.1}$$

where ε_e^l, ε_n^l ,ε_u^l are the three misalignment errors in the local-level frame, f_e, f_n, f_u are three specific force components in the local-level frame, b_e, b_n, b_u are the accelerometer biases in the local-level frame. Equation (6.1) indicates that ε_e^l affects the velocity error through f_n and f_u, ε_n^l through f_e and f_u, ε_u^l through f_e and f_n. f_u includes gravity and is therefore always large, f_e and f_n are only different from zero when the vehicle has a maneuver in the horizontal plane; ε_u^l is therefore only observable through velocity measurements when the vehicle has a maneuver in the horizontal plane, either by vehicle acceleration or a turn. In contrast, ε_e^l and ε_n^l are always observable. When using

GPS Doppler observations to update INS, ε_e^l and ε_n^l can be much better estimated than ε_u^l especially in cases where constant vehicle motion is required.

In an INS, the position is obtained by integrating the velocity. Position errors do not contain more information about the misalignments than velocity errors do. When GPS pseudorange observations are used to update the INS, the situation does not change. The ε_e^l and ε_n^l can be much better estimated than the ε_u^l, and the estimation of ε_u^l depends on vehicle maneuvers in the horizontal plane.

In the local-level frame, the relationship between the misalignment errors and the transformation matrix $\mathbf{C}_b^l$ is given by

$$\begin{bmatrix} 1 & -\varepsilon_u^l & \varepsilon_n^l \\ \varepsilon_u^l & 1 & -\varepsilon_e^l \\ -\varepsilon_n^l & \varepsilon_e^l & 1 \end{bmatrix} \mathbf{C}_b^l(\text{true}) = \mathbf{C}_b^l(\text{computed}) \tag{6.2}$$

In Equation (6.2)

$$\mathbf{C}_b^l = \begin{bmatrix} \cos\psi\cos\varphi - \sin\psi\sin\theta\sin\varphi & -\sin\psi\cos\theta & \cos\psi\sin\varphi + \sin\psi\sin\theta\cos\varphi \\ \sin\psi\cos\varphi + \cos\psi\sin\theta\sin\varphi & \cos\psi\cos\theta & \sin\psi\sin\varphi - \cos\psi\sin\theta\cos\varphi \\ -\cos\theta\sin\varphi & \sin\theta & \cos\theta\cos\varphi \end{bmatrix} \tag{6.3}$$

where (φ, θ, ψ) are the three attitude angles, roll, pitch and yaw. Defining the attitude errors as

$$\begin{aligned} \delta\psi &= \psi(\text{computed}) - \psi(\text{true}) \\ \delta\theta &= \theta(\text{computed}) - \theta(\text{true}) \\ \delta\varphi &= \varphi(\text{computed}) - \varphi(\text{true}) \end{aligned} \tag{6.4}$$

Equation (6.2) yields

$$\delta\varphi = -\varepsilon_e^l \frac{\sin\psi}{\cos\theta} + \varepsilon_n^l \frac{\cos\psi}{\cos\theta} \tag{6.5}$$

$$\delta\theta = \varepsilon_e^l \cos\psi + \varepsilon_n^l \sin\psi \tag{6.6}$$

$$\delta\psi = \varepsilon_e^l \sin\psi \tan\theta - \varepsilon_n^l \cos\psi \tan\theta + \varepsilon_u^l \tag{6.7}$$

Equations (6.5) to (6.7) indicate that the roll error $\delta\varphi$ and the pitch error $\delta\theta$ depend on ε_e^l and ε_n^l, and the yaw error $\delta\psi$ mainly depends on ε_u^l. Because ε_e^l and ε_n^l are much better estimated than ε_u^l from GPS updates, the roll error $\delta\varphi$ and the pitch error $\delta\theta$ of the low-cost integrated INS/GPS system are much smaller than the yaw error $\delta\psi$.

Since the attitude errors are estimated using double differenced GPS pseudorange and Doppler observations, the attitude accuracy achievable with the low-cost integrated INS/GPS system depends not only on the vehicle trajectory, accelerometer biases and gyro drifts, but also on the PDOP value and the synchronization error between GPS and the MotionPak.

6.6 MOVING BASE ALIGNMENT

As discussed in Chapter 3, the initial azimuth alignment of the MotionPak can only be realized by using other external measurements because its gyro drifts are too large. In the low-cost integrated INS/GPS system, the north and east components of GPS velocity are used to compute an approximate initial heading. The error of this estimated initial heading can be very large. It is desirable in most applications that the heading error will be reduced and its effect on system accuracy be eliminated after a period of time. Figure 6.10 shows the convergence of the heading with time for the low-cost integrated INS/GPS system,

when starting from an arbitrary initial heading.

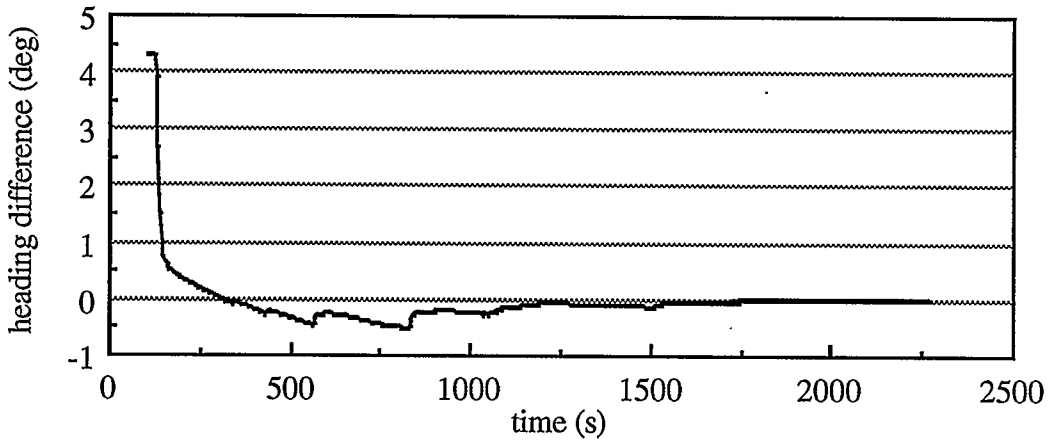

Figure 6.10 Heading Difference due to Different Initial Headings

Figure 6.10 indicates that the effect of the initial heading error decreases with time, and is eliminated after about 20 minutes. This means that the integrated system has in-flight alignment capabilities when using GPS observations to update the MotionPak. The alignment time and accuracy depends on both the vehicle maneuvers and the geometry of the satellites configuration observed. The van motion in test #1 is varied enough to improve the alignment of the MotionPak through normal vehicle maneuvers.

The moving base alignment capability of the low-cost integrated system is very important because it ensures sufficient heading accuracy even in case of large initial heading errors. Otherwise accurate static heading alignment would be necessary, which is impossible with a low-cost IMU, or the system has to be constrained by a given external heading.

6.7 RESULTS OF VAN TEST #2

The second van test was conducted in the research park of The University of Calgary. Its

objective was to test the integrated system under less than ideal conditions. The master station was set upon the roof of the Engineering Building. Figure 6.11 shows the trajectory of the test. The number of satellites observed and the PDOP during the test are shown in Figures 6.12 and 6.13. Due to buildings and trees, only four or five satellites were observed during most of the time, and at some times only three satellites were observable. Because of the poor geometry of the observed satellites, the PDOP is often larger than 3.0. Figures 6.14 and 6.15 show the attitude and velocity change during the test.

The velocity, position an attitude errors of the low-cost integrated INS/GPS are shown in Figures 6.16, 6.17 and 6.18, respectively. Statistical values of these errors are summarized in Tables 6.4, 6.5 and 6.6, respectively.

Table 6.4 Velocity Errors of the Low-Cost Integrated INS/GPS

	Ve error	Vn error	Vu error
mean (m/s)	0.002	-0.003	0.003
RMS (m/s)	0.082	0.095	0.067

Table 6.5 Position Errors of the Low-Cost Integrated INS/GPS

	latitude error	longitude error	height error
mean (m)	0.826	-2.139	-2.554
RMS (m)	4.483	3.471	5.121

Table 6.6 Attitude Errors of the Low-Cost Integrated INS/GPS

	roll error	pitch error	heading error
mean (deg)	-0.177	0.066	0.112
RMS (deg)	0.185	0.088	0.657

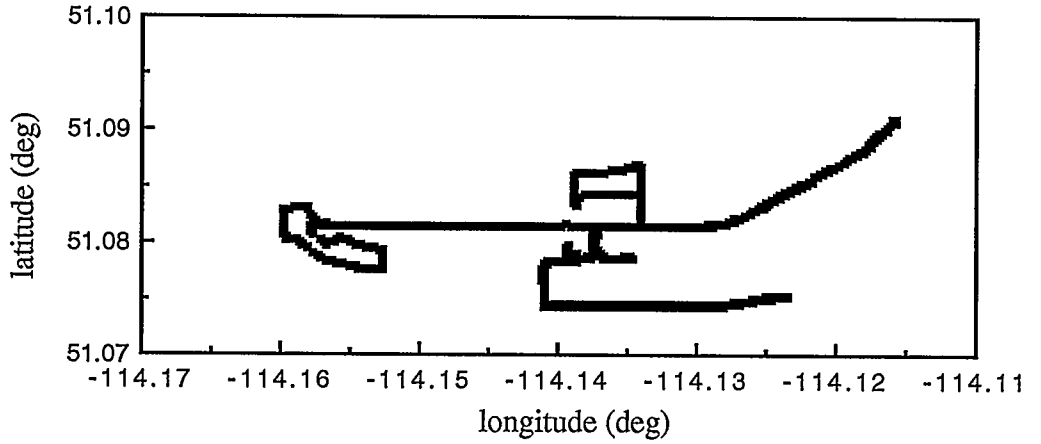

Figure 6.11 Trajectory of Van Test #2

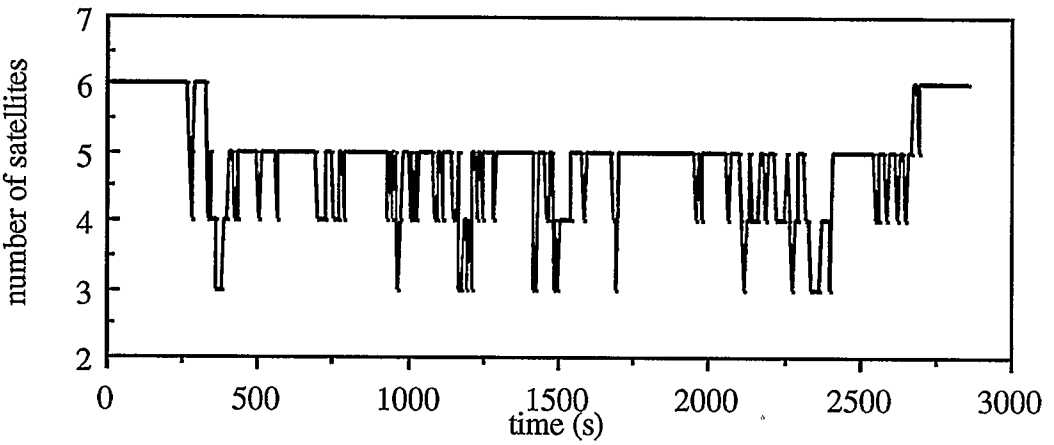

Figure 6.12 Number of Satellites Observed During Van Test #2

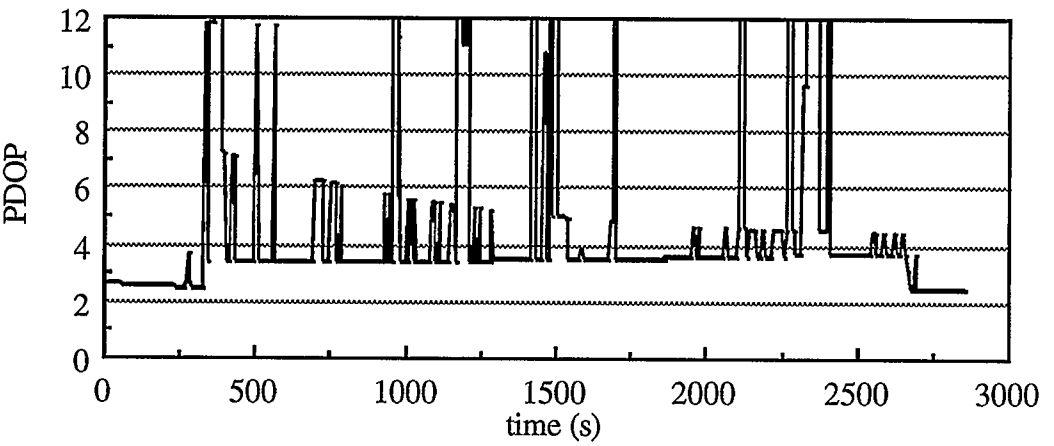

Figure 6.13 PDOP During Van Test #2

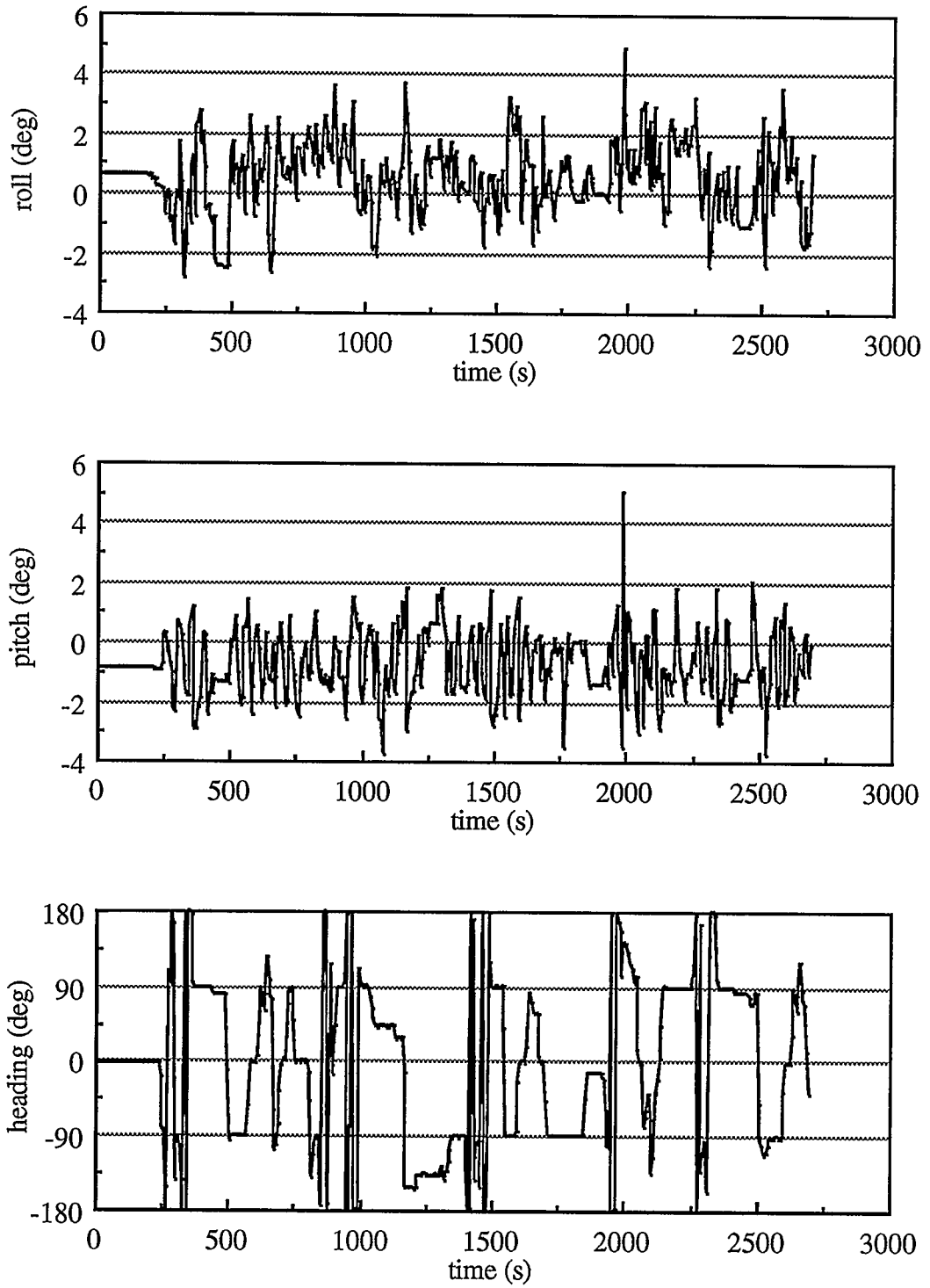

Figure 6.14 Van Attitude During Van Test #2

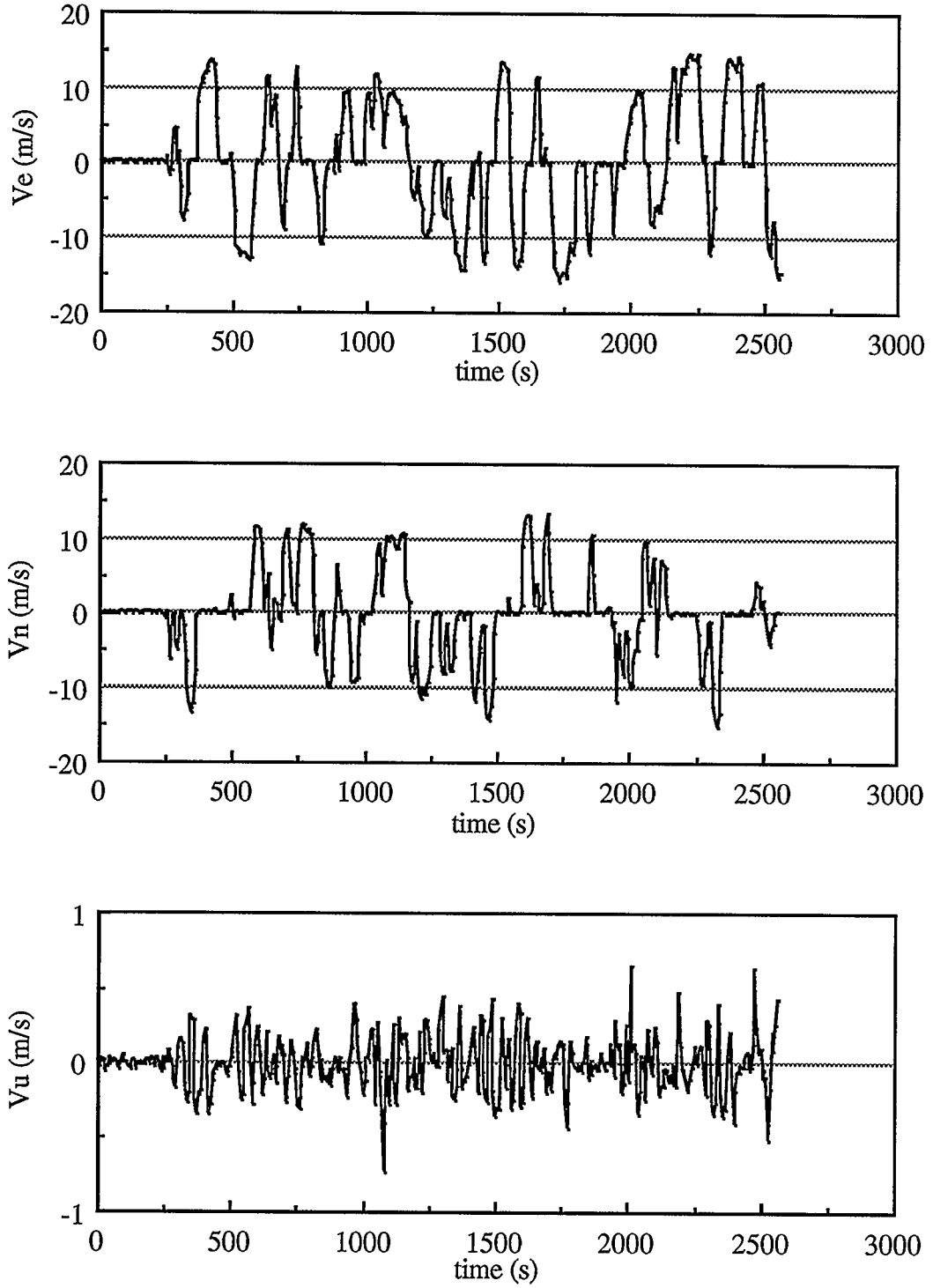

Figure 6.15 Van Velocity During Van Test #2

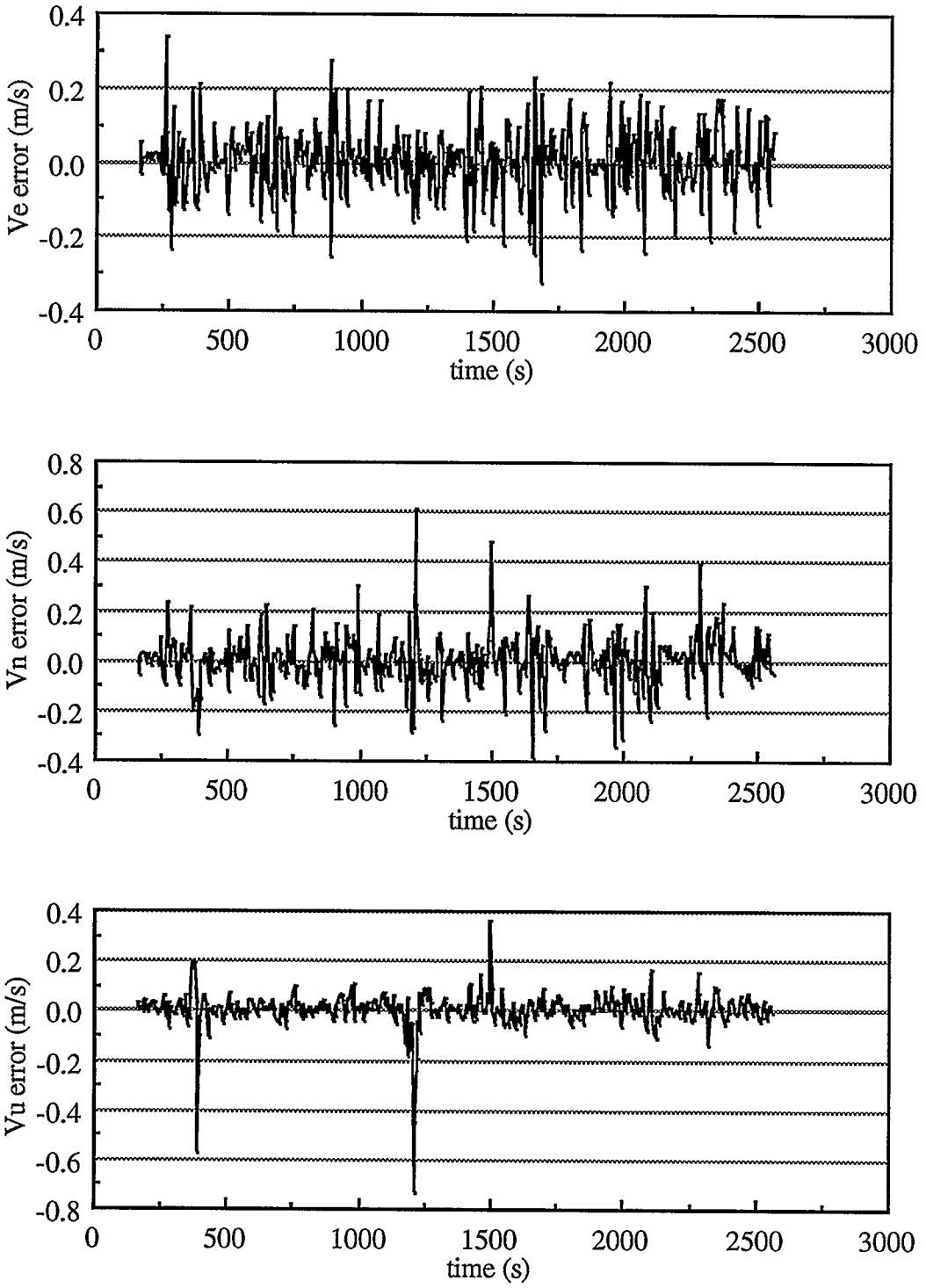

Figure 6.16 Velocity Errors of the Low-Cost Integrated INS/GPS

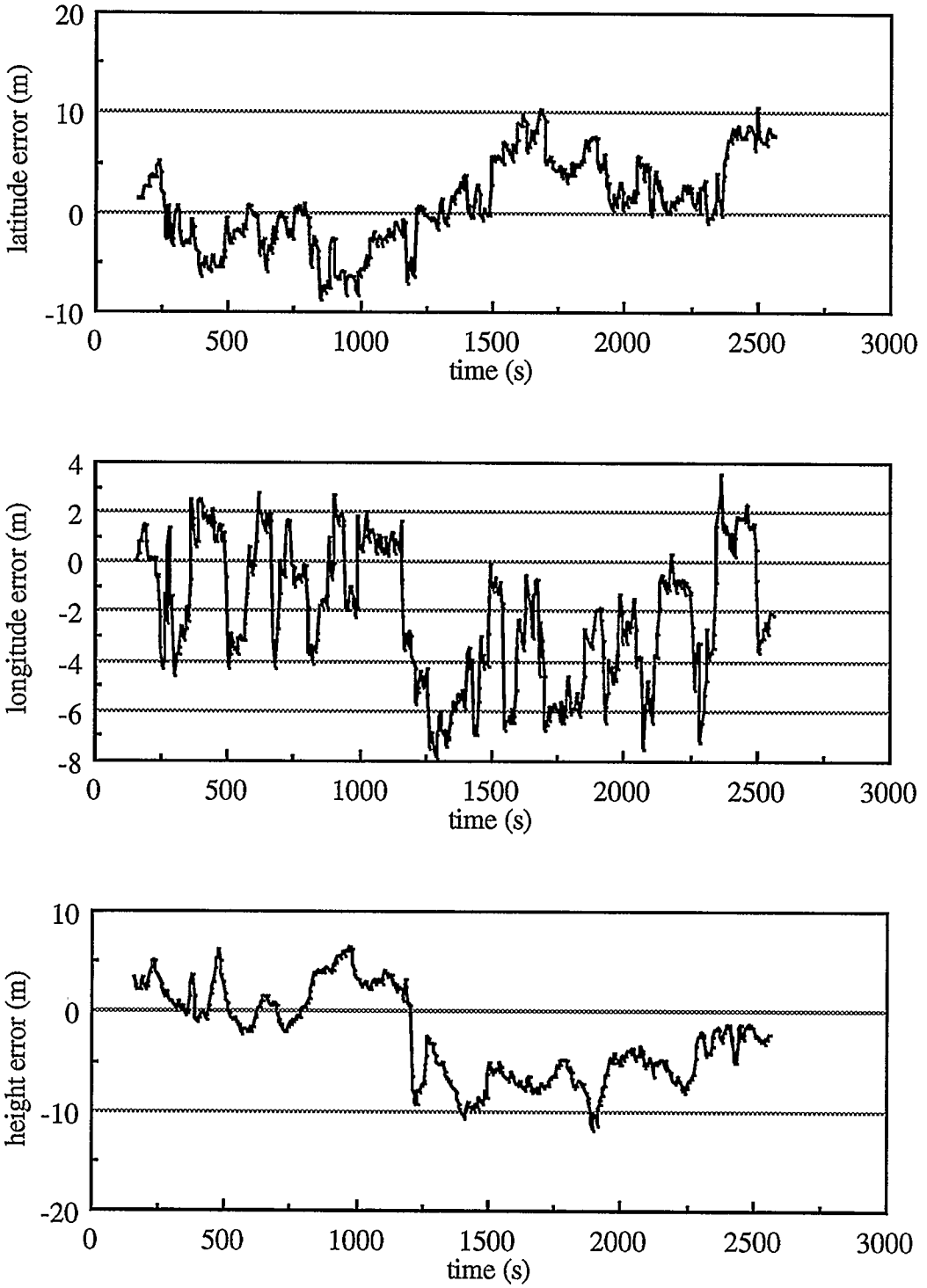

Figure 6.17 Position Errors of the Low-Cost Integrated INS/GPS

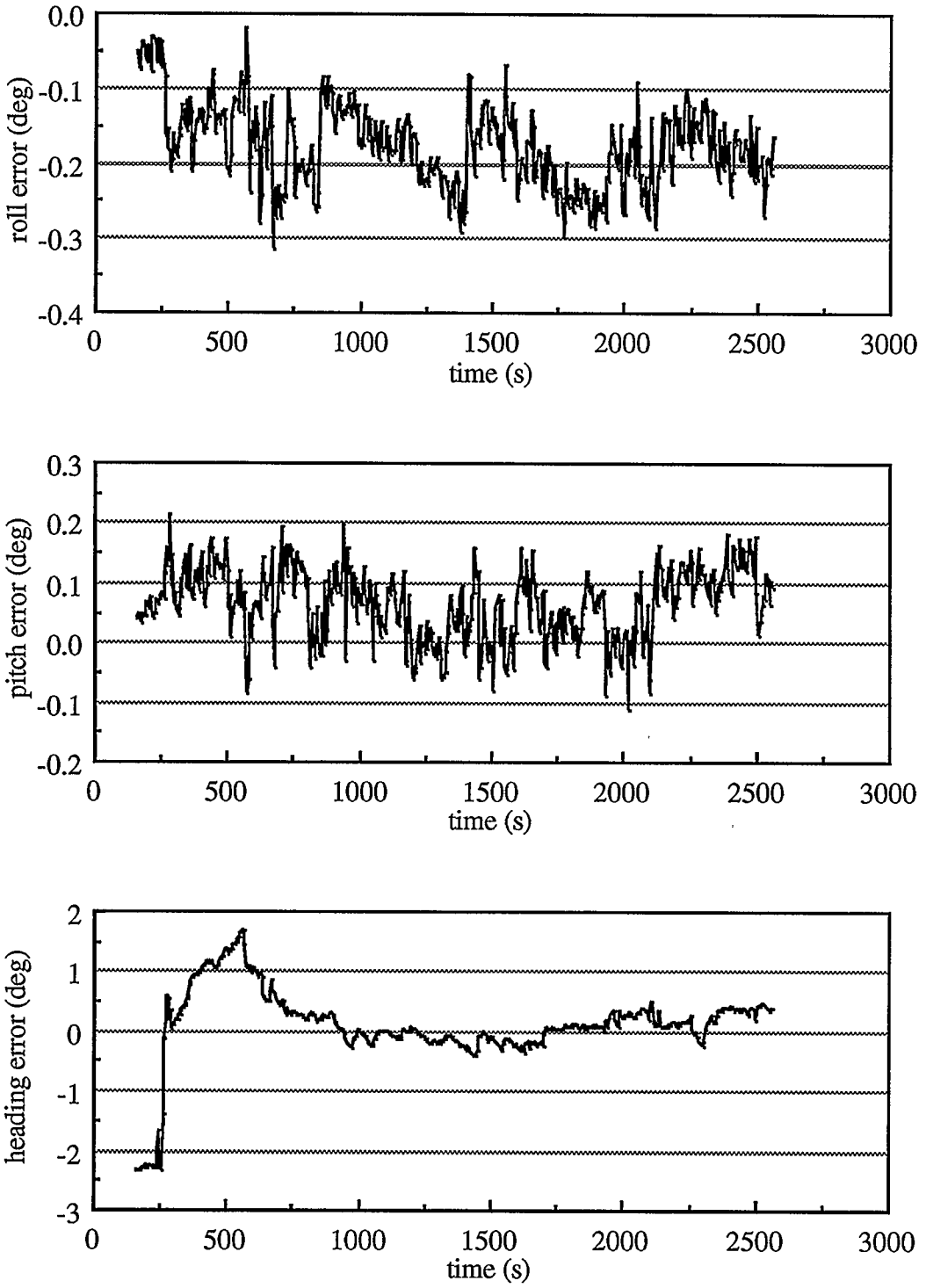

Figure 6.18 Attitude Errors of the Low-Cost Integrated INS/GPS

When comparing the second set of test results with the first one, it becomes clear that PDOP values influence the accuracy of the integrated INS/GPS system to a considerable extent. This shows mainly in large bias values for position and attitude, and in large variances for velocity and position. In terms of attitude components only the variance of the roll is considerably increased. The system accuracy, however, is still marginal for the accuracy requirements of airborne resource mapping applications.

In airborne applications, aircraft maneuvers, such as sharp banked turns, may shade some GPS signals (Sun, 1994a). Since the performance of the low-cost integrated INS/GPS system largely depends on the PDOP value, two airborne GPS antennas should be used, which can largely overcome the satellite signal shading problem (Sun, 1994b). The two antennas can also be used to determine vehicle heading and pitch, which is very important for the heading updates and will be discussed in Chapter 7.

CHAPTER 7

INTEGRATION OF THE MOTIONPAK WITH A GPS MULTI-ANTENNA SYSTEM

As discussed in Chapter 6, the heading accuracy achievable with the low-cost integrated INS/GPS system using double differenced GPS pseudorange and Doppler observations is marginal for airborne resource mapping applications and depends very much on vehicle maneuvers. In order to provide accurate heading information, vehicle maneuvers, such as horizontal turns or accelerations are needed from time to time. This, however, will impose restrictions on the vehicle trajectory and thus mission planning. If the application can not provide such maneuvers, as in cases where constant velocity is the desired operational environment, the heading accuracy will decrease with time and could become very poor. The reason for this limitation is that the INS attitude can only be indirectly improved since the pseudorange observations are primarily used to improve the position accuracy and the Doppler observations are primarily used to improve the velocity accuracy. To overcome this limitation and to meet heading accuracy requirements for resource mapping applications in any operational environment, direct attitude measurements, especially heading measurements, are highly desirable for the integrated INS/GPS system.

The recent development in attitude determination using GPS multi-antenna systems makes it possible to integrate an inertial system with GPS by using not only pseudorange and Doppler observations, but also attitude measurements, see Miller et al. (1993). In this

chapter, heading measurements from a GPS dual-antenna system are added to the integration described in Chapter 5 and 6. Test results are analyzed and compared to those of the integration in Chapter 6.

7.1 ATTITUDE MEASUREMENTS OF A GPS MULTI-ANTENNA SYSTEM

In the first van test described in Chapter 6, a four-antenna Ashtech 3DF receiver was also installed on the van. Figure 7.1 illustrates the antenna configuration and their spacing. The carrier phase measurements collected from the four antennas were used to compute the van attitude. Figure 7.2 shows the attitude errors of the 3DF receiver and Table 7.1 gives their statistical values. For a detailed description of the attitude determination algorithm, see El-Mowafy (1994).

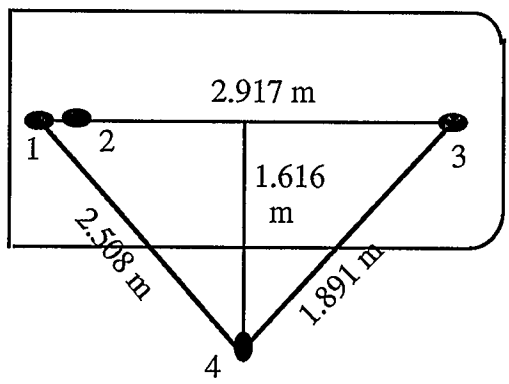

Figure 7.1 Antenna Configuration

Only heading measurements from the 3DF receiver are used in the system integration. The use of heading measurements only is based on the following considerations:

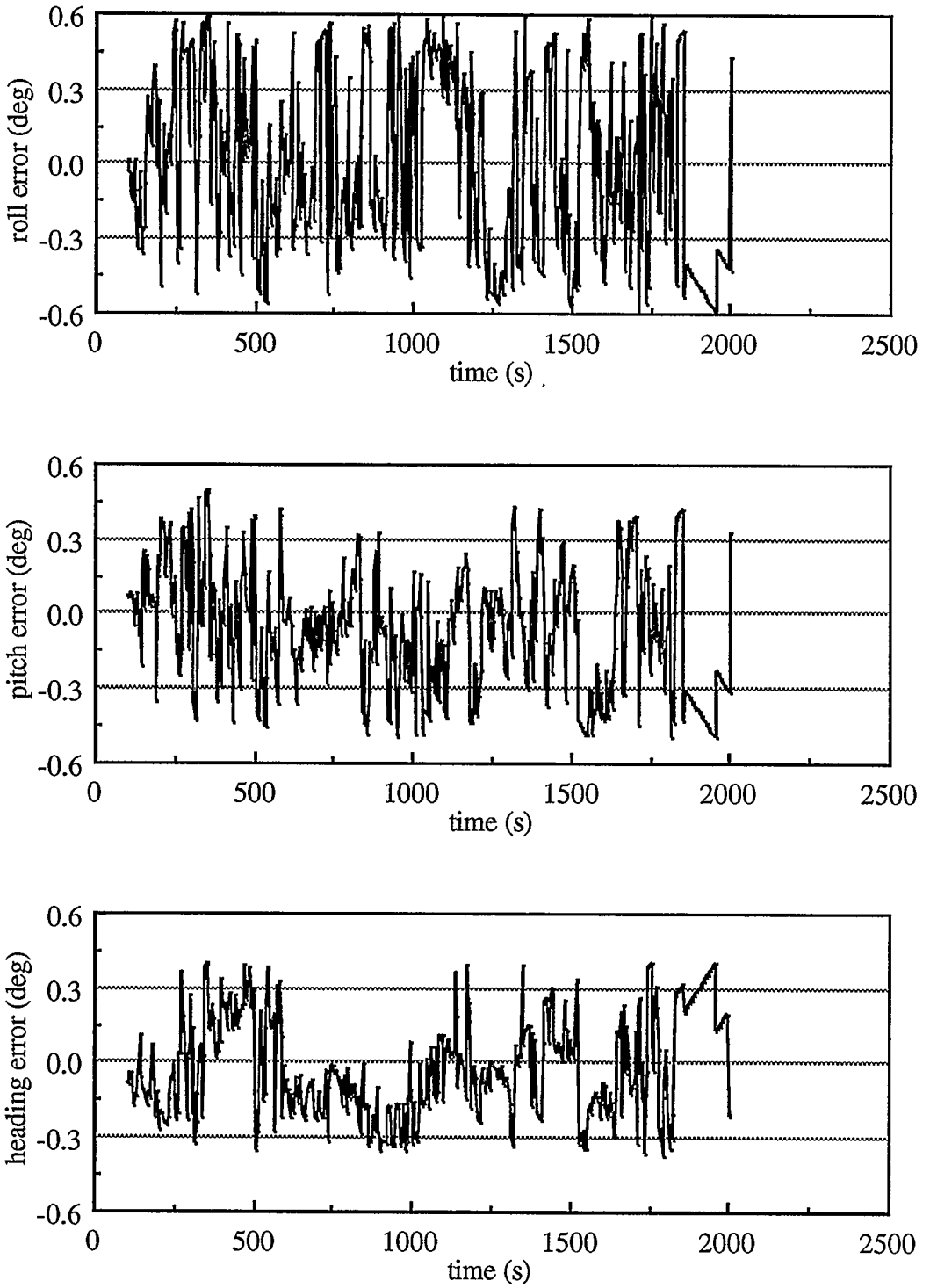

Figure 7.2 Attitude Errors of the 3DF Receiver

Table 7.1 Attitude Errors of the 3DF Receiver

	roll error	pitch error	heading error
mean (deg)	-0.016	-0.062	-0.027
RMS (deg)	0.351	0.243	0.199

(1) Additional heading measurements are needed to make the low-cost integrated INS/GPS system meet the heading accuracy requirements of airborne resource mapping applications in any operational environment while the accuracy requirements in roll and pitch can be satisfied by using double differenced pseudorange and Doppler observations;

(2) Only two remote GPS antennas installed along the longitudinal axis of the vehicle are needed to determine heading and pitch. To determine the roll, one more GPS antenna has to be installed, which will increase the system cost;

(3) In airborne applications, the resulting roll measurements will be affected by the wing flexure in airborne applications (Cannon, 1994), and will most likely deviate considerably from the roll of the remote sensing system;.

(4) The pitch accuracy of this test is much worse than that of the integrated system using double differenced pseudorange and Doppler observations.

7.2 INTEGRATION OF THE MOTIONPAK WITH A GPS DUAL-ANTENNA SYSTEM

A centralized Kalman filter is employed to estimate inertial navigation errors and inertial sensor errors of the MotionPak using heading measurements from a GPS dual-antenna

system, double differenced GPS pseudorange and Doppler observations. Figure 7.3 shows the concept of this centralized Kalman filter. The state vector (5.8) is used in the integration Kalman filter. In order to also integrate the GPS dual-antenna system, the heading differences between the INS and the GPS dual-antenna system must be modelled.

In the earth-fixed frame, the relationship between the misalignment errors and the transformation matrix $\mathbf{C}_b^e$ is given by

$$\begin{bmatrix} 1 & -\varepsilon_z^e & \varepsilon_y^e \\ \varepsilon_z^e & 1 & -\varepsilon_x^e \\ -\varepsilon_y^e & \varepsilon_x^e & 1 \end{bmatrix} \mathbf{C}_l^e(\text{true})\mathbf{C}_b^l(\text{true}) = \mathbf{C}_l^e(\text{computed})\mathbf{C}_b^l(\text{computed}) \tag{7.1}$$

After the differential GPS pseudorange and Doppler updates, the errors in the $\mathbf{C}_l^e$ matrix are much smaller than the errors in $\mathbf{C}_b^l$ matrix. Neglecting the errors of $\mathbf{C}_l^e$, equation (7.1) becomes

$$(\mathbf{C}_l^e)^T \begin{bmatrix} 1 & -\varepsilon_z^e & \varepsilon_y^e \\ \varepsilon_z^e & 1 & -\varepsilon_x^e \\ -\varepsilon_y^e & \varepsilon_x^e & 1 \end{bmatrix} \mathbf{C}_l^e\mathbf{C}_b^l(\text{true}) = \mathbf{C}_b^l(\text{computed}) \tag{7.2}$$

Comparing equation (7.2) with (6.2), we have

$$\begin{bmatrix} 1 & -\varepsilon_u^l & \varepsilon_n^l \\ \varepsilon_u^l & 1 & -\varepsilon_e^l \\ -\varepsilon_n^l & \varepsilon_e^l & 1 \end{bmatrix} = (\mathbf{C}_l^e)^T \begin{bmatrix} 1 & -\varepsilon_z^e & \varepsilon_y^e \\ \varepsilon_z^e & 1 & -\varepsilon_x^e \\ -\varepsilon_y^e & \varepsilon_x^e & 1 \end{bmatrix} \mathbf{C}_l^e \tag{7.3}$$

This is equivalent to

$$\begin{bmatrix} \varepsilon_e^l \\ \varepsilon_n^l \\ \varepsilon_u^l \end{bmatrix} = (\mathbf{C}_l^e)^T \begin{bmatrix} \varepsilon_x^e \\ \varepsilon_y^e \\ \varepsilon_z^e \end{bmatrix} \tag{7.4}$$

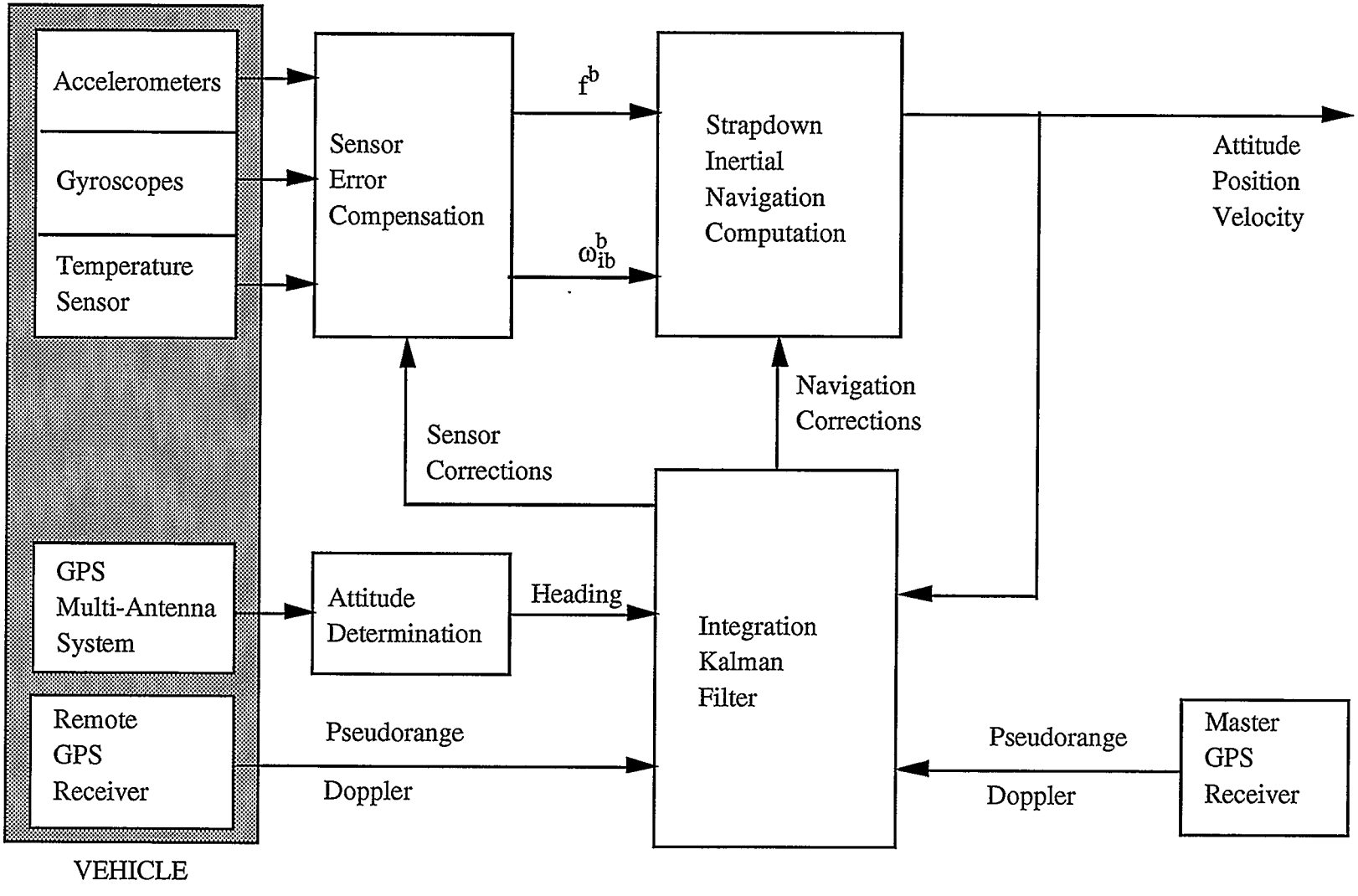

Figure 7.3 Integration of the MotionPak with a GPS Multi-Antenna System

Inserting equation (7.4) into (6.7) results in

$$d\psi = \begin{bmatrix} \dfrac{C_b^l(1,2)C_b^l(3,2)}{(C_b^l(3,1))^2+(C_b^l(3,3))^2} & \dfrac{C_b^l(2,2)C_b^l(3,2)}{(C_b^l(3,1))^2+(C_b^l(3,3))^2} & 1 \end{bmatrix} (C_l^e)^T \begin{bmatrix} \varepsilon_x^e \\ \varepsilon_y^e \\ \varepsilon_z^e \end{bmatrix} \tag{7.5}$$

Equation (7.5) is the relationship between $\delta\psi$ and $\varepsilon_x^e, \varepsilon_y^e, \varepsilon_z^e$.

7.3 VAN TEST RESULTS AND ANALYSIS

The low-cost integrated INS/GPS system using double differenced pseudorange and Doppler observations as well as heading measurements from the 3DF receiver was implemented for van test #1. Figures 7.4, 7.5 and 7.6 show the attitude, velocity and position errors, respectively. The error statistics are given in Tables 7.2, 7.3 and 7.4 respectively. The tables show that the accuracy requirements of airborne resource mapping applications are satisfied by integrating the MotionPak with GPS using double differenced pseudorange and Doppler observations as well as heading measurements from a GPS dual-antenna system.

Table 7.2 Attitude Errors of the Integrated System

	roll error	pitch error	heading error
mean (deg)	-0.007	-0.028	-0.075
RMS (deg)	0.047	0.070	0.189

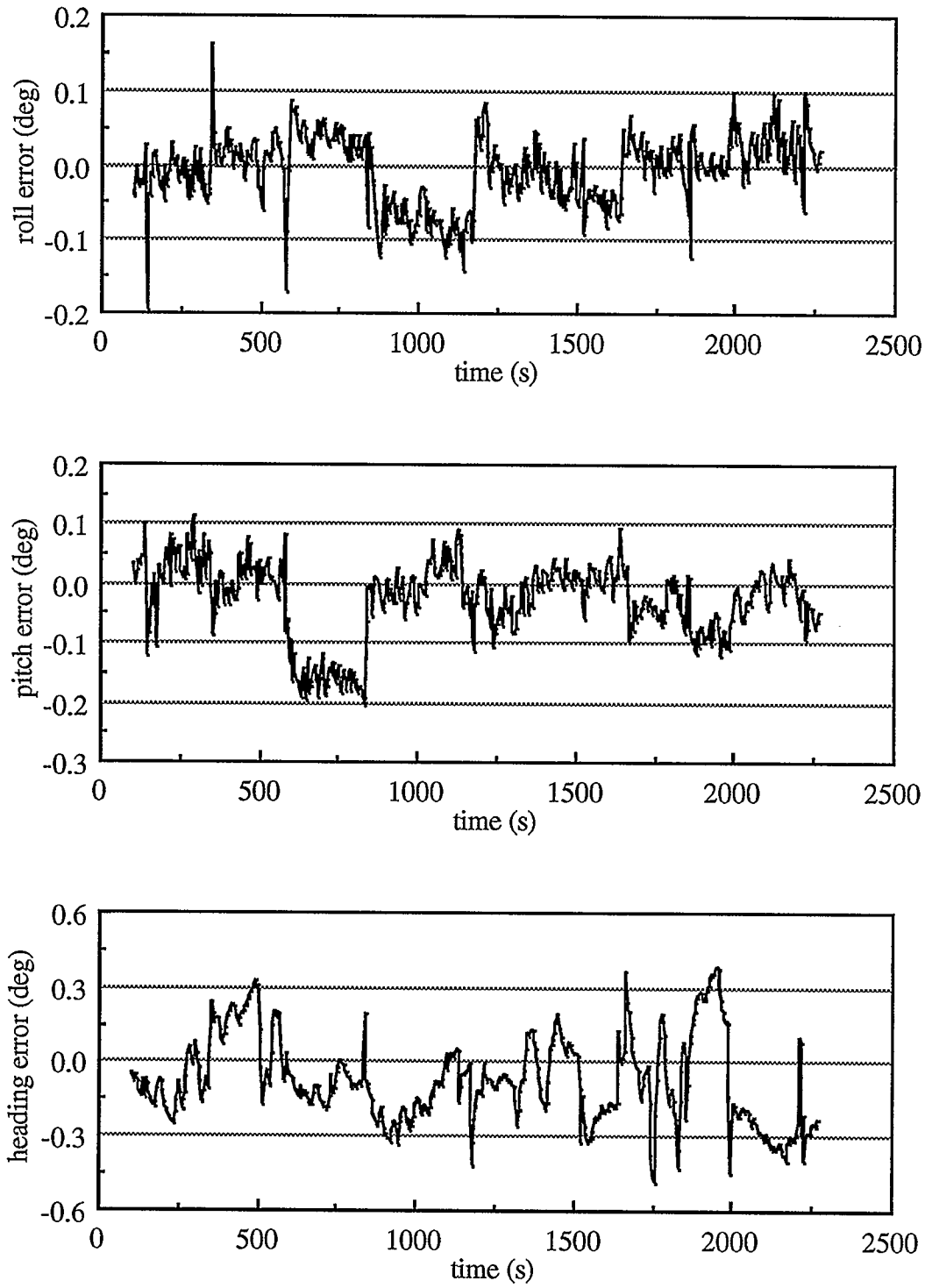

Figure 7.4 Attitude Errors of the Integrated System

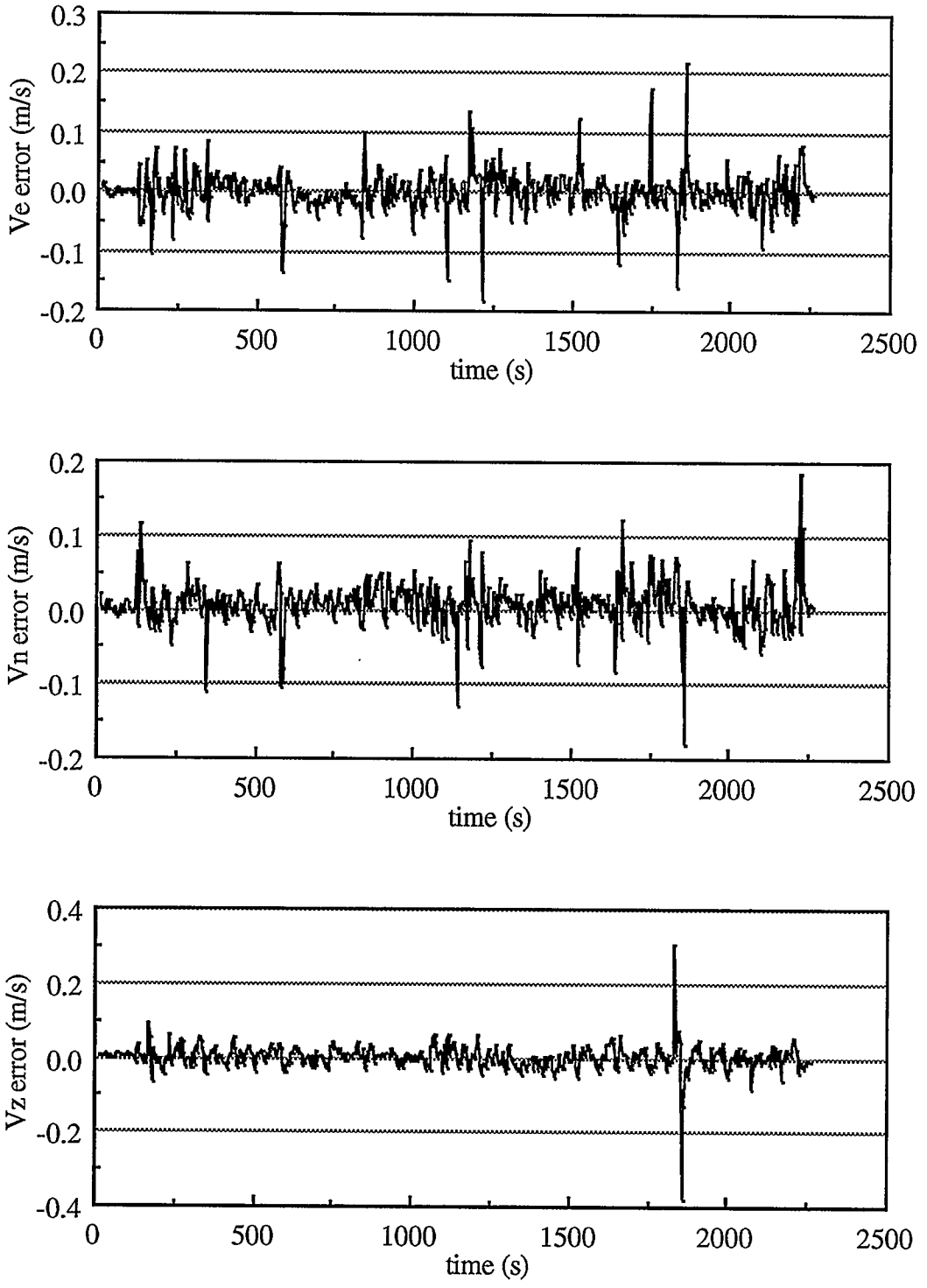

Figure 7.5 Velocity Errors of the Integrated System

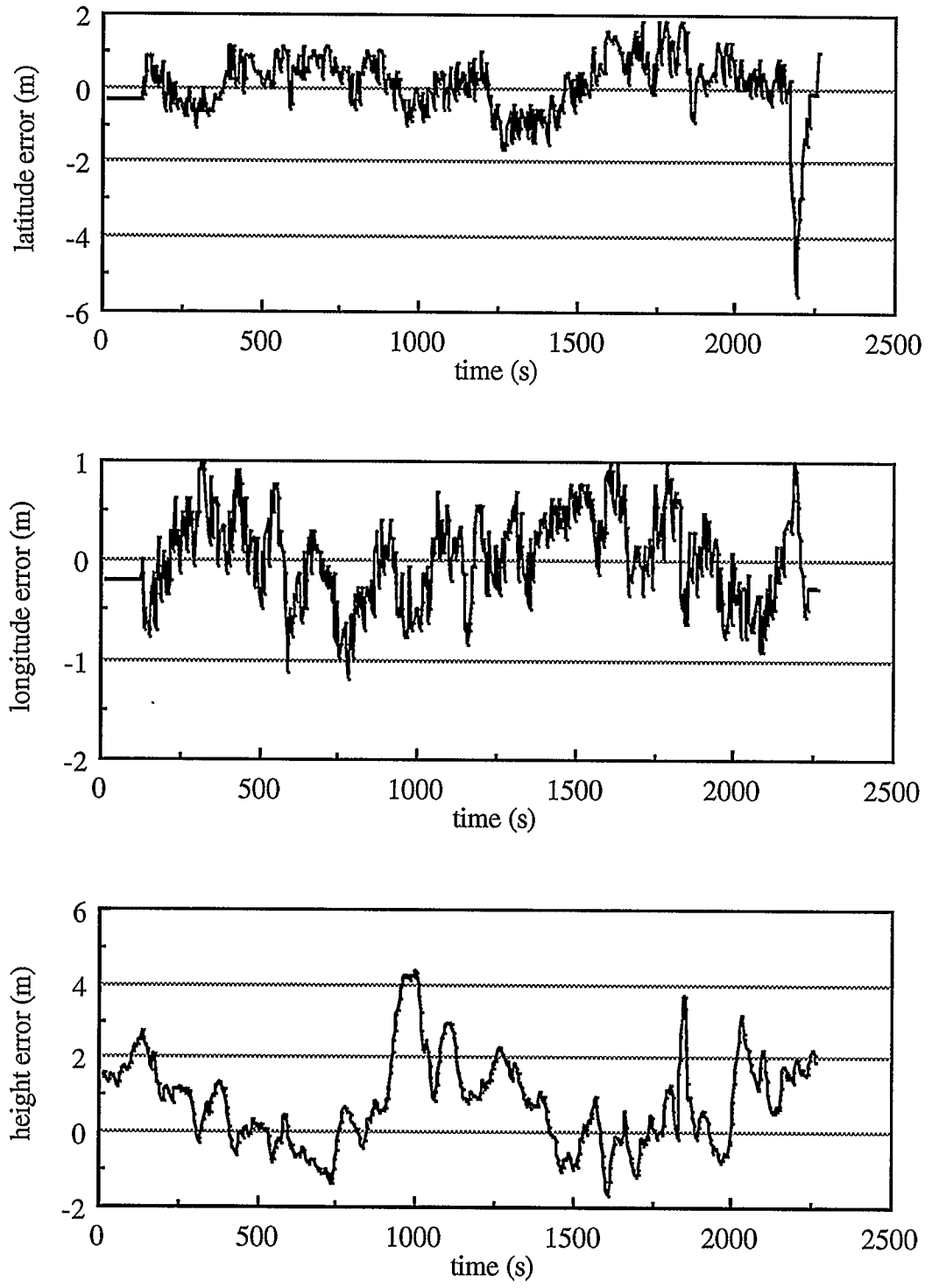

Figure 7.6 Position Errors of the Integrated System

Table 7.3 Velocity Errors of the Integrated System

	V_e error	V_n error	V_u error
mean (m/s)	-0.000	-0.005	-0.001
RMS (m/s)	0.030	0.031	0.030

Table 7.4 Position Errors of the Integrated System

	latitude error	longitude error	height error
mean (m)	0.078	0.008	0.809
RMS (m)	0.848	0.459	1.458

Comparing Figure 7.4 and Table 7.2 with Figure 6.9 and Table 6.3, it is clear that heading measurements from a GPS dual-antenna system limits error growth in heading and results in accurate attitude information even during long periods of constant velocity movements along straight lines. The accuracy achievable in roll and pitch, however, is about the same as before. Since ε_e^l and ε_n^l have been well estimated using double differenced pseudorange and Doppler observations, the yaw error $\delta\psi$ mainly depends on ε_u^l in case of a small pitch angle, see Equation (6.7). Therefore, the heading measurements from the GPS multi-antenna system can significantly improve the ε_u^l estimation accuracy and only slightly improve the estimation accuracy of ε_e^l and ε_n^l. Equations (6.5) to (6.7) explain why the better estimation of ε_u^l will improve the heading accuracy but will leave the roll and pitch accuracy about the same.

The better estimation of ε_u^l enhances the INS velocity performance, see Equation (6.1). Since the Kalman filter can use the advantages of both systems, the velocity accuracy of the

low-cost integrated INS/GPS system is also improved by using heading measurements from a GPS dual-antenna system. The improvement in velocity enhances the position accuracy as well since the INS position is obtained by only integrating the velocity.

The heading measurements from a GPS multi-antenna system are also used in the initial alignment of the MotionPak. In this case, the initial heading is taken from the heading measurements of the GPS multi-antenna system rather than computed from the GPS velocity.

The performance of a GPS multi-antenna system can also be enhanced in the following aspects through integrating with the MotionPak:

(1) Comparing Figure 7.4 and Table 7.2 with Figure 7.2 and Table 7.1, it is clear that high frequency error components of the heading from a GPS multi-antenna system are smoothed out through the integration.

(2) The MotionPak can provide attitude outputs with excellent short-term accuracy to enhance the ambiguity determination ability of a GPS multi-antenna system.

(3) Instead of low data rate attitude outputs of a GPS multi-antenna system, high-rate attitude outputs are available from the integrated system.

CHAPTER 8

CONCLUSIONS AND RECOMMENDATIONS

8.1 CONCLUSIONS

The contribution of this research was in the development and testing of a low-cost integrated INS/GPS system for airborne resource mapping applications. Based on the prototype system developed and the test results obtained, the following conclusions can be drawn.

(1) The low-cost integrated INS/GPS system is developed to the prototype stage by using a low-cost inertial sensor assembly and by optimally combining the measurements from the inertial sensors and GPS. All the hardware and software designs for the prototype system have been verified by tests.

(2) The design of the analogue-to-digital conversion and the inertial error compensation for the MotionPak makes it possible to use low-cost and low-quality inertial sensor assemblies to develop low-cost integrated INS/GPS systems with sufficient accuracy for a wide range of applications.

(3) For airborne resource mapping applications, double differenced GPS pseudorange and Doppler as well as attitude from a GPS dual-antenna system are suitable measurements for updating an INS.

(4) The GPS 1PPS signal can be used to synchronize the measurements between GPS and INS with sufficient accuracy.

(5) In order to maintain the adequacy of the linear inertial error equations for a low-quality inertial sensor assembly, a feedback configuration must be used.

(6) The centralized Kalman filter gives a tight coupling of the INS and GPS measurements and is suitable for the low-cost integrated INS/GPS system.

(7) The integrated INS/GPS system using double difference GPS pseudorange and Doppler observations can meet the accuracy requirements of airborne resource mapping applications in position, roll and pitch. The heading accuracy, however, is marginal and depends on the vehicle trajectory.

(8) In addition to using double difference GPS pseudorange and Doppler observations, heading measurements from a GPS dual-antenna system can enhance the integrated system performance. In this case, the low-cost system will meet the accuracy requirements of airborne resource mapping in any operational environment.

(6) Due to the low cost, small size and accuracy achievable, such a system can be used in a wide range of applications.

8.2 RECOMMENDATIONS

Up to now, only a prototype of the low-cost integrated INS/GPS system has been developed and tested. In order to build the production system, additional work is needed. The following are recommendations for further work.

(1) The system has to be flight-tested and its performance in this environment has to be analyzed.

(2) The gyros and accelerometers in the MotionPak are very temperature sensitive. The models currently used to compensate the temperature-induced sensor errors are not very stable. Since they are the major source of system errors, an internal temperature control device should be added to keep the MotionPak at constant temperature and thus eliminate these errors.

(3) Analogue anti-aliasing filters should be used to replace the digital low-pass filters currently used.

(4) Stand-alone GPS receivers and GPS multi-antenna systems have been used in the prototype system. With the advances in GPS technology, low-cost, small-size and accurate GPS cards are available. This kind of GPS cards should be used in the low-cost integrated INS/GPS system to replace the stand-alone GPS receivers used right now.

(5) A small-size analogue-to-digital conversion board should be designed to replace the general-purpose data acquisition board currently used. The production version of the low-cost integrated INS/GPS system should put the analogue-to-digital board, one GPS card and the MotionPak in the same box.

(6) Two airborne GPS antennas should be used in the production version of the low-cost integrated INS/GPS system since dual antennas can largely overcome the satellite signal shading problem and determine the vehicle heading. The general attitude determination algorithm should be specialized to a simple heading and pitch algorithm for use with two nondedicated GPS cards.

(7) If the low-cost integrated INS/GPS system is used for applications which require higher position accuracy, double differenced GPS carrier phase observations can be used.

REFERENCES

Bader, J. (1993): *Low Cost GPS/INS*, Proceedings of ION GPS-93, Salt Lake City, Utah, pp. 235-244.

Baumker, M. and A. Mattissek (1992): *Integration of a Fiber Optical Gyro Attitude and Heading Reference System with Differential GPS*, Proceedings of ION GPS-92, Albuquerque, New Mexico pp. 1093-1101.

BEI Electronics Company (1993): ***MotionPak User Manual***, Concord, California.

Britting, K.R. (1971): ***Inertial Navigation System Analysis***, Wiley-Interscience, New York.

Brown, R.A., R.F. Cox and R.E. Ebner (1992): *Global Positioning Inertial Navigation System Development*, Proceedings of ION GPS-92, Albuquerque, New Mexico pp. 697-705.

Cannon, M.E. (1991): *Airborne GPS/INS with an Application to Aerotriangulation*, UCSE Report #20040, Department of Surveying Engineering, The University of Calgary, Calgary, Canada.

Cannon, M.E., H. Sun, T. Owen and M. Meindl (1994): *Assessment of a Non-Dedicated GPS Receiver System for Precise Airborne Attitude Determination*, Proceedings of ION GPS-94, Salt Lake City, Utah, pp. 645-654.

Cohen, C.E., B.W. Parkinson and B.D. Mcnally (1994): *Flight Tests of Attitude Determination Using GPS Compared Against an Inertial Navigation Unit,* **Navigation**, Journal of The Institute of Navigation, Vol. 41, pp. 83-97.

Cox, D.B. (1978): *Integration of GPS with Inertial Navigation System*, **Navigation**, Journal of The Institute of Navigation, Vol. 25, No. 2, pp. 236-245.

Dally, J.W., W.F. Riley, and K.G. McConnell (1993): ***Instrumentation for Engineering Measurements***, John Wiley & Sons Inc., New York.

El-Mowafy, A. (1994): *Kinematic Attitude Determination from GPS*, UCGE Report #20074, Department of Geomatics Engineering, The University of Calgary, Calgary, Canada.

Gao, Y., E.J. Krakiwsky, M.A. Abousalem and J.F. McLellan (1993): *Comparison and Analysis of Centralized, Decentralized, and Federated Filters*, **Navigation**, Journal of The Institute of Navigation, Vol. 40, No. 1, pp. 69-86.

Geis, L.J. (1989): ***Transform Analysis and Filters***, Prentice-Hall, Inc., New Jersey.

Gelb, A. (ed.) (1974): ***Applied Optimal Estimation***, The M.I.T. Press, Cambridge, Massachusetts.

Hartman, R.G. (1988): *An Integrated GPS/IRS Design Approach*, **Navigation**, Journal of The Institute of Navigation, Vol. 35, No. 1, pp. 121-134.

Howell, G. and W. Tang (1994): *A Universal GPS/INS Kalman Filter Design*, Proceedings of ION GPS-94, Salt Lake City, Utah, pp. 443-451.

Hutchinson, C.E. (1984): *The Kalman Filter Applied to Aerospace and Electronic Systems*, **IEEE Transactions on Aerospace and Electronic Systems**, AES-24, 4, pp. 500-504.

Karatsinides, S.P. (1994): *Enhancing Filter Robustness in Cascade GPS-INS Integrations*, **IEEE Transactions on Aerospace and Electronic Systems**, AES-30, 4, pp. 1001-1007.

Knight D.T., A.W. Osborne, R.W. Snow and D.G. Kim (1993): *Demonstration of a New, Tightly-Coupled GPS/INS*, Proceedings of ION GPS-93, Salt Lake City, Utah, pp. 205-214.

Kwan, W., W.R. Lee, L.O. Lupash and J.A. McLean (1993): *The Design and Implementation of the AC-130U GPS/INS Integrated Filter*, Proceedings of ION GPS-93, Salt Lake City, Utah, pp. 225-234.

Lachapelle, G. and G. Lu (1994): *Precise Shipborne Attitude Determination Using Wide Antenna Spacing*, Proceedings of KIS-94, Banff, Canada, pp. 323-330.

Lapucha, D. (1990): *Precise GPS/INS Positioning for a Highway Inventory System*, UCSE Report #20038, Department of Surveying Engineering, The University of Calgary, Calgary, Canada.

Lipman, J.S. (1992): *Trade-Offs in the Implementation of Integrated GPS Inertial Systems*. Proceedings of ION GPS-92, Albuquerque, New Mexico pp. 1125-1133.

Liu, Z. (1992): *Comparison of Statistical Methods for the Alignment of Strapdown Inertial System*, UCGE Report #20047, Department of Geomatics Engineering, The University of Calgary, Calgary, Canada.

Lu, G., M.E. Cannon, G. Lachapelle, and P. Kielland (1994): *Attitude Determination Using Dedicated and Nondedicated Multiantenna GPS Sensors*, **IEEE Transactions on Aerospace and Electronic Systems**, AES-30, 4, pp. 1053-1058.

Maybeck, P.S. (1979): ***Stochastic Models, Estimation, and Control***, Vol. 1, Academic Press, New York.

McMillan, J.C. (1994a): *A GPS Attitude Error Model for Kalman Filtering*, Proceedings of IEEE Position Location and Navigation Symposium, Las Vegas, pp. 329-336.

McMillan, J.C. and D.A.G. Arden (1994b): *Sensor Integration Options for Low Cost Position and Attitude Determination*, Proceedings of IEEE Position Location and Navigation Symposium, Las Vegas, pp. 453-459.

Meyer-Hilberg, J. and T. Jacob (1994): *High Accuracy Navigation and Landing System Using GPS/IMU System Integration*, Proceedings of IEEE Position Location and Navigation Symposium, Las Vegas, pp. 293-305.

Miller, B.L., C.A. Phillips, A.G. Evans and J.E. Bibel (1993): *A Kalman Filter Implementation for a Dual-Antenna GPS Receiver and an Inertial Navigation System*, Proceedings of ION GPS-93, Salt Lake City, Utah, pp. 593-602.

Morrison, R. (1984): ***Instrumentation Fundamentals and Applications***, Wiley-Interscience, New York.

National Instruments (1993): ***AT-MIO-16X User Manual***, Austin, Texas.

Nelthropp, D., J. Campanile and L. Federici (1992): *Integration of Embedded GPS/INS on the T-45A Aircraft*, Proceedings of ION GPS-92, Albuquerque, New Mexico pp. 215-223.

Schmidt, G.T. (1989): *Kalman Filter Integration of Modern Guidance and Navigation Systems*, **AGARD Lecture Series No. 166**, Neuily Sur Seine, France.

Schmidt, G.T. (1978): *Strapdown Inertial Systems*, **AGARD Lecture Series No. 95**, Neuily Sur Seine, France.

Schmidt, S.F. (1981): *The Kalman Filter: Its Recognition and Development for Aerospace Applications*, **Journal on Guidance and Control**, Vol. 4, No. 1, pp. 4-7.

Schwarz, K.P., M.A. Chapman, M.E. Cannon, P. Gong (1993): *An Integrated INS/GPS Approach to the Georeferencing of Remotely Sensed Data*, **Photogrammetric Engineering and Remote Sensing**, Vol. 59, 11, pp. 1667-1674.

Schwarz, K.P., M.A. Chapman, M.E. Cannon, P. Gong, D. Cosandier (1994a): *A Precise Positioning/Attitude System in Support of Airborne Remote Sensing*, Proceeding of the GIS/ISPRS Conference, Ottawa, Canada.

Schwarz, K.P. and G.S. Zhang (1994b): *Development and Testing of a Low Cost Integrated GPS/INS*, Proceedings of ION GPS-94, Salt Lake City, Utah, pp. 1137-1144.

Schwarz, K.P. and M. Wei (1994c): *Aided Versus Embedded --- A Comparison of Two Approaches to GPS/INS Integration*, Proceedings of IEEE Position Location and Navigation Symposium, Las Vegas, pp. 314-322.

Schwarz, K.P. and M. Wei (1995): ***Inertial Geodesy and INS/GPS Integration***, ENGO 623 Lecture Notes, Department of Geomatics Engineering, The University of Calgary, Calgary, Canada.

Shale, R. and J, Bader (1994): *Flight Test Result of the Rockwell MIGITS*, Proceedings of IEEE Position Location and Navigation Symposium, Las Vegas, pp. 306-309.

Silva, R.N. and G.W. Murray (1994): *Low Cost Quartz Rate Sensors Applied to Tactical Guidance IMUs*, Proceedings of IEEE Position Location and Navigation Symposium, Las Vegas, pp. 37-42.

Stambough, J.S. (1973): *Propagation and System Accuracy Impact of Major Sensor Errors on a Strapdown Aircraft Navigator*, **IEEE Transactions on Aerospace and Electronic Systems**, AES-9, 6, pp. 838-846.

Sun, H. (1994a): *GPS/INS Integration for Airborne Applications*, UCGE Report #20069, Department of Geomatics Engineering, The University of Calgary, Calgary, Canada.

Sun, H. (1994b): *Integration of INS with Multiple GPS Antennas for Airborne Applications*, Proceedings of ION GPS-94, Salt Lake City, Utah, pp. 1401-1409.

Tang, W. and G. Howell (1993): *Integrated GPS/INS Kalman Filter Implementation Issues*, Proceedings of ION GPS-93, Salt Lake City, Utah, pp. 217-224.

Tazartes, D.A. and J.G. Mark (1988): *Integration of GPS Receivers into Existing Inertial Navigation Systems*, **Navigation**, Journal of The Institute of Navigation, Vol. 35, No. 1.

Upadhyay, T.N., S. Cotterill, A.W. Deaton (1994): *Autonomous GPS/INS Navigation Experiments for Space Transfer Vehicle*, **IEEE Transactions on Aerospace and Electronic Systems**, AES-29, 3, pp. 772-785.

Vieweg, W. (1994): *Using Low Cost Inertial Sensors for Integrated Satellite/Inertial Navigation*, Proceedings of ION GPS-94, Salt Lake City, Utah, pp. 417-425.

Wei, M. and K.P. Schwarz (1990a): *A Strapdown Inertial Algorithm Using an Earth-Fixed Cartesian Frame*, **Navigation**, Journal of The Institute of Navigation, Vol. 37, No. 2, pp. 153-167.

Wei, M. and K.P. Schwarz (1990b): *Testing a Decentralized Filter for GPS/INS Integration*, Proceedings of IEEE Position Location and Navigation Symposium, Las Vegas, pp. 429-435.

Wells, D., N. Beck, D. Delikaraoglu, A. Kleusberg, E. Krakiwsky, G. Lachapelle, R. Langley, M. Nakiboglu, K.P. Schwarz, J. Tranquilla and P.Vanicek (1986): ***Guide to GPS Positioning***, The University of New Brunswick, Fredericton, New Brunswick, Canada.

Woolven, S., B.H. Kliewer and B.M. Scherzinger (1994): *Application of Integrated Navigation Technology to Road and Rail Survey*, Proceedings of KIS-94, Banff, Canada, pp. 409-417.

Wong, R.V.C. (1988): *Development of a RLG Strapdown Inertial Survey System*, UCSE Report #20027, Department of Surveying Engineering, The University of Calgary, Calgary, Canada.